



GEOLOGY OF THE INTERMOUNTAIN WEST

an open-access journal of the Utah Geological Association

ISSN 2380-7601

Volume 10

2023

THE KANARRA FOLD-THRUST STRUCTURE—THE LEADING EDGE OF THE SEVIER FOLD-THRUST BELT, SOUTHWESTERN UTAH

William J. Chandonia and John P. Hogan



© 2023 Utah Geological Association. All rights reserved.

This is an open-access article in which the Utah Geological Association permits unrestricted use, distribution, and reproduction of text and figures that are not noted as copyrighted, provided the original author and source are credited. Email inquiries to GIW@utahgeology.org.



GEOLOGY OF THE INTERMOUNTAIN WEST

an open-access journal of the Utah Geological Association

ISSN 2380-7601

Volume 10

2023

Editors

| | |
|--|---|
| Douglas A. Sprinkel Azteca Geosolutions 801.391.1977 GIW@utahgeology.org dsprinkel@gmail.com | Thomas C. Chidsey, Jr. Utah Geological Survey 801.824.0738 tomchidsey@gmail.com |
| Bart J. Kowallis Brigham Young University 801.380.2736 bkowallis@gmail.com | John R. Foster Utah Field House of Natural History State Park Museum 435.789.3799 eutretauranosuchus@ gmail.com |
| Steven Schamel GeoX Consulting, Inc. 801.583-1146 geox-slc@comcast.net | |

Production

Cover Design and Desktop Publishing
Douglas A. Sprinkel

Cover

View from the Kanarra Falls trail looking north upon overturned, thrust Permo-Triassic carbonates and siliciclastics. The Timpoweap Member of the Triassic Moenkopi Formation forms the higher, eastern ridge. Duplication of the lower red member on either side of the Timpoweap Member reveals a major fold accommodation fault along the east limb of the Kanarra fold-thrust structure—the Kanarra Creek thrust. Inset: View south near the entrance to Spring Creek Canyon of a break-thrust fold in the Fossil Mountain Member of the Permian Kaibab Formation, which is a smaller, partial mimic of the larger Kanarra fold-thrust structure (see figure 12, p. 23 for a complete description).



Geology of the Intermountain West (GIW) is an open-access journal in which the Utah Geological Association permits unrestricted use, distribution, and reproduction of text and figures that are not noted as copyrighted, provided the original author and source are credited.

2022–2023 UGA Board

| | | | |
|------------------|------------------|----------------------------|--------------|
| President | Rick Ford | rford@weber.edu | 801.915.3188 |
| President-Elect | Eugene Syzmanski | eugenes@utah.gov | 801.537.3364 |
| Co-Program Chair | Megan Crocker | meganlynncrocker@gmail.com | 801.538.5290 |
| Treasurer | Aubrey DeReuil | aubrey@zanskar.us | 850.572.2543 |
| Secretary | Tom Chidsey | tomchidsey@gmail.com | 801.824.0738 |
| Past President | John South | johnvsouth@gmail.com | 801.367.9292 |

UGA Committees

| | | | |
|-----------------------|------------------|--------------------------|--------------|
| Environmental Affairs | Craig Eaton | eaton@ihi-env.com | 801.633.9396 |
| Geologic Road Sign | Greg Gavin | greg@loughlinwater.com | 801.541.6258 |
| Historian | Paul Anderson | paul@pbageo.com | 801.364.6613 |
| Outreach | Greg Nielsen | gnielsen@weber.edu | 801.626.6394 |
| Public Education | Zach Anderson | zanderson@utah.gov | 801.537.3300 |
| | Matt Affolter | gfl247@yahoo.com | |
| Publications | Paul Inkenbrandt | paulinkenbrandt@utah.gov | 801.537.3361 |
| Publicity | Paul Inkenbrandt | paulinkenbrandt@utah.gov | 801.537.3361 |
| Social/Recreation | Roger Bon | rogerbon@xmission.com | 801.942.0533 |

AAPG House of Delegates

| | | | |
|----------------|-----------------|------------------------------|--------------|
| 2020–2023 Term | David A. Wavrek | dwavrek@petroleumsystems.com | 801.322.2915 |
|----------------|-----------------|------------------------------|--------------|

State Mapping Advisory Committee

| | | | |
|--------------------|---------------|------------------------|--------------|
| UGA Representative | Bill Loughlin | bill@loughlinwater.com | 435.649.4005 |
|--------------------|---------------|------------------------|--------------|

Earthquake Safety Committee

| | | | |
|-------|--------------|------------------|--------------|
| Chair | Grant Willis | gwillis@utah.gov | 801.537.3355 |
|-------|--------------|------------------|--------------|

UGA Website — www.utahgeology.org

| | | | |
|-----------|------------------|--------------------------|--------------|
| Webmaster | Paul Inkenbrandt | paulinkenbrandt@utah.gov | 801.537.3361 |
|-----------|------------------|--------------------------|--------------|

UGA Newsletter

| | | | |
|-------------------|-----------|--------------------------|--------------|
| Newsletter Editor | Bill Lund | uga.newsletter@gmail.com | 435.590.1338 |
|-------------------|-----------|--------------------------|--------------|

Become a member of the UGA to help support the work of the Association and receive notices for monthly meetings, annual field conferences, and new publications. Annual membership is \$30 and annual student membership is only \$5. Visit the UGA website at www.utahgeology.org for information and membership application.

The UGA board is elected annually by a voting process through UGA members. However, the UGA is a volunteer-driven organization, and we welcome your voluntary service. If you would like to participate please contact the current president or committee member corresponding with the area in which you would like to volunteer.



The Kanarra Fold-Thrust Structure—The Leading Edge of the Sevier Fold-Thrust Belt, Southwestern Utah

William J. Chandonia¹ and John P. Hogan^{1,2}

¹Department of Geosciences and Geological Engineering and Petroleum Engineering, Missouri University of Science and Technology, 129 McNutt Hall, 1400 North Bishop, Rolla, MO 64509 USA; williamjchandonia@gmail.com; ² jhogan@mst.edu

ABSTRACT

The multiple origins proposed for the Kanarra anticline in southwestern Utah as a drag-fold along the Hurricane fault, a Laramide monocline, a Sevier fault-propagation fold, or a combination of these processes, serve to muddy its tectonic significance. This in part reflects the structural complexity of the exposed eastern half of the fold. The fold evolved from open and up-right to overturned and tight, is cross-cut by multiple faults, and was subsequently dismembered by the Hurricane fault. The western half of the fold is obscured because of burial, along with the hanging wall of the Hurricane fault, beneath Neogene and younger sediments and volcanics. We present the results of detailed bedrock geologic mapping, and geologic cross sections restored to Late Cretaceous time (prior to Basin and Range extension), to demonstrate the Kanarra anticline is a compound anticline-syncline pair inextricably linked with concomitant thrust faulting that formed during the Sevier orogeny. We propose the name Kanarra fold-thrust structure to unambiguously identify the close spatial and temporal association of folding and thrusting in formation of this prominent geologic feature. We identify a previously unrecognized thrust, the Red Rock Trail thrust, as a forelimb shear thrust that was in a favorable orientation and position to have been soft-linked, and locally hard-linked, with the thrust ramp of the basal detachment to form a break thrust. The east verging Red Rock Trail thrust is recognized by a distinctive cataclasite in the Lower Jurassic Navajo Sandstone. The hanging wall of the Red Rock Trail thrust is displaced eastward over the Middle Jurassic Carmel Formation and Upper Cretaceous formations and can be traced for at least 27 km and possibly farther. We contend the Kanarra fold-thrust structure unambiguously defines the leading edge of the Sevier fold-thrust belt in southwestern Utah. Stratigraphic relationships in the southern and northern part of the Kanarra fold-thrust structure constrain its development between the early and late Campanian (about 84 to 71 Ma) but possibly younger. In southwestern Utah, initial movement along the Iron Springs thrust at about 100 Ma (Quick and others, 2020) and subsequent eastward advancement of the Sevier deformation front to the Red Rock Trail thrust at about 84 to 71 Ma coincided with well-documented magmatic flare ups in the Cordilleran arc in the hinterland of the Sevier fold-thrust belt. This temporal relationship between magmatic flare ups and thrusting is consistent with a close correspondence between arc-related processes and episodic foreland deformation.

Citation for this article.

Chandonia, W.J., and Hogan, J.P., 2023, The Kanarra fold-thrust structure—the leading edge of the Sevier fold-thrust belt, southwestern Utah: *Geology of the Intermountain West*, v. 10, p. 1–64, <https://doi.org/10.31711/giw.v10.pp1-64>.

INTRODUCTION

The Sevier fold-thrust belt (Armstrong, 1968; Burchfield and Davis, 1972) is an integral component of the more extensive Cordilleran orogenic belt that affected western North America from the Late Jurassic (about 165 Ma) to the Eocene (about 50 Ma) (Yonkee and Weil, 2015; Herring and Greene, 2016). Magmatism, deformation, and accompanying sedimentation during this time was in response to subduction of the oceanic Farallon plate along the western edge of the North America plate, and accretion of various outboard terranes (Lageson and others, 2001; DeCelles, 2004; DeCelles and others, 2009; DeCelles and Graham, 2015; Ducea and others, 2015). Across the Cordilleran retro-arc several prominent east-directed thin-skinned thrusts folded and imbricated Proterozoic to Mesozoic miogeoclinal and terrestrial sediments resulting in at least 350 km of shortening at the latitude of central to northern Utah (DeCelles, 2004; Herring and Greene, 2016).

Significant advancement in the understanding of the structural style, spatial progression, and effect on foreland sedimentation during collisional orogenesis have come from extensive investigation of the Sevier fold-thrust belt in northern and central Utah (Constenius, 1996; Constenius and others, 2003; DeCelles, 2004; DeCelles and Coogan, 2006; Chidsey and others, 2007; Herring and Greene, 2016; Pujols and others, 2020) as well as in Nevada (Long, 2015; Giallorenzo and others, 2018; Di Fiori and others, 2021). However, the temporal and spatial evolution of deformation associated with the Sevier fold-thrust belt varies considerably along strike (e.g., see figure 1, p. 77, in Quick and others, 2020). In central to northern Utah, at the latitude of the Salt Lake salient (about 41° N.), the Sevier fold-thrust belt remained active longer (ca., 100 myr) over a wider deformation belt (about 500 km) and propagated farther inland (e.g., Hogsback thrust, which continued moving east up to 56 Ma). In contrast, in the southern part of the fold-thrust belt, at the latitude of the Las Vegas recess (about 36° N.), thin-skinned deformation was of shorter duration (ca., 50 myr) and formed a narrower deformation belt (about 100 km wide). Quick and others (2020) attributed this along strike spatial and temporal variation in the advancement of the Sevier de-

formation front to structural inheritance; the location of the buried western edge of Precambrian continental crust least affected by extension (i.e., the “hingeline,” see Kay, 1951; Stokes, 1976; Picha and Gibson, 1985; Picha, 1986 for a complete discussion) as well as the location of prominent extensional basement structures (e.g., transform faults). The sinuous trace defined by the multiple salients and recesses of the retro-arc Sevier fold-thrust belt reflects the form of the rifted Precambrian North American continental margin and the prominent role reactivated extensional structures in the basement had on the eastward advancement of the Sevier deformation front (Picha and Gibson, 1985; Paulsen and Marshak, 1999; Quick and others, 2020).

The location and timing of arrival of the Sevier deformation front in southwestern Utah, the region linking the northern and southern parts of the fold-thrust belt (figure 1), remains a subject of debate (Biek and others, 2009, p. 29, 31). This is due, in part, to the complexity of the bedrock and surficial geology of southwestern Utah. Here contractional structures associated with the Sevier orogeny are variably dissected by Cenozoic Basin and Range extensional faulting (e.g., the Hurricane fault), obscured by intrusion of Miocene laccoliths (e.g., the Pine Valley and/or Three Peaks laccolith), covered by Neogene to Holocene volcanic units, or buried by significant landslides (Biek, 2003a, 2003b; Hurlow and Biek, 2003; Biek and others, 2009; Knudsen, 2014a, 2014b; Biek and Hayden, 2016; Quick and others, 2020). Biek and others (2009, p. 5) defined the leading edge of the Sevier fold-thrust belt deformation in southwestern Utah by the location of the Square Top Mountain thrust (their easternmost significant thrust) and the Virgin, Pintura, and Kanarra anticlines. The Square Top Mountain thrust is linked with the Keystone-Muddy Mountain-Tule Spring thrust system in southeastern Nevada and its northern extension is linked with the Blue Mountain-Iron Springs-Canyon Range thrust system (see figure 5, p. 6, figure 40, p. 26, in Biek and others, 2009). Arrival of the leading edge of the Sevier fold-thrust belt in southwestern Utah is thus constrained by the emergence of the Square Top Mountain thrust and the erosional beveling of the Pintura anticline, which is unconformably overlain by the Cretaceous Canaan Peak Formation. The Canaan

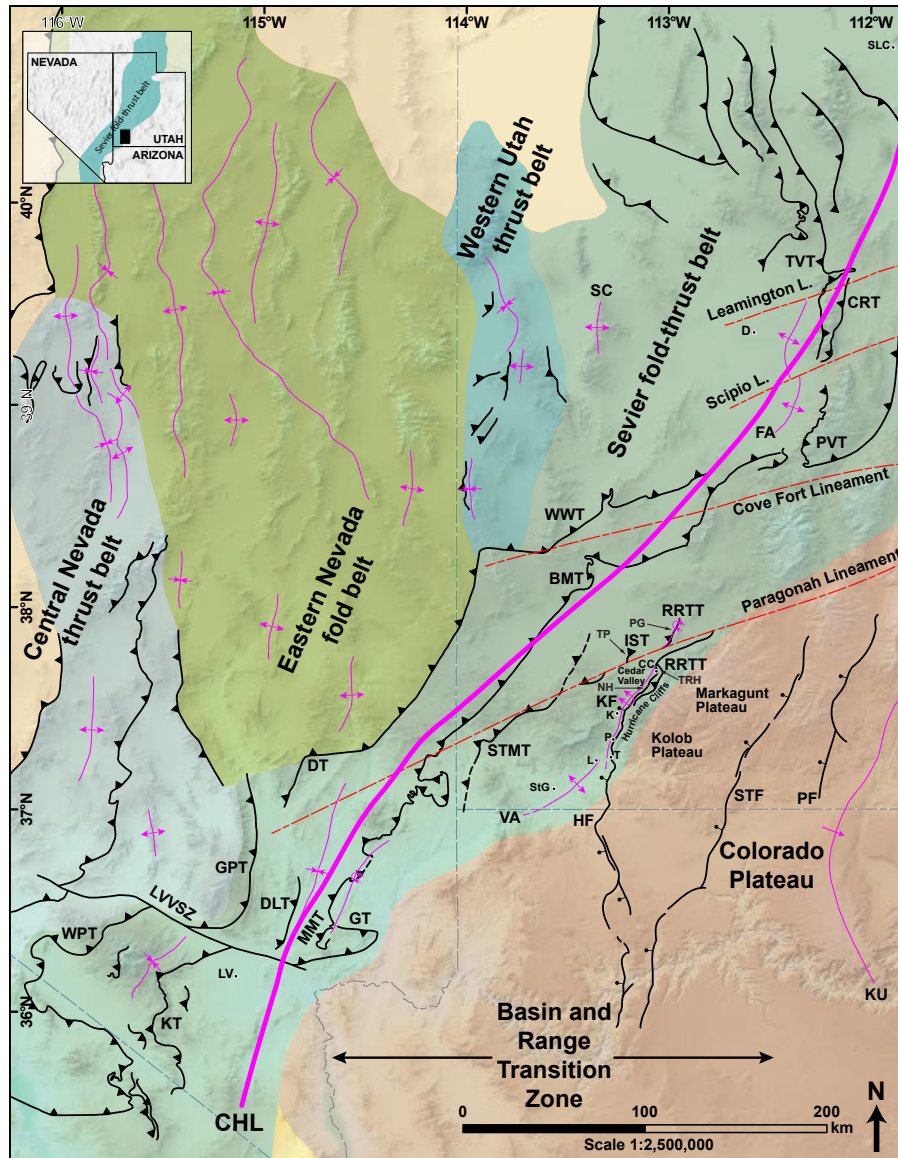


Figure 1. Regional overview map showing the Sevier frontal fold-thrust belt in relation to Cordilleran hinterland deformation belts and the craton. Included are Proterozoic rift-related lineaments, the Cordilleran hinge line (CHL), and Basin and Range structures. Geographic abbreviations: SLC—Salt Lake City; D—Delta; CC—Cedar City; K—Kanarra; P—Pintura; T—Toquerville; L—Leeds; StG—St. George; LV—Las Vegas; TRH—The Red Hill; NH—North Hills; PG—Parowan Gap; TP—Three Peaks. Fold abbreviations: VA—Virgin anticline; KF—Kanarra fold. FA—Fillmore arch; SC—Sevier culmination; KU—Kaibab uplift (Laramide). Thrust abbreviations: KT—Keystone thrust; DLT—Dry Lake thrust; MMT—Muddy Mountains thrust; GT—Glendale thrust; BMT—Blue Mountain thrust; WPT—Wheeler Pass thrust; GPT—Gass Peak thrust; DT—Delamar thrust; WWT—Wah Wah thrust; STMT—Square Top Mountain thrust; IST—Iron Springs thrust; RRTT—Red Rock Trail thrust; PVT—Pahvant thrust (formerly spelled Pavant thrust); CRT—Canyon Range thrust; TVT—Tintic Valley thrust. Basin and Range structures: LVVSZ—Las Vegas Valley shear zone; HF—Hurricane fault; STF—Sevier-Toroweap fault; PF—Paunsaugunt fault. After Quick and others (2020); compiled from Stokes and others (1963), Picha and Gibson (1985), Wernicke and others (1988), Willis (1999), Page and others (2005), Long (2012, 2015), Biek and others (2015), Yankee and Weil (2015), Herring and Green (2016), Giallorenzo and others (2018). DEM visualization from the USGS National Map 3D Elevation Program (3DEP).

Peak is broadly thought to be early to late Campanian, about 84 to 71 Ma, although these dates are poorly constrained and the timing of continued Sevier deformation in this area may be younger (Biek and others, 2009 p. 30–31). Quick and others (2020) suggested an earlier arrival for the deformation front associated with the Sevier fold-thrust belt in southwestern Utah is constrained by emergence of the Iron Springs thrust at The Three Peaks. They used a 100.18 ± 0.04 crystallization age for zircons extracted from a previously unrecognized dacite lapilli ash-fall tuff associated with the Marshall Creek Breccia to constrain movement of the Iron Springs thrust (also see Fillmore, 1991) to latest Albian–earliest Cenomanian (about 100 Ma); an age considerably earlier than previously proposed but similar in age to the about 99 Ma Keystone thrust of Fleck and Carr (1990). Subsequently, Biek and others (2015, p. 91) proposed the presence of an earlier period of cryptic thrusting for the Paunsaugunt normal fault on the Paunsaugunt Plateau as the easternmost leading edge of the Sevier fold-thrust belt.

The discrepancy in the timing of arrival and location of the leading edge of the Sevier fold-thrust belt in southwestern Utah highlights the uncertainty associated with episodic Sevier deformation in the region. We suggest this, in part, stems from long-lived uncertainty associated with the nature of the Kanarra anticline (Gregory and Williams, 1947; Averitt, 1962; Threet, 1963a, 1963b; Armstrong, 1968; Biek, 2007a; Biek and others, 2009; Biek and Hayden, 2016) and along strike correlation of structures (e.g., faults) and stratigraphic units. The Kanarra anticline is coincident with the trace of the Cordilleran hingeline in southwestern Utah, extending from near Toquerville to Cedar City for about 53 km (figure 1). The development of the Kanarra anticline has been contentious since it was first described by Dutton (1880), who did not recognize the fold as a separate feature from the Hurricane fault. Over time, it has alternately been interpreted as forming during Mesozoic reverse faulting along the Hurricane fault (e.g., Lovejoy, 1978), a Laramide monocline (e.g., figure 1, p. 548 and figure 2, p. 549, in Enriquez St. Pierre and Johnson, 2021), and as a Sevier-age thin-skinned fault propagation fold (Grant and others, 1994) modified by rotation of the footwall of the Hurricane fault during Basin and

Range extension (Stewart and Taylor, 1996). The ambiguity in the strain significance of the Kanarra anticline reflects complications due to dismemberment of the anticline by the Hurricane fault (i.e., the west-dipping limb may be buried beneath Neogene and younger fill of Cedar Valley), offset of the axial trace of the fold (e.g., along the Proterozoic Paragonah lineament), and burial by prominent landslides (Threet, 1963b; Picha and Gibson, 1985; Biek and others, 2015). Current consensus recognizes the Kanarra anticline as a contractional fault propagation fold formed during the Sevier orogeny (see Biek and others, 2009) although alternative interpretations as a Laramide age monocline persist (see figure 1, p. 548 and figure 2 p. 549, in Enriquez St. Pierre and Johnson, 2021).

The role of thrusting in the development of the Kanarra anticline is poorly understood. Grant and others (1994) and Nowir and Grant (1995) show the Kanarra anticline near Kanarraville, Utah, to be an asymmetric, overturned anticline, with imbricate thrust splays merging into a high-level detachment fault that soles along the base of the Permian Kaibab Formation (see figure 6, p. 201, in Nowir and Grant, 1995). Older flank thrusts are shown on both limbs of the fold; the flank thrust on the overturned eastern limb corresponds to the Taylor Creek thrust system of Kurie (1966) who interpreted it as a back thrust. The easternmost thrust fault is a “rollover-break-thrust,” a term assigned by Nowir and Grant (1995, p. 200), which displaced the overturned limb of the anticline to the east and is shown to have breached the surface. Several of these thrusts, including the rollover-break thrust, were inferred and necessary to produce a balanced cross section through the Kanarra anticline (Nowir and Grant, 1995). However, in their cross section the rollover-break thrust is shown to have simultaneously both normal and reverse separation along its length (see figure 6, p. 201, in Nowir and Grant, 1995). Previous geologic maps (e.g., Averitt, 1967) and subsequent geologic maps (e.g., Biek and Hayden, 2016) of the Kanarra anticline include the west-directed Taylor Creek thrust system but do not show the presence of a leading edge east-directed thrust. As a result, many publications show the Keystone-Muddy Mountain-Square Top Mountain-Iron Springs-Canyon Range thrusts as the leading edge of

the Sevier orogeny in southwestern Utah (e.g., see figure 66, p. 61, in Hintze, 2005).

Establishing the location of the leading edge of the Sevier fold-thrust belt in southwestern Utah is critical to linking the spatial and temporal advancement of the Sevier deformation front along its strike length and interpretation of its effect on foreland sedimentation. We report the results of new detailed geologic mapping and structural cross sections of the Kanarra anticline, near Kanarraville, Utah. Our work demonstrates that thrust faults and folding are inextricably linked in all stages of formation of the Kanarra anticline. Our geologic mapping identifies the previously speculated (i.e., Nowir and Grant, 1995 rollover-break thrust), but unsubstantiated leading edge thrust of the Sevier fold-thrust belt along the eastern overturned limb of this part of the Kanarra anticline—our Red Rock Trail thrust. Following Butler and others (2020), we propose the name Kanarra fold-thrust structure to unambiguously identify the close spatial and temporal association of folding and thrusting in formation of this prominent geologic feature. We characterize the complete profile of this fold-thrust structure, demonstrate regional continuity in tectonic style along its strike (e.g., The Red Hill), and identify the Kanarra fold-thrust structure as the leading edge of the Sevier fold-thrust belt in southwestern Utah during the Late Cretaceous.

STRUCTURAL SETTING

In southwestern Utah, the Colorado Plateau Province consists of a set of high plateaus that are dissected by three large north-trending normal fault systems. These fault systems are 100s of kilometers long of which some continue southward into Arizona and the Grand Canyon region. They form a series of structural blocks that step down to the west towards the Basin and Range Province defining the Basin and Range-Colorado Plateau transition zone (figure 1). From east to west, these transition zone normal faults are the Paunsaugant, Sevier-Toroweap, and Hurricane fault systems (Biek and others, 2015). The Markagunt Plateau is the westernmost of the High Plateaus. The Hurricane Cliffs and Hurricane fault lie just east of the Cordilleran hingeline and mark the western edge of the Markagunt Plateau

and the Basin and Range transition zone (figure 1).

Cropping out along the Hurricane Cliffs, between St. George and Cedar City, are upper Paleozoic to Upper Cretaceous sediments that have been uplifted, dissected, and are now well exposed in the rugged topography of the footwall of the Hurricane fault. Stratigraphic separation on the Hurricane fault is estimated to be up to 2500 m just north of St. George near Toquerville (Stewart and Taylor, 1996). North of St. George, from the town of Toquerville to Cedar City, these strata were deformed into the Kanarra fold-thrust structure (i.e., the Kanarra fold of Gregory and Williams, 1947) during the Sevier orogeny (plate 1; figure 1). Here the eastern limb of the Kanarra fold-thrust structure trends north-northeast for over 50 km and is well exposed along its length in several across-strike canyons incised into the footwall of the Hurricane fault (Gregory and Williams, 1947; Averitt, 1962; Biek, 2007a). Part of the anticline of the fold-thrust structure has been displaced downward along with the hanging wall of the Hurricane fault and is buried beneath Neogene to Holocene sediments and volcanics in the Cedar Valley graben (plate 1). Beginning at Shurtz Creek, the anticline of the Kanarra fold-thrust structure (i.e., the Shurtz Creek anticline of Averitt, 1962) plunges northwards and a part of a fold closure is preserved near Cedar City in the vicinity of The Red Hill (i.e., the Squaw Creek anticline of Hintze, 2005, p. 175). The fold is likely a doubly plunging anticline (i.e., a pericline); however, the presumed southern closure of the fold has been sheared away along the Hurricane fault near Toquerville (plate 1). Plates 1, 2A, 2B, and 3, and the supplemental files can be found at https://scholarsmine.mst.edu/geosci_geo_peteng_facwork/2025/.

Near Kanarraville, the approximate center of the fold-thrust structure, exposed strata preserve significant structural complexity in terms of folding and faulting (e.g., see Nowir and Grant, 1995; Biek and Hayden, 2016). Here, bedding abruptly overturns along a 10-km section of the fold-thrust structure and is displaced and repeated along multiple faults. Understanding the spatial and temporal evolution of this part of the Kanarra fold-thrust structure through detailed geologic mapping is critical to resolving its tectonic significance to the evolution of the Sevier orogeny in southwestern Utah. Our detailed 1:110,000-scale structural map of

the Kanarra fold-thrust structure and our 1:15,000 geologic map of the central part of the Kanarra fold-thrust structure are presented on plates 1 and 2A, respectively, and the stratigraphic column on plate 2B.

STRATIGRAPHIC SETTING

Deposition of Paleozoic miogeoclinal sediments along the passive margin of the western coast of Laurentia was strongly controlled by subsidence from post-rift lithospheric cooling and structural lineaments formed during rifting. During this time, cyclical deposition generated a zone of westward-thickening marine-marginal marine strata beginning at the craton edge, known as the Cordilleran hingeline (Kay, 1951; Stokes, 1976; Picha and Gibson, 1985; Wernicke and others, 1988). Thick packages of competent strata—locally including the Middle and Upper Cambrian Bonanza King Formation, Upper Cambrian Nopah Dolomite, Mississippian Redwall Limestone, and Permian Queantoweap Sandstone—were deposited on top of the Lower Cambrian Tapeats Sandstone and Lower and Middle Cambrian Bright Angel Shale during this period (Hintze, 1986, 2005; Hurlow and Biek, 2003). Whereas these competent units are unexposed in the map area, their presence in the subsurface and contribution to the mechanical response of the stratigraphic package are important to the development of the Kanarra fold-thrust structure. The response of Paleoproterozoic rocks in this area during Sevier contraction appears to be limited to reactivation of basement structures or “structural inheritance” leading to formation of local promontories and reentrants along the Kanarra fold-thrust structure as discussed in later sections. The ages, names, rock type, thicknesses, and patterns of formations cropping out in the map area, or included in the cross sections, are shown on plate 2B and are available in the supplementary data repository.

Towards the end of the Permian, basin conditions began to change significantly (Hintze, 1986, 2005; Biek and others, 2009). A dwindling pattern of shorter and shorter cycles, marked by thinner strata, followed deposition of the Queantoweap Sandstone. During the beginning of the Triassic, base level fell, and an unconformity (i.e., the TR-1 unconformity) surface developed

on exposed, previously deposited marine sediments (Pipiringos and O’Sullivan, 1978). The absence of the incompetent Harrisburg Member of the Permian Kaibab Formation marks the presence of this major unconformity (Hintze, 1986). In the field area, the Rock Canyon Conglomerate or the Timpoweap Members of the Lower Triassic Moenkopi Formation rests unconformably on either the Harrisburg or Fossil Mountain Members of the Kaibab Formation as discussed in later sections. Following the Rock Canyon Conglomerate, the final cycles of the passive margin sequence deposition are recorded in the Moenkopi Formation. Higher frequency, relatively short-lived cycles led to deposition of relatively thin (e.g., meters), competent limestones and sandstones interbedded with thicker (e.g., tens of meters), incompetent mudstones and siltstones (see figures 3A and 3B, p. 152, in Hofmann and others, 2013). The thicker incompetent packages of rock are also known as the Triassic red beds: lower red member, middle red member, Shnabkaib Member, and upper red member of the Moenkopi Formation. The major competent layers within this package are found in the Timpoweap and Virgin Limestone Members, though both primarily consist of incompetent siltstone and shale as discussed in later sections.

A switch to terrestrial (i.e., fluvial and lacustrine) conditions beginning in the Late Triassic and into the Early Jurassic, led to deposition of thin, competent layers of sandstone and conglomerate interbedded within relatively thicker layers of mudstone and siltstone (Biek and others, 2009). Significant thin (meters to tens of meters), competent strata within this package include the Shinarump Conglomerate Member of the Upper Triassic Chinle Formation, the Dinosaur Canyon Member of the Upper Triassic-Lower Jurassic Moenave Formation, the Springdale Sandstone Member of the Lower Jurassic Kayenta Formation, and the Shurtz Tongue of the Lower Jurassic Navajo Sandstone (plate 2B). This package is capped by the last thick (hundreds of meters), competent layer deposited in the stratigraphic section, the Navajo Sandstone.

Unconformably overlying the Navajo Sandstone are the Middle Jurassic Temple Cap and Carmel Formations, which consist of interbedded competent layers of limestone and/or sandstone and incompetent layers

of mudstone and gypsum (Sprinkel and others, 2011; Knudsen, 2014a; Biek and Hayden, 2016). The upper part of the Carmel Formation was partially removed by erosion during the Cretaceous, and is unconformably overlain by the thin, dispersed orogenic Cedar Mountain Formation (Biek and others, 2009; Biek and Hayden, 2016). The sub-Cretaceous unconformity is capped everywhere on the plateau by the Cretaceous Naturita and Straight Cliffs Formations. In the map area, the Jurassic Carmel Formation and Cretaceous strata crop out as gentle, vegetated slope formers and sub-horizontal ledges at the top of the Hurricane Cliffs. The incompetent pink member of the Claron Formation unconformably overlies the Navajo Sandstone in the North Hills indicating considerable erosional beveling of Mesozoic strata before or during the Paleogene (plate 2B; Biek and Hayden, 2016). This unconformity has temporal significance as it constrains the timing of deformation associated with development of the Kanarra fold-thrust structure during the Sevier orogeny as discussed in a later section.

METHODS

Geologic Maps

Boots-on-the-ground geologic mapping using traditional techniques that included topographic base maps, aerial imagery, geologic compasses, GPS units, and field notebooks was conducted during the summers of 2016 to 2019. Approximately 2000 in-person field observations were collected—including structural orientation measurements—and used to construct the geologic maps (plates 2A and 3). The orientation of all planar features (e.g., bedding, faults, etc.) is reported using the following format – the three digits for the azimuth of the strike is reported first followed by the two digits for the angle of the dip. The orientation of all linear features (e.g., slicken line, mineral lineation, etc.) is reported using the following format—the two digits for the angle of the plunge is reported first followed by the three digits for the azimuth of the trend. For example, a fault plane (040, 65) contains slicken lines (63, 038) and mineral accretion steps (e.g., chatter marks) indicating normal-slip. Field data were backed up in real time with FieldMove (from 2017 to 2018; Muir, 2015) and StraboSpot (Walker and others,

2019). Across-strike and along-strike traverses at Camp Creek, Spring Creek, Kanarra Creek, Short Creek, Murrie Creek, and along Kanarra Mountain Road (plate 2A) were completed to efficiently cover ground. The location of all contacts mapped in person (particularly difficult and concealed contacts) were refined using a combination of Geologic Map Data Extractor (GMDE) (Allmendinger, 2020), Google Earth, and LIDAR data collected in 2020 by the Utah Geospatial Resource Center and the Utah Division of Emergency Management. In addition, we also used 107 strike and dip measurements extracted from previous geologic maps (Averitt, 1962, 1967; Biek and Hayden, 2016). Using our geologic map, aerial imagery, Digital Elevation Models (DEM), and GMDE (Allmendinger, 2020) we constrained unit thickness, three-dimensional projections of geologic contacts (e.g., faults), and axial traces at a regional scale (as opposed to outcrop scale) for the 1:15,000-scale geologic map and 1:10,000-scale structural map (plates 2A and 3, respectively). This allowed us to test structural interpretations in three-dimensions, thus removing ambiguity inherent in two-dimensional interpretations based upon separation (e.g., Davis and others, 2011, p. 275). The 1:110,000-scale map of the Kanarra fold-thrust structure (plate 1) was compiled from our field mapping, previous 7.5-minute quadrangles (Averitt, 1962, 1967; Averitt and Threet, 1973; Hurlow and Biek, 2003; Biek 2007a, 2007b; Knudsen, 2014a, 2014b; Biek and Hayden, 2016), and three 30' x 60' quadrangles (Rowley and others, 2006; Biek and others, 2009, 2015). Solely for the purpose of emphasizing structural relationships pertinent to the Kanarra fold-thrust structure, we choose to show on the map the lower red member, middle red member, and upper red member using the same color scheme, as well as including the Temple Cap Formation in with the Carmel Formation and displaying the Upper Cretaceous formations with one color (plates 2A, 2B, and 3). We do not attach, nor imply, any stratigraphic significance to these groupings; they are strictly for illustrative purposes such that the structures in the map area are readily visible in the figures. Each map plate was compiled in ArcMap 10.8.1 and finalized using Adobe Illustrator. The information used to construct the geologic maps presented in plates 2A and 3, are available in data repository files.

Geologic Cross Sections

The geologic cross sections are constructed using our geologic map (plate 2A), published unit thicknesses, and unit thicknesses based upon our current mapping, and using GMDE (Allmendinger, 2020) and the Move™ software by Petroleum Experts (see Supplemental Data Tables A1 and A2). We invoke “Pumpelly’s rule,” which states that small-scale structures mimic the style and orientation of larger structures of the same episode of deformation in the same area (Pumpelly and others, 1894). Thus, establishing the geometrical forms of the folded rocks is an essential step in constructing the cross section. The Kanarra fold-thrust structure includes inextricably related buckle folds, forced folds, a regional detachment fault, and early- and late-forming fold accommodation faults (e.g., Mitra, 2002a). These geometrical fold styles are well exposed and well developed within the Timpoweap Member of the Moenkopi Formation and the Fossil Mountain Member of the Kaibab Formation (plates 2A and 3; figure 2) and are also observed in several other units as well. The fold shapes and position of fold accommodation faults (e.g., Cloos, 1961, 1964; Mitra, 2002a) within the layering suggest a component of buckling before faulting. Each fold is comprised of smooth-hinged “kinks” formed by kink panels of varying size and number (figure 2; Fail, 1973; also see p. 138–150 and figure 61, p. 143, in Fail and Wells, 1974).

Map-scale views of folded layers (plates 1, 2A, and 3) show smooth-hinged kinks in the field (figure 2). The southern cliff face at the mouth of Spring Creek hosts a large, outcrop-scale composite fold-thrust structure and buckle fold train immediately above the west-verging thrust within the Fossil Mountain Member (figure 2A). At the western end of this fold train is a break-thrust fold (figure 2A; also see plate 33, p. 228, in Willis, 1893; Fischer and others, 1992). This family of folds and faults (cf., Dahlstrom, 1969) mimics the structural style of the Kanarra fold-thrust structure (see Pumpelly and others, 1894). Thus, we employed the kinked, parallel fold break-thrust model in construction of all our cross sections to reflect the geometrical style of folding and faulting observed in the field. The cross sections are based upon our geologic mapping (this study and unpublished

geologic mapping) and where noted utilize data from the geologic maps of Averitt and Threet (1973) and Knudsen (2014a).

Shear Fracture Measurements

Shear fracture sets occur within competent strata along the Kanarra fold-thrust structure. They are found along the mapped traces of major fold accommodation faults. Elsewhere, these shear fractures are commonly mesoscale or outcrop-scale faults. For clarity, we restrict the term fault to hundreds of meter-scale structures and shear fracture to meter-scale structures. For each shear fracture, the strike, dip, and rake of slickenlines are measured and recorded. Rakes are measured down from right-hand rule strike directions along the fracture plane, and slip sense is interpreted separately. Slip sense is interpreted from R-type and P-type fracture steps (common in sandstones) or mineral fibers (common in carbonates) on the fracture surface (Petit, 1987; Allmendinger and others, 1989). The slip sense is also constrained, where possible, by offset of marker beds, drag folds, and oblique exposures of shear fracture sets. These shear fractures are analyzed using FaultKin and Stereonet (Marrett and Allmendinger, 1990; Allmendinger and others, 2013; Cardozo and Allmendinger, 2013) to produce a fault plane solution, which can be used to estimate the aggregate, map-scale orientation and slip sense of the fault plane at several locations on the fold limb. Using the average bedding orientation at each shear fracture set location, we rotate the fault plane solutions model so that local bedding fits the average orientation of bedding at Camp Creek where the fold is upright and open. This allows for direct comparison of fault plane solutions along the length of the fold. We undertake these analyses primarily to document the presence and deformation history of early formed thrusts as the fold evolves from a gentle, open fold in the southern part of the map area to a steep, tight, overturned fold in the northern part of the map area. This serves as an approximate temporal progression of structural development and strain accumulation during folding.

RESULTS

The results of our field investigations are presented

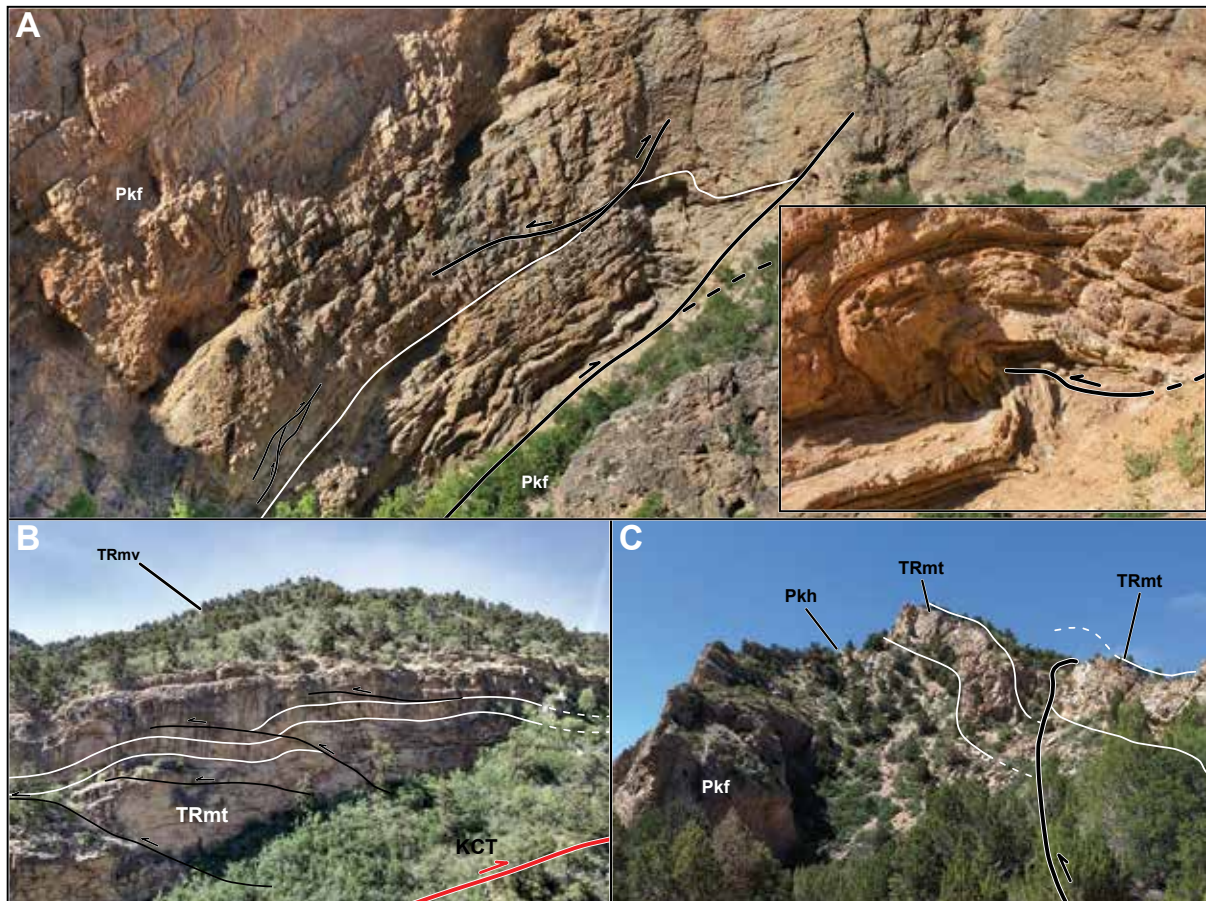


Figure 2. (A) View south on a composite fold-thrust structure within the Fossil Mountain Member of the Kaibab Formation in the core of the leading anticline. Inset: Close-up of the “leading” fold, a fractal model of the Kanarra fold. (B) View south above the entrance to Camp Creek. Folds within the lower ledge-forming unit of the Timpoweap Member of the Moenkopi Formation, cut by later, antithetic thrusts in the hanging wall of the Kanarra Creek thrust. (C) View north onto the leading anticline of the Kanarra fold-thrust structure from the Spring Creek Canyon trail. Here, the lower ledge-forming unit in the Timpoweap is duplicated along an early formed thrust—this may be a piece of the discontinuous Kanarra Creek thrust exposed to the north and south. Structure initializations: Kanarra Creek thrust—KCT. See plate 2B (stratigraphic column) for explanation of map unit symbols.

as (1) a 1:110,000 bedrock geologic map of the Kanarra fold-thrust structure (plate 1), (2) a 1:15,000 geologic map emphasizing the bedrock geology and structure of the central part of the Kanarra fold-thrust structure (plate 2A), (3) a geologic cross section through the central part of the 1:15,000 geologic map of the Kanarra fold-thrust structure, and (4) a 1:10,000 geologic map emphasizing faults, fold axes, field photo locations, and fault plane solutions along the central part of the Kanarra fold-thrust structure (plate 3). In the following sections we expand upon significant details of the results of our geologic mapping as applied to specific topics related to the stratigraphy and structures present in this

region as they relate to defining the Kanarra fold-thrust structure.

Distinguishing the Timpoweap Member from the Virgin Limestone Member of the Moenkopi Formation

Stratigraphic nomenclatural changes have been suggested for several Mesozoic and Cenozoic units in the map area within the past two decades (e.g., Lucas and Tanner, 2006; Lucas and others, 2007; Hautmann and others, 2013; Hofmann and others, 2013, 2014; Carpenter, 2014). Some have been accepted, but not all

suggested changes are reflected in current maps. For this reason, we adopted the convention of using member and formation names based upon recent local mapping (e.g., Knudsen, 2014a, 2014b; Biek and Hayden, 2016). Nevertheless, the detailed characteristics of certain units—particularly the Timpoweap and Virgin Limestone Members of the Moenkopi Formation—are critical to unravelling the complex structural relationships along the eastern limb of the Kanarra fold-thrust structure, especially the relative timing of early- versus late-forming thrust faults in the development of the Kanarra fold-thrust structure.

In southwestern Utah, the Timpoweap and Virgin Limestone Members of the Moenkopi Formation represent a series of intertonguing lithofacies (e.g., Lucas and others, 2007; Hofmann and others, 2013; figure 2 this paper). They record a cyclic stratigraphic pattern reflecting sequential transgressions and regressions along the Cordilleran hingeline during the Lower Triassic. The shallow-marine and sabkha units generally represent transgressive packages, which correlate to units elsewhere as part of the Thaynes Formation (or Thaynes Group) of northern Utah, whereas the red beds represent regressive packages (Lucas and others, 2007). The shallow-marine lithosomes, particularly the Timpoweap and the Virgin Limestone Members, have similar lithologies and fossil distributions. This can make them difficult to distinguish in the field, especially in complexly faulted areas where they are juxtaposed and overturned. For accurate discernment between the Timpoweap and Virgin Limestone Members, careful consideration must be given to their topographic expression (i.e., “fingerprint”), distribution of lithologies, and characteristic local fossil assemblages.

Timpoweap Member

The topographic signature of the Timpoweap Member is distinct from that of the Virgin Limestone Member (plates 2A and 3). The unit can be divided approximately in half. The lower half forms a thick (over 20 m) ledge, whereas the upper half forms a slope. The ledge is a thick-bedded, gray to pale yellow-orange to yellow-gray limestone (10YR 8/6 and 5Y 8/4, see Munsell Color, 2009), whereas the slope former is an incompe-

tent, yellow micritic shale (plates 2A and 3; figure 3).

Where the Rock Canyon Conglomerate Member is present, the conglomeratic facies grades upward into the ledge-forming Timpoweap, so that the lowermost limestone beds may contain isolated, thin, pebble conglomerate lenses. Some limestone beds in the ledge forming Timpoweap are sand rich; others appear sandy on their weathered faces, particularly the light to medium gray (N6 to N7) to pale yellow-orange to yellow-gray beds, yet most of these are a crystalline limestone (see Dunham, 1962) as revealed by fresh surfaces. This contrasts markedly with thick, yellowish-orange, yellowish-brown, and moderate yellow-gray (10YR 6/6, 10YR 5/4, and 5Y 7/6) quartz arenite beds in the Virgin Limestone. The upper slope-forming part of the Timpoweap includes thin, discontinuous, dark-brown, sand-bearing limestone. Locally, the top of the yellow micritic shale unit can abruptly darken to a deep purple-gray before the contact with the overlying lower red member (figure 4). This purple-gray (5P 6/2 to 5P 4/2) layer is distinctly part of the Timpoweap Member (cf., Lucas and others, 2007, p. 111), but it is not always present in the Timpoweap, particularly at thrust contacts. However, where present, it can lead to a misidentification between the Timpoweap and Virgin Limestone Members because it resembles the purple mudstone beds within the Virgin.

Fossils in the Timpoweap Member are scarce, particularly in comparison to the abundant fossiliferous Virgin Limestone Member. The fossil assemblages of the Timpoweap and the Virgin Limestone contain genera that are common to both members. However, there are key fossils intrinsic to the Timpoweap that distinguish it from the Virgin Limestone assemblage (Lucas and others, 2007; figure 5 this paper). A characteristic Timpoweap fossil includes the ammonite *Wasatchites* (figures 5A and 5C), which is exclusive to the Timpoweap Member; however, it is also rare and typically poorly preserved. The discovery of *Wasatchites* (figure 5C) on the ridge north of Kanarra Creek confirms this unit as the Timpoweap Member (see plate 3 for location).

Virgin Limestone Member

The most distinct map- to outcrop-scale characteristic of the Virgin Limestone is its topographic signa-

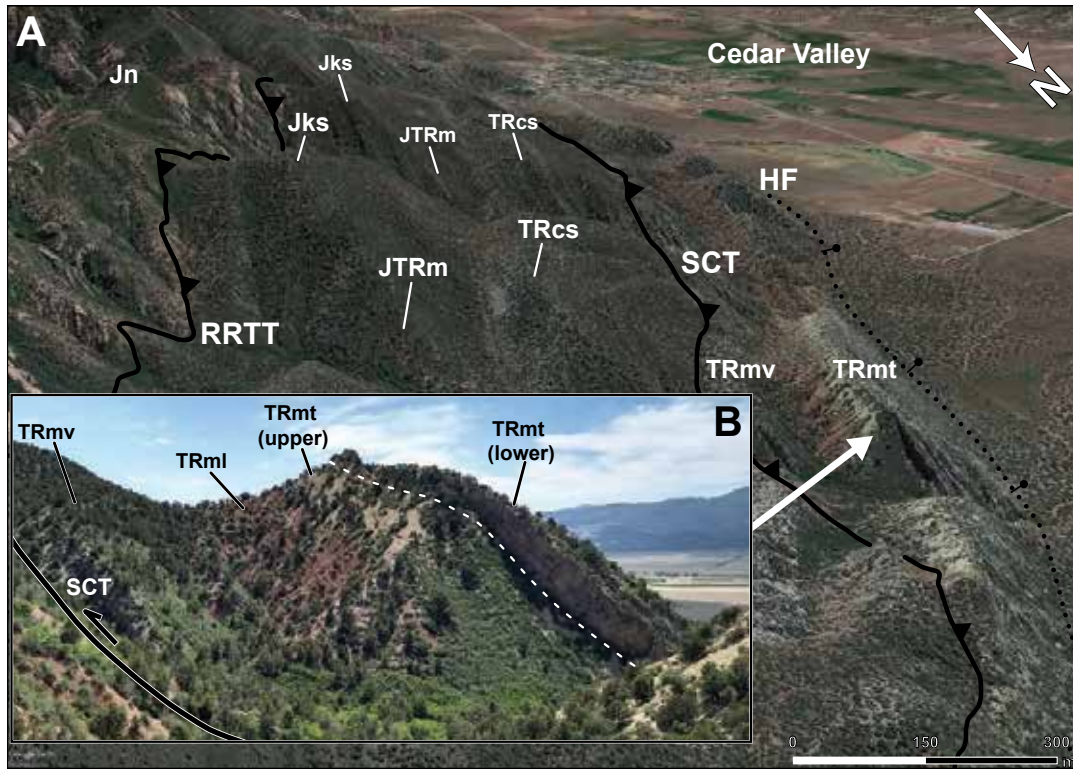


Figure 3. (A) Google Earth 3D terrain view of the overturned stratigraphy along the Kanarra fold limb, looking southwest into Short Creek. The Spring Creek and Red Rock Trail thrusts are included to orient the reader to the map. Here, the Timpoweap Member forms the first of several ridges rising above Cedar Valley. The ledge-forming gray to yellow lower limestone unit holds up the ridge, with the yellow calcareous shale upper unit outcropping beneath. (B) Field photograph of the same view, looking farther westward onto the ridge of Timpoweap Member of the Moenkopi Formation. The dashed white line marks the transition into the upper yellow shale unit. Near the contact with the lower red member, the shale grades vertically into a deep purple-gray color. Structure initializations: HF–Hurricane fault; SCT–Spring Creek thrust; RRTT–Red Rock Trail thrust. See plate 2B (stratigraphic column) for explanation of map unit symbols.

ture (figure 4). Within the field area, the Virgin Limestone is dominantly composed of sandstone, siltstone or mudstone, and minor limestone, with the incompetent strata comprising over two-thirds of the total thickness. Where depositional contacts are preserved, the top of the Virgin Limestone is marked by a sharp transition into a double layer of gypsum at the base of the middle red member. The Virgin Limestone consists of several thin, competent, resistant fins set within a much thicker (tens of meters) interval of incompetent mudstone and siltstone. The fins are gray (N7 to N5), medium to very thick bedded packstone and wackestone or tan (10YR 6/6 to 10YR 5/4 on weathered faces, and 5Y 7/6 on fresh faces) fine-grained quartz arenite. Locally, a fin can contain both lithologies separated by a sharp contact between sandstone and limestone. The fins are typically 1

to 4 m thick, although fins up to 8 m thick are reported (see Knudsen, 2014a). Where the fins are steeply dipping, they stand high above the intervening incompetent strata (figure 4B). The incompetent intervals contain mudstone and siltstone, typically varying in color from gray (N7 to N5) to brown (5YR 4/4) and locally purple (5P 6/2 to 5P 4/2).

The Virgin Limestone Member is also distinguished from the Timpoweap Member by the abundance of fossils and the presence of the following key marker trace fossils and fossils: (1) the trace fossil *Thalassinoides* and two major body fossil types, (2) the brachiopod *Rhynchonella*, and (3) the crinoid *Holocrinus (smithi?)* (figure 6). The trace fossil *Thalassinoides* was found only within the Virgin Limestone, along the bottom of a very thick bedded, tan quartz arenite ledge, which commonly

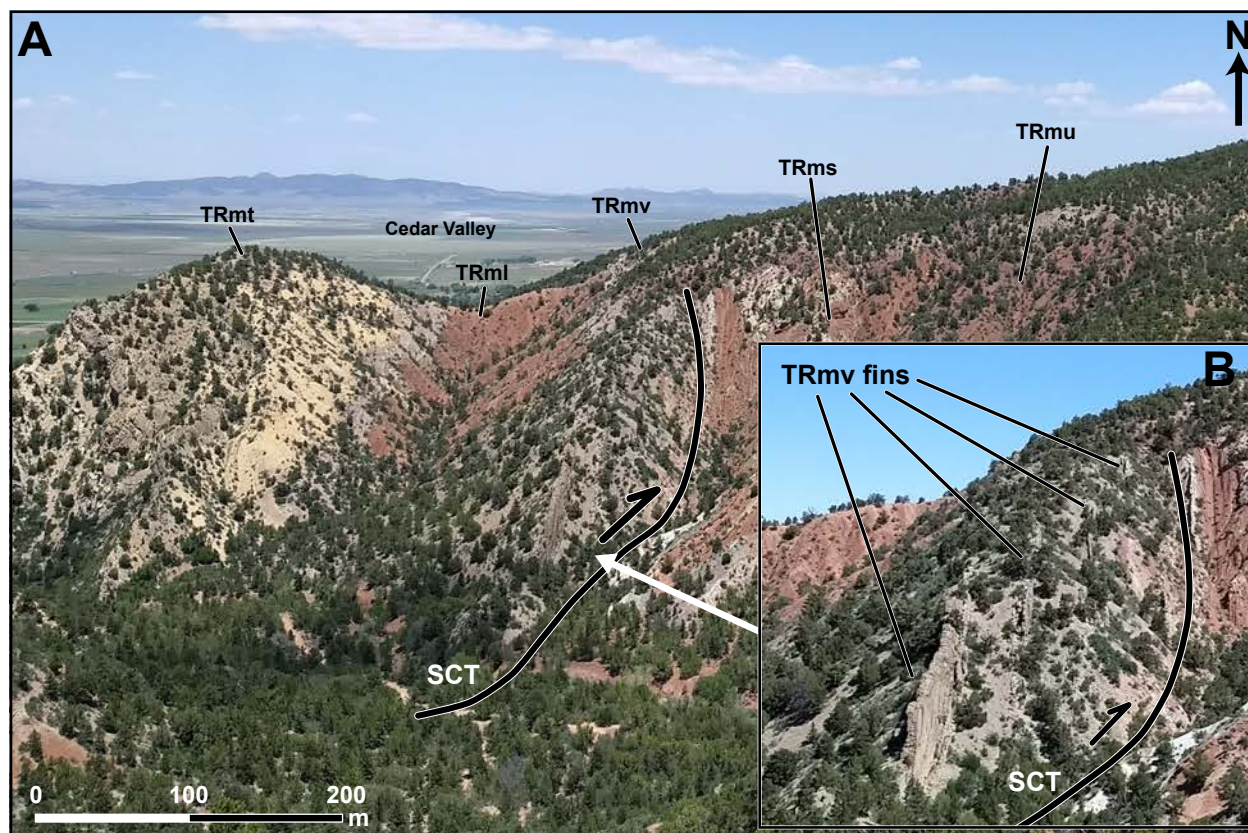


Figure 4. (A) Field photograph view of the lower units in the exposed stratigraphic section—primarily Moenkopi Formation—looking north across Spring Creek. The leading anticline hinge of the Kanarra fold forms the hill to the west. The western hilltop is capped by the Timpoweap Member of the Moenkopi Formation—yellow shale underlain by the gray-yellow ledge forming lower unit. The yellow shale grades into the deep purple-gray mudstone near the contact with the lower red member of the Moenkopi. Looking east across a saddle of lower red member, vertical to overturned gray limestone and tan sandstone fins interbedded with gray-purple mudstone form a ridge of the Virgin Limestone Member of the Moenkopi. The Virgin Limestone ridge is displaced by the Spring Creek thrust, truncating the middle red member of the Moenkopi. Inset (B) emphasizes the alternating competent fins and mudstone in the Virgin Limestone. Structure initializations: SCT—Spring Creek thrust. See plate 2B (stratigraphic column) for explanation of map unit symbols.

outcrops near the top of the unit (figure 6A). The trace fossil is preserved as interweaving casts of tunnels with triple junctions and is interpreted as *Thalassinoides* (cf., see figure 16A, p. 166, in Hofmann and others, 2013); this trace fossil was found at Kanarra Creek where the Virgin Limestone Member is overturned. In addition, the brachiopod *Rhynchonella* is common only to the Virgin Limestone (figure 6C), where it is restricted to the limestone layers. The brachiopod is most like *Rhynchonella* from the Thaynes Formation of southeastern Idaho (see plate 1, p. 311–312, in Perry and Chatterton, 1979); however, its size and plications also resemble *Piarorhynchella* (cf., figure 9C1, p. 161, in Hofmann and others, 2013) and *Lissorhynchia* (Wang and others,

2017). The brachiopods commonly form thin shell beds, and complete, individual shell fossils can be found near outcrops where they weather out of the limestone fins (figure 6C). They are small, with their long axes typically less than 2 cm long, and contain rounded, relatively wide, plications, which greatly increase in amplitude at the shell midpoint (figure 6C, inset).

The crinoid *Holocrinus (smithi?)* was found exclusively in the limestone or sandstone layers of the Virgin Limestone Member as scattered stem plates (figure 6; cf., figure 3c, p. 101, in Schubert and others, 1992). We observed two forms of crinoid stem plates. One has more rounded corners, straighter sides, and more closely resembles a pentagon (figure 6B), whereas the other



Figure 5. Fossils used in the field to distinguish the Timpoweap Member of the Moenkopi Formation. Ammonites of differing levels of preservation—this fossil type was scarce and poorly preserved in the field area. (A) The ammonite specimen appears to be *Anasibirites* and is entirely replaced by calcite. (B) The ammonite specimen appears to be *Wasatchites* identified from the shell decorations and size (cf., figure 5, p. 115, in Lucas and others, 2007), although the level of preservation makes interpretation difficult. This specimen was found in a sandstone bed along the ridge capped by the Timpoweap Member north of Kanarra Creek. (C and D) Specimens of *Eumorphotis* (cf., figure 6, p. 161, in Hautmann and others, 2013; figure 11, p. 562, in Hofmann and others, 2014), a bivalve genus dominantly found in the Timpoweap Member in the field area. Ammonites are known to occur in the Virgin Limestone Member (Hofmann and others, 2011), but none were found in the Kanarraville area.

resembles a five-sided star (figure 6D). The crinoid *Holocrinus* is entirely unique to the Virgin Limestone and, along with the brachiopods, were used as marker fossils.

DESCRIPTION OF THE KANARRA FOLD-THRUST STRUCTURE

The complexity of structural elements, folds, and faults of the Kanarra fold-thrust structure reflects the



Figure 6. Trace fossil and fossils used in the field to distinguish (identify) the Virgin Limestone Member of the Moenkopi Formation. (A) Interweaving bioturbations reminiscent of trace fossil *Thalassinoides* found as casts on the bottom of an overturned, thick-bedded sandstone ledge capping the southern ridge near the entrance to Kanarra Creek. (B) *Holocrinus* in gray limestone of the Virgin Limestone just north of Spring Creek. (C) Brachiopod shell bed and well-preserved specimen (inset) found at Kanarra Creek. These are similar to *Lissorhynchia* or the *Rhynchonella* species found elsewhere in the Thaynes Formation but were not found outside the Virgin Limestone in the Kanarraville area. (D) *Holocrinus* within tan, fine-grained sandstone in the Virgin Limestone.

protracted, multi-phase geologic history of an area that straddles several major long-lived lithospheric boundaries: (1) the Cordilleran hingeline, (2) the leading edge of the Sevier fold-thrust belt, and (3) the boundary between the Basin and Range Province and the Colorado Plateau Province (figure 1). Resolving the tectonic significance of the Kanarra fold-thrust structure in the context of this extended geologic history requires understanding the inextricable temporal and spatial re-

relationship of contractional faults (i.e., thrusts) to the development of the Kanarra fold-thrust structure. Due to the abundance of faults associated with the Kanarra fold-thrust structure, we have assigned names to the major faults and their splays, or closely associated faults, for clarity (tables 1 and 2).

The relationship of folding and faulting is well preserved in the central part of the Kanarra fold-thrust structure (plate 1) and is best understood using the detailed geologic map of this area (plates 2A and 3) and a structural cross section through the Kanarra fold-thrust structure prior to its dismemberment by the Hurricane fault during Basin and Range extension (figure 7). This cross section shows the full profile of the restored Kanarra fold-thrust structure at the time of the Sevier orogeny—prior to the western trailing limb of the Kanarra anticline being severed and buried, along with the hanging wall of the Hurricane fault in Cedar Valley, beneath a thick mantle of alluvium shed off the Hurricane Cliffs (plates 1 and 2A). The compound nature of the Kanarra anticline is readily discernible in the cross section (figure 7). The central part of the compound Kanarra anticline is defined by a broad sub-horizontal hinge zone that connects two anticlines. We refer to the anticline on the eastern half as the leading anticline, and the anticline on the western half as the trailing anticline. These terms reflect the spatial position of these folds within the Kanarra anticline and are introduced for clarity in the **Discussion** section (figure 7).

The Kanarra Anticline

The Kanarra anticline is an asymmetric, east verging, overturned anticline with a compound geometric form (figure 7). The fold form has many of the characteristics of idealized fault propagation folds that develop in the hanging wall of blind thrust faults (e.g., Mitra, 2002b; Davis and others, 2011, p. 414–428). The anticline is defined by a long, shallow west-dipping trailing limb, a relatively flat hinge zone, and a shorter leading limb that is steeply dipping west and overturned. The overturned leading antichinal limb verges eastward and transitions into a tight, east-verging syncline.

Field exposure of sparse, isolated remnants of the hinge zone along the strike of the leading anticline of

the Kanarra anticline (see figures 2A inset and 2C) exhibit a kink style geometry of folding. In cross section, the Kanarra anticline-syncline pair can be represented with a series of kink panels (figure 7); collectively these kink panels contribute to defining the overall form of the anticline and the syncline. However, the leading anticline hinge zone also has an overall rounded form, which is characteristic of buckle folds. Buckling (Willis, 1893; Fischer and others, 1992) may have contributed to the initial stages of folding of these strata.

The trailing limb of the Kanarra anticline includes an early fold accommodation fault, which has merged with the later, exposed Spring Creek thrust (figure 7; see later section for more detail). Displacement along the Spring Creek thrust forms a trailing or distal fault-bend fold (e.g., Davis and others, 2011, p. 409–413) in the hanging wall of the trailing limb of the Kanarra anticline. This fault-bend fold modifies the overall geometric form of the Kanarra anticline into a composite fold with a trailing anticline and a leading anticline (figure 7). The trailing and central part of the Kanarra anticline, along with the hanging wall of the Hurricane fault are buried beneath younger geologic units in Cedar Valley and their relationship to the Pintura anticline is presented in the **Discussion** section.

The axial trace of a fold, the line formed by the intersection of the axial surface of the fold with any other surface, occurs within the hinge zone of the fold (Davis and others, 2011). The hinge zone of the leading anticline, where shallow west-dipping strata rotate into the eastern leading limb of the anticline, is sparsely exposed (plate 1). The remnants of the hinge zone are used to define the discontinuous axial trace of the leading anticline axial surface along the length of the Kanarra fold-thrust structure (plate 1). Previously, the hinge zone of the leading anticline was interpreted as the hinge zone of the Kanarra anticline, and because of the discontinuous, dissected, nature of the leading anticline hinge zone along strike, was locally assigned other names (e.g., Hintze, 2005, Squaw Creek anticline, p. 175). In the central part of the Kanarra fold-thrust structure, there are three locations where the leading anticline hinge zone is well exposed: (1) Camp Creek, (2) Spring Creek, and (3) just south of Kanarra Creek (plates 2A and 3).

Table 1. Locations of faults on the Kanarra fold-thrust structure that outcrop in the Kanarraville area.

| Fault Name | Fault Type | Timing | Initials | Vrg.* | Locality | UTM (E) | UTM (N) |
|---------------------------------|-----------------------|---------------|------------------|-------|----------------|---------|---------|
| Kanarra Creek thrust | Limb wedge thrust | Early | KCT | W | Kanarra Creek | 308241 | 4157135 |
| Taylor Creek thrust | Limb wedge thrust | Early | TCT | W | Camp Creek | 307079 | 4152057 |
| Hicks Creek thrust | Limb wedge thrust | Early | HCT | W | Kanarra Creek | 308528 | 4156697 |
| Spring Creek thrust | Forelimb shear thrust | Late | SCT splay | E | Kanarra Creek | 308180 | 4157130 |
| primary splay | | | | | | | |
| Spring Creek thrust | Limb wedge thrust | Early-late** | SCT | E | Spring Creek | 307538 | 4154717 |
| main trace | | | | | | | |
| Murie Creek thrust ¹ | Forelimb shear thrust | Late | MCT ¹ | E | Spring Creek | 307900 | 4154058 |
| Murie Creek thrust ² | Forelimb shear thrust | Late | MCT ² | E | Murie Creek | 309957 | 4157749 |
| Red Rock Trail thrust | Forelimb shear thrust | Late | RRTT | E | Red Rock Trail | 308756 | 4155360 |
| Murie Creek fault | Oblique-slip (RL) | Early-late*** | MCF | RL | Murie Creek | 312353 | 4159903 |

* Vergence or displacement direction (cardinal)

** Initially an east-verging limb wedge thrust; late movement observed in the field cuts across leading anticline hinge and limb

*** Initial movement uncertain, but we suggest it is likely syn-folding

Table 2. Locations of faults on the Kanarra fold-thrust structure that outcrop at The Red Hill.

| Fault Name | Fault Type | Timing | Initials | Vrg.* | Locality | UTM (E) | UTM (N) |
|---------------------------------|-----------------------|--------------|----------|-------|---------------------------|---------|---------|
| Spring Creek thrust | Limb wedge thrust | Early-late | SCT | E | Stephens Canyon | 319059 | 4172923 |
| Stephens Canyon thrust (W) | Hinge wedge thrust | Early-late** | StCT(W) | W | Stephens Canyon | 319288 | 4172058 |
| Stephens Canyon thrust (E) | Limb wedge thrust | Early*** | StCT(E) | W | Stephens Canyon | 319288 | 4172058 |
| Hicks Creek thrust | Limb wedge thrust | Early | HCT | W | Hicks Creek | 319592 | 4172798 |
| Coal Creek thrusts | Hinge wedge thrust | Late | CCTS | NW | Coal Creek | 319470 | 4172283 |
| | | | | | Lone Tree Mtn. | | |
| Red Rock Trail thrust | Forelimb shear thrust | Late | RRTT | E | (W slope) | 320413 | 4170036 |
| Thunderbird Gardens Trail fault | Oblique-slip | Late | TGTF | LL | Thunderbird Gardens Trail | 319835 | 4173373 |

* Vergence or displacement direction (cardinal)

** Late movement observed by truncation of TRmm and indicated in cross section

Parallels strike of beds—likely began early and related to StCT(E)

*** Duplicates Shnabkaib Member roughly parallel to strike

Hinge Zone at Camp Creek

At Camp Creek, the leading anticline is upright and open. The axial trace is exposed in Lower Moenkopi units and the Fossil Mountain Member of the Kaibab Formation, which crop out in the canyon at the mouth of Camp Creek. Fault splays of the Hurricane fault cut the hinge zone near the creek mouth (figure 8A) and the axial trace is lost south of the creek where it has been

sheared away (plates 2A and 3). Within the canyon, a steep axial surface separates consistently westward dipping (about 10 to 15° W.) from east dipping (about 15° E.) bedding in limestone of the Fossil Mountain Member of the Kaibab Formation. Here, in the core of the hinge zone, multiple meter-scale kink panels in the limestone impart an open, gentle flexure best seen at the bottom of the canyon (figure 8B). The geometry of the leading anticline is reflected in the shape of the hinge

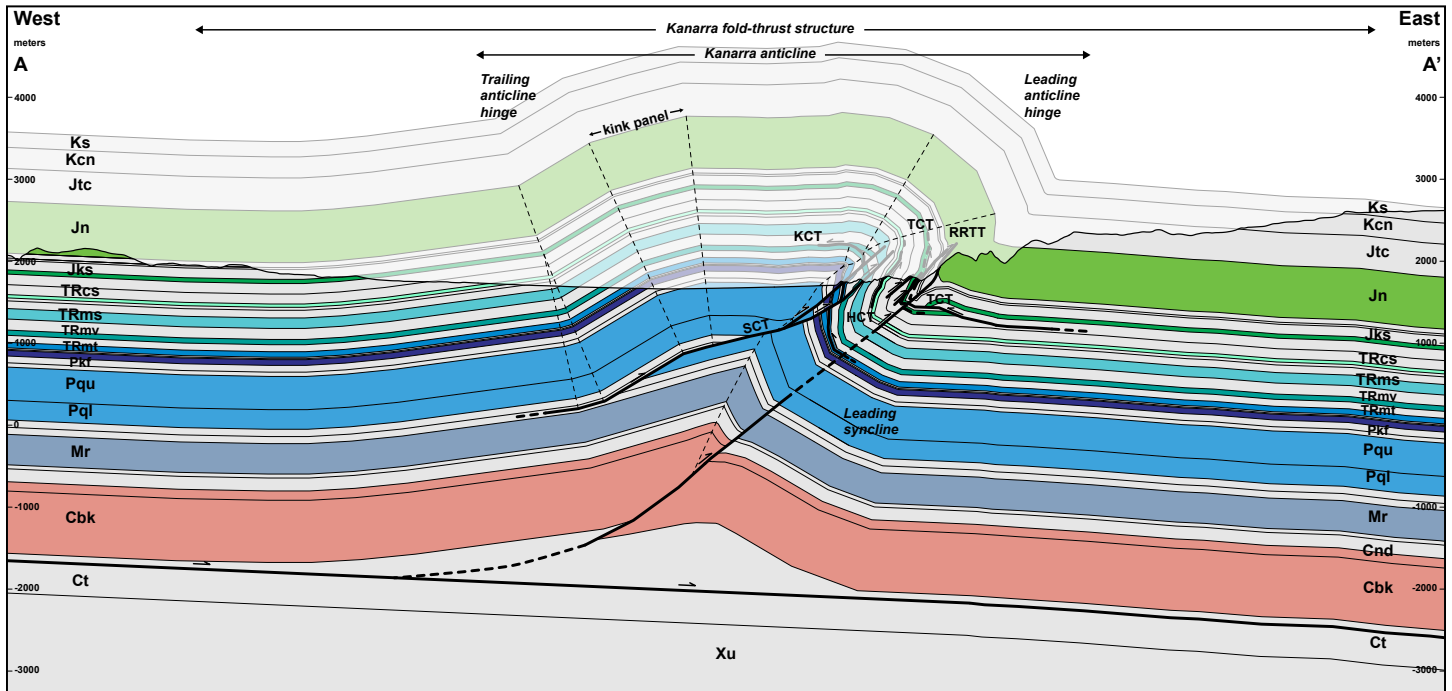


Figure 7. Cross section A–A' of the Kanarra fold-thrust structure at Kanarra Creek showing the restored Sevier structure circa 80 Ma, based on field mapping along Kanarra Creek. Kink axes and components of the hinge zone are annotated for reference. Eroded geology is faded out. The pre-extension trailing limb and fold crest are constrained by the tilted, sub-horizontal layering along the Hurricane Cliffs and the shape of the closely related Pintura anticline (Hurlow and Biek, 2003). No strata below the Fossil Mountain Member of the Kaibab Formation (Pkf) are exposed at the location of the cross section; unexposed layer thickness and presence are constrained by local data sources (Hintze, 1986; Van Kooten, 1988; Hurlow and Biek, 2003; Biek and others, 2009). Unexposed, thick, competent layers (Cbk–Cnd, Mr, Pq) are colored according to age; exposed ridge-former colors correspond to the map. Present-day topography is included to emphasize the ridge-formers. Structure west of the Hurricane Cliffs, within the present-day Cedar Valley graben, does not represent present-day bedrock geology. Structure initializations: SCT–Spring Creek thrust; KCT–Kanarra Creek thrust; HCT–Hicks Creek thrust; TCT–Taylor Creek thrust; RRTT–Red Rock Trail thrust. See plate 2B (stratigraphic column) for explanation of all map unit symbols. Line of section shown on plates 1 and 2.

zone, which is horizontal and open, with the enclosing strata forming an interlimb angle of about 150° (gentle).

Hinge Zone at Spring Creek

The axial trace within the hinge zone of the leading anticline is well exposed within a 60-m-high canyon wall at the mouth of Spring Creek. The cliff face exposes the Fossil Mountain Member of the Kaibab Formation capped by the Timpoweap Member of the Moenkopi Formation. The hinge zone, appearing rounded, tightens considerably between Camp Creek and Spring Creek. At Spring Creek, the interlimb angle is about 65° (close) and much tighter than the interlimb angle of 150° (gentle) at Camp Creek. Here, the

steep (about 80°), west-dipping axial surface roughly parallels the trace of the Hurricane fault. Farther east along Spring Creek, the transition from steeply dipping to overturned strata is readily shown by rotation of the primary bedding in the Kaibab Formation. In addition, steep, vertical, and overturned dips are recorded by the resistant “fins” in the Virgin Limestone Member of the Moenkopi Formation (figures 4 and 9; plates 2A and 3).

Hinge Zone near Kanarra Creek

Just north of Spring Creek, about 500 m from the transition to overturned bedding in the Timpoweap Member, the hinge zone of the leading anticline is truncated by the Hurricane fault (plate 2A). East of this



Figure 8. (A) Google Earth 3D terrain view with Landsat/Copernicus imagery of the Hurricane fault zone along the length of the exposed Kanarra fold-thrust structure in the study area. Splays of the Hurricane fault zone in the area are exposed here at Camp Creek. (B) Low-displacement normal faults within the eastward-diminishing Hurricane fault zone at the mouth of Camp Creek. (C) Larger-displacement normal faults; westernmost fault displaces the Timpoweap Member of the Moenkopi Formation next to the Kaibab Formation. Field assistant Dylan Webb is 1.72 m tall. Also shown is the Permian unconformity, here seen as Rock Canyon Conglomerate Member of the Moenkopi Formation over black-banded, chert-rich Kaibab Formation. Structure initializations: HF–Hurricane fault; KCT–Kanarra Creek thrust; TCT–Taylor Creek thrust. See plate 2B (stratigraphic column) for explanation of map unit symbols.

truncation, several thrust faults of the Spring Creek thrust system cut through the hinge zone (see the later discussion on faults). The largest splay of the Spring Creek thrust system displaces overturned Timpoweap Member onto shallow, west-dipping (about 8° W.), and presumably upright Virgin Limestone Member. A low topographic ridge underlain by the Virgin Limestone Member east of the thrust truncation hosts a closed (about 35° interlimb angle), gently inclined, overturned fold. On the east side of this topographic ridge, between Spring Creek and Kanarra Creek, part of the reclined fold nose is preserved (figure 9B), and the middle red

member double-gypsum layer is disharmonically folded into an “S-fold” on the eastern limb (307700 m E.; 4155810 m N.). Bedding taken west of the fold nose indicate a shallow-dipping (15 to 35° W.), upright western limb, whereas bedding on its steeper (60 to 75° W.) eastern limb is overturned.

The axial trace of this fold can be mapped northwards for nearly the entire length of the low Virgin Limestone Member ridge (about 1000 m) until it dies out at Kanarra Creek, likely cut by the Spring Creek thrust. A small, later thrust (also about 1000 m long), cuts through the western limb of this fold (plates 2A and 3, also see Aver-

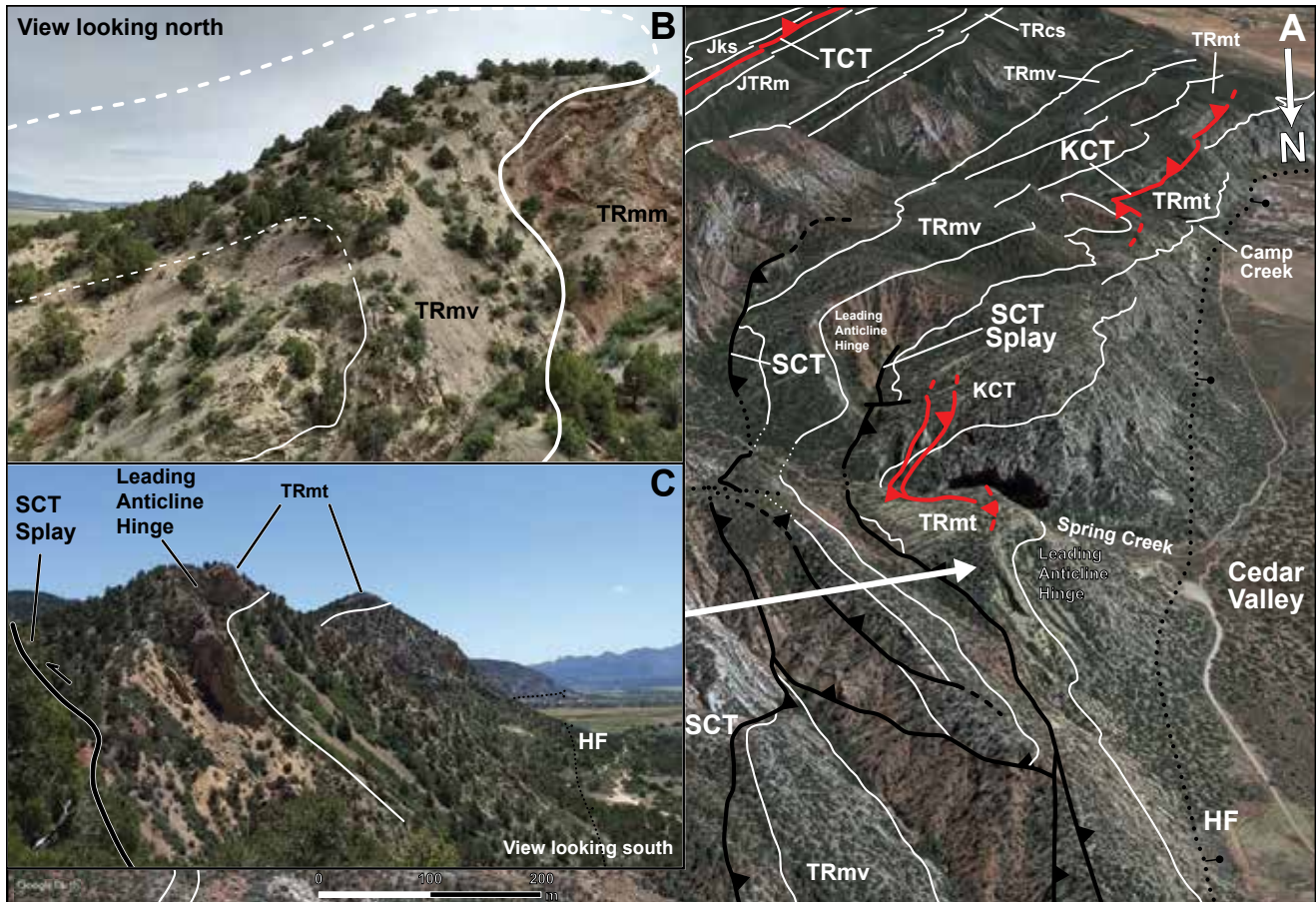


Figure 9. (A) Google Earth 3D terrain view with Landsat/Copernicus imagery looking south into Spring Creek where the Kanarra fold-thrust structure overturns. Selected faults and sedimentary contacts are shown for reference to the map. Part of the leading anticline hinge here is defined by the shape of folded Timpoweap and Virgin Limestone Members of the Moenkopi Formation and Kaibab Formation strata. (B) View to the north onto a tight, gently reclined closure on the leading anticline hinge within the Virgin Limestone Member just to the north of (A) and east of (C). (C) Field photograph looking south of upright (middle and background) and overturned (middle ground) Timpoweap, outlined by the white Harrisburg Member–Timpoweap Member contact. Structure initializations: HF–Hurricane fault; KCT–Kanarra Creek thrust; SCT–Spring Canyon thrust; TCT–Taylor Creek thrust. See plate 2B (stratigraphic column) for explanation of map unit symbols.

itt, 1967). This thrust likely formed to accommodate strain within the overtightened fold hinge. The entire structure is transported eastward along the main trace of the Spring Creek thrust just to the east of the ridge. We interpret the tightly folded Virgin Limestone here to be the northernmost remnant of the leading anticline hinge zone in the study area, cut and modified by transport along the Spring Creek thrust.

Contraction Faults

The Kanarra anticline-syncline pair is faulted along its length (plate 2A). The greatest density of faults crops

out in the central section where the eastern limb is overturned (plate 3). Typically, these faults (i.e., fault planes) are poorly exposed and inaccessible to direct observation. They are mappable through observations of truncation, folding, or attenuation of incompetent strata along competent ridge formers. Where possible, striated, stepped shear fracture sets within competent units were measured in the field to determine the aggregate sense of slip of the larger thrust surfaces (e.g., Petit, 1987; Marrett and Allmendinger, 1990). Most of these faults are contraction faults associated with the Sevier orogeny and the formation of the Kanarra fold-thrust structure.

Early Contraction Faults

Contraction faults associated with the Kanarra fold-thrust structure can be subdivided into early and late contraction faults relative to the evolution of the anticline-syncline pair from open and upright to tight, overturned, and asymmetric (tables 1 and 2). Early contraction faults include the Kanarra Creek, Taylor Creek, and Hicks Creek thrust faults. These early contraction faults all have the following attributes consistent with their inception as thrust faults at the earliest stages of folding: (1) the strike of these faults is typically sub-parallel to parallel to bedding (plates 2A and 3); (2) the map-scale patterns of the fault traces through the topography constrain the dips on these faults to be typically 10 to 25° steeper than dip of the bedding in their footwalls, consistent with early thrusts that are now folded (Cloos, 1961, p. 106); (3) ridge-forming units are commonly duplicated by these thrusts, doubling, or tripling the original thickness of these units; (4) statistical solutions of measurements of rake, displacement direction, and orientation of striated, stepped shear fracture populations along these duplications indicate thrust sense of slip (plate 3; table 3); and (5) asymmetric folds, while not always present, indicate displacement consistent with thrusting (e.g., figures 2 and 9). In the central section of the Kanarra anticline, several early formed contraction faults were folded and are overturned along with the eastern limb of the leading anticline—these faults can exhibit an apparent normal sense of displacement in the field (figure 7; plates 2A and 3).

These early thrusts occur at all scales, with the largest, the Taylor Creek thrust (Kurie, 1966; Biek, 2007a) being tens of kilometers long (plate 2A). Due to dismemberment of the Kanarra anticline by the Hurricane fault, these thrusts crop out only within the hinge zone of the leading anticline and the eastern limb of the Kanarra anticline. However, similar early contraction thrusts are present on the western limb of the closely associated Virgin anticline (e.g., at Leeds, Utah, to the southwest) and along its crest (Biek, 2003a, 2003b). Because these faults tend to form on the limbs (flanks) of folds, we refer to these early formed thrusts as flank thrusts (e.g., Grant, 1987), though they are known by other names (a type of fold accommodation fault or

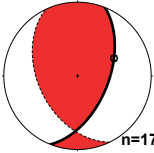
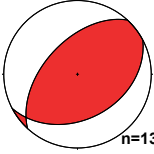
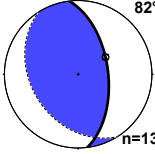
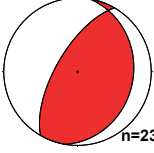
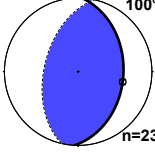
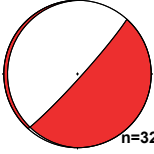
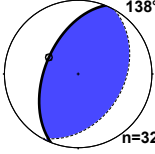
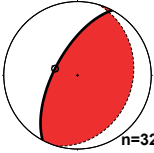
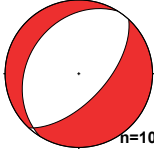
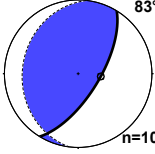
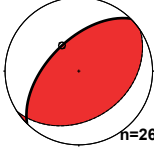
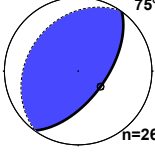
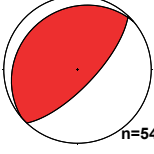
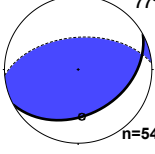
wedge faults (cf., Cloos, 1961; Fail and Wells, 1974; Mitra, 2002a). We infer that flank thrusts were also present on the trailing limb of the Kanarra anticline (i.e., the Spring Creek thrust) and their presence is supported by our mapping and structural cross section of the Kanarra fold-thrust structure (figure 7; plates 2A and 3). The significant flank thrusts within the central parts of the Kanarra fold-thrust structure are discussed in the following sections.

Kanarra Creek thrust: The Kanarra Creek thrust is the westernmost exposed thrust in the map area (plate 2A). It is commonly associated with repetition of stratigraphic units lower in the section, typically the Timpoweap and lower red members of the Moenkopi Formation and crops out close to the hinge zone of the leading anticline of the Kanarra anticline. We infer its trace is discontinuous along the length of the Kanarra anticline due to the structural level of exposure and to its removal from view because of displacement of the hanging wall of the Hurricane fault.

The southernmost occurrence of the Kanarra Creek thrust in the map area is at Camp Creek (plate 2A). Here the leading anticline is upright and open. The Kanarra Creek thrust crops out along the hinge of the fold where it duplicates the ledge-forming limestone layer in the Timpoweap Member (figure 10). The thrust has been affected by folding and dips shallowly eastward at about 20° (about 10° greater than the strata in its footwall) and displaces strata in the hanging wall to the west. In the hanging wall of the thrust is an asymmetric (tops-to-the-west) fold within the lower red member (figure 8A) (306380 m E.; 4153120 m N.). Based on structural level and repetition of stratigraphic units, the Kanarra Creek thrust continues southwards along strike into Wayne Canyon (see plates 2A and 3); farther south it may correlate to the thrust along the Black Ridge in the Pintura 7.5-minute quadrangle (e.g., Hurlow and Biek, 2003).

In Spring Creek, the Kanarra Creek thrust crops out along the hinge zone of the leading anticline (figure 9; plates 2A and 3). North of Spring Creek, parts of the fault and the hinge zone of the fold have been removed by the Hurricane fault. Continuing northward, remnants of the hinge zone of the leading anticline are complexly faulted by both early and late thrust faults. The inten-

Table 3. Fault plane solutions for selected thrusts in the Kanarra fold-thrust structure.

| Location, Fault Name | Local Bedding | Unrotated | Rotated* | Fault Plane (S,D,R**) |
|---|---------------|---|--|---|
| Camp Creek Taylor Creek thrust | (041, 38) |  | NA | (022, 25, 122) |
| Spring Creek Taylor Creek thrust | (185, 60) |  |  | (353, 57, 105) |
| Kanarra Creek Taylor Creek thrust | (206, 42) |  |  | (003, 39, 82) |
| Kanarra Creek Murie Creek thrust fold-thrust structure | (213, 81) |  |  | (202, 53, 85) |
| Kanarra Creek Spring Creek thrust | (211, 57) |  | NA | (208, 64, 95) |
| Kanarra Creek Kanarra Creek thrust movement*** | (211, 57) |  |  | (032, 67, 100) |
| Short Creek Taylor Creek thrust | (235, 67) |  |  | Early**** (036, 60, 91) Late (225, 56, 83) |
| Murie Creek Taylor Creek thrust | (236, 65) |  |  | (064, 39, 71) |

Strike (S), Dip (D) in degrees

* Rotated to the inclination at Camp Creek (38°)

** "R" is the rake, shown in Aki-Richards format (e.g., Allmendinger, 2012)

*** May be related to the folded Kanarra Creek thrust

**** Late (current) orientation favorable for reactivation, see text for explanation

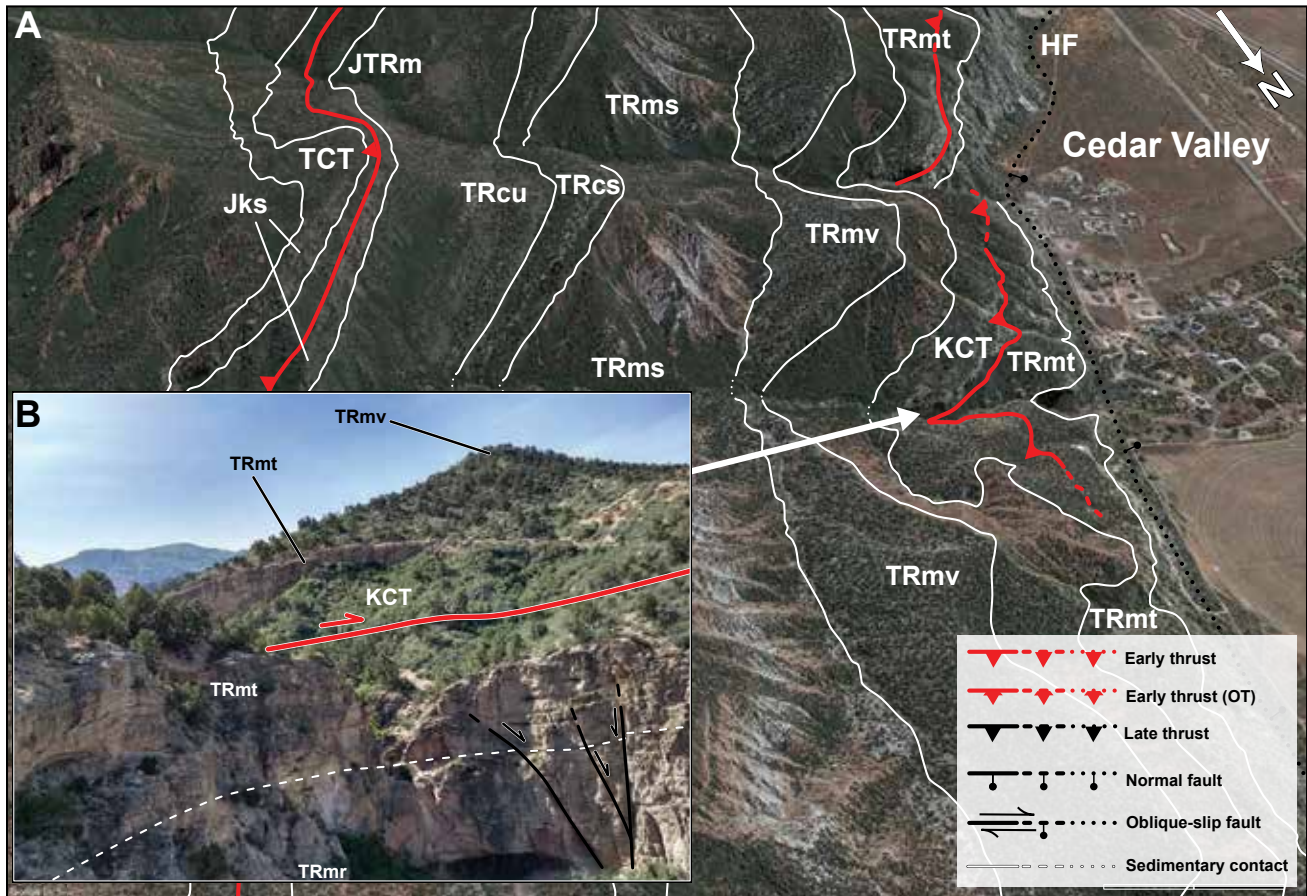


Figure 10. (A) Google Earth 3D terrain view into Camp Creek, looking south. The Kanarra Creek thrust is seen here as an upright, west-directed thrust duplicating the Timpoweap Member. This thrust continues southward along strike into Wayne Canyon (background). Bottom right inset: legend for this and subsequent Google Earth 3D terrain views. (B) Field photograph of the Kanarra Creek thrust looking southeast. Ledge-forming Timpoweap Member of the Moenkopi Formation in the middle ground is thrust over the Timpoweap and Rock Canyon Conglomerate of the Moenkopi outcropping on the Kanarra fold crest in the foreground (southern side of Camp Creek). We place the laterally variable, gradational contact from where the Rock Canyon Conglomerate weathers into hoodoos closer to the mouth of the creek (foreground). Structure initializations: HF—Hurricane fault; KCT—Kanarra Creek thrust; TCT—Taylor Creek thrust. See plate 2B (stratigraphic column) for explanation of map unit symbols.

sity of deformation requires accurate identification of stratigraphic units and their spatial relationships to determine the location of the Kanarra Creek thrust. Near the mouth of Kanarra Creek is a low hill with a water storage tank that is underlain by the Kaibab and Moenkopi Formations up to the Timpoweap Member (figure 11). Looking to the north (figure 11B) these same strata have been thrust eastward in the hanging wall of a splay of the Spring Creek thrust (discussed below). Just east of this hill is a resistant ridge of overturned Timpoweap Member comprised of yellow limestone, stratigraphi-

cally overlain by yellow micritic shale, and capped by purple mudstone. The Timpoweap is followed eastward (up section) by the lower red member and then the Virgin Limestone Member. The succession of strata, confirmed by outcrop appearance, lithology, and fossils (cf., figures 3 to 6), shows an uninterrupted, overturned, stratigraphic section up to the main trace of the Spring Creek thrust (figure 11). The lower red member of the Moenkopi Formation also crops out on the western side of the ridge formed by the overturned limestone of the Timpoweap Member (figure 11; plates 2A and 3). This

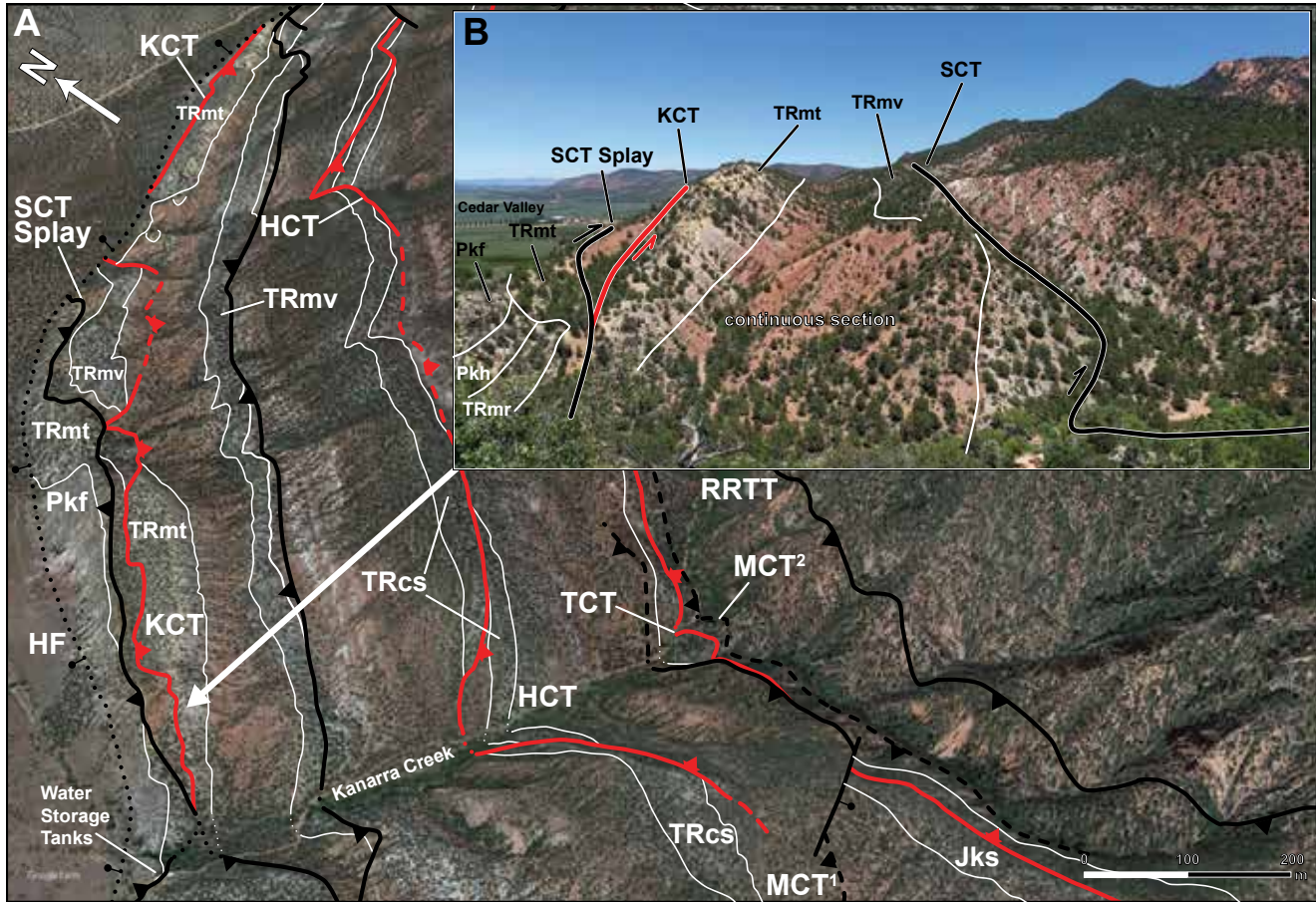


Figure 11. (A) Google Earth 3D terrain view into Kanarra Creek looking northeast. Selected faults and sedimentary contacts are included for reference to the map. (B) Along-strike view upon ridges of the Timpoweap and Virgin Limestone Members of the Moenkopi Formation to the east. The lower red member of the Moenkopi Formation is also present west of the Timpoweap, marking the Kanarra Creek thrust. Farther west, the Kaibab Formation and part of the Timpoweap Member are thrust over this older thrust system on the Spring Creek thrust primary splay. The Permian-Triassic unconformity is marked by Rock Canyon Conglomerate overlying the Harrisburg Member near the bottom of the Kaibab Formation-Timpoweap Member ridge (white contact) and absence of these units to the north. Structure initializations: HF-Hurricane fault; KCT-Kanarra Creek thrust; SCT-Spring Creek thrust; HCT-Hicks Creek thrust; TCT-Taylor Creek thrust; MCT^{1,2}-Murie Creek thrust system; RRTT-Red Rock Trail thrust. See plate 2B (stratigraphic column) for explanation of map unit symbols.

repetition within overturned strata marks the presence of an early thrust, the Kanarra Creek thrust, that was folded and overturned during formation of the leading anticline (figures 7 and 12; plate 2A).

The Kanarra Creek thrust can be followed farther to the north as it continues along the resistant ridge defined by the limestone ledge of the Timpoweap Member. The trace of the thrust veers obliquely eastward across the ridge as it ramps up section (plates 2A and 3). Displacement along the Kanarra Creek thrust ramp is revealed on the north side of the ridge, where the Timpoweap

Member is juxtaposed directly adjacent the Virgin Limestone Member (figure 13) (308635 m E.; 4157735 m N.). Farther north along strike, the Kanarra Creek thrust soles into red beds of the Moenkopi Formation, placing the lower red member onto a sliver of the middle red member (figures 13B and 13C). A complex set of thrust splays followed by a synform in the Timpoweap Member marks the northern exposure of this part of the Kanarra Creek thrust before its main trace veers back to the west and is truncated by the Hurricane fault (plates 2A and 3).

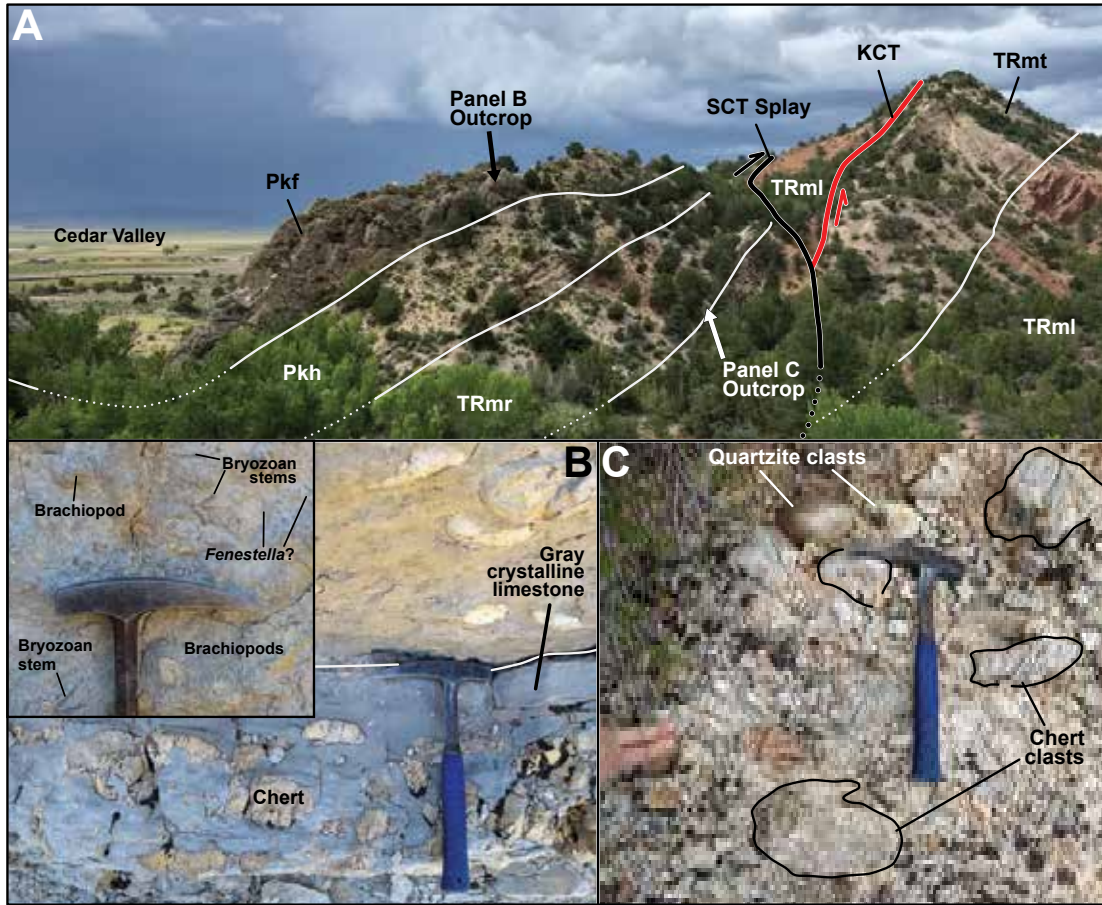


Figure 12. (A) View looking northwest across Kanarra Creek onto faulted Permian and Triassic strata. The Kanarra Creek thrust (red) places the Timpoweap Member over the lower red member; the Spring Creek thrust primary splay truncates the older Kanarra Creek thrust. (B) Overturned, fossiliferous and cherty limestone of the Fossil Mountain Member of the Kaibab Formation. Hammer handle points to stratigraphic top. Inset: Brachiopod and bryozoan fossils exposed along the top of the limestone bed pictured in (B), which reflect the greater diversity of Kaibab fossils in comparison to adjacent younger strata. Bryozoan shape reminiscent of *Fenestella*. (C) Rounded chert and quartzite clasts in the Rock Canyon Conglomerate Member of the Moenkopi Formation. Structure initializations: SCT—Spring Creek thrust; KCT—Kanarra Creek thrust. See plate 2B (stratigraphic column) for explanation of map unit symbols.

The northernmost appearance of the Kanarra Creek thrust in the map area is at the mouth of Short Creek (plates 2A and 3). Here the thrust duplicates the Timpoweap Member (figure 14). The ledge-forming lower part of the Timpoweap Member defines the hanging wall, which is thrust over the lower red member, the upper yellow shale beds of the Timpoweap, and the lower ledge-forming Timpoweap in the footwall (figure 14A). The section here remains overturned, and the thrust is contained within these overturned units. Along strike, to the north and to the south of Short Creek, the thrust

soles into the Timpoweap Member, approximately doubling its thickness, before the thrust trace tips are truncated by the Hurricane fault (plates 2A and 3).

Taylor Creek thrust: The Taylor Creek thrust is a significant, west-directed, flank thrust, which can be traced over several kilometers along the eastern limb of the leading anticline (plates 2A and 3), from its type area in Taylor Creek (Kurie, 1966; Biek, 2007a) to the northernmost extent of the field area at Murie Creek (plates 2A and 3). In its type area at Kolob Canyon, the thrust is east

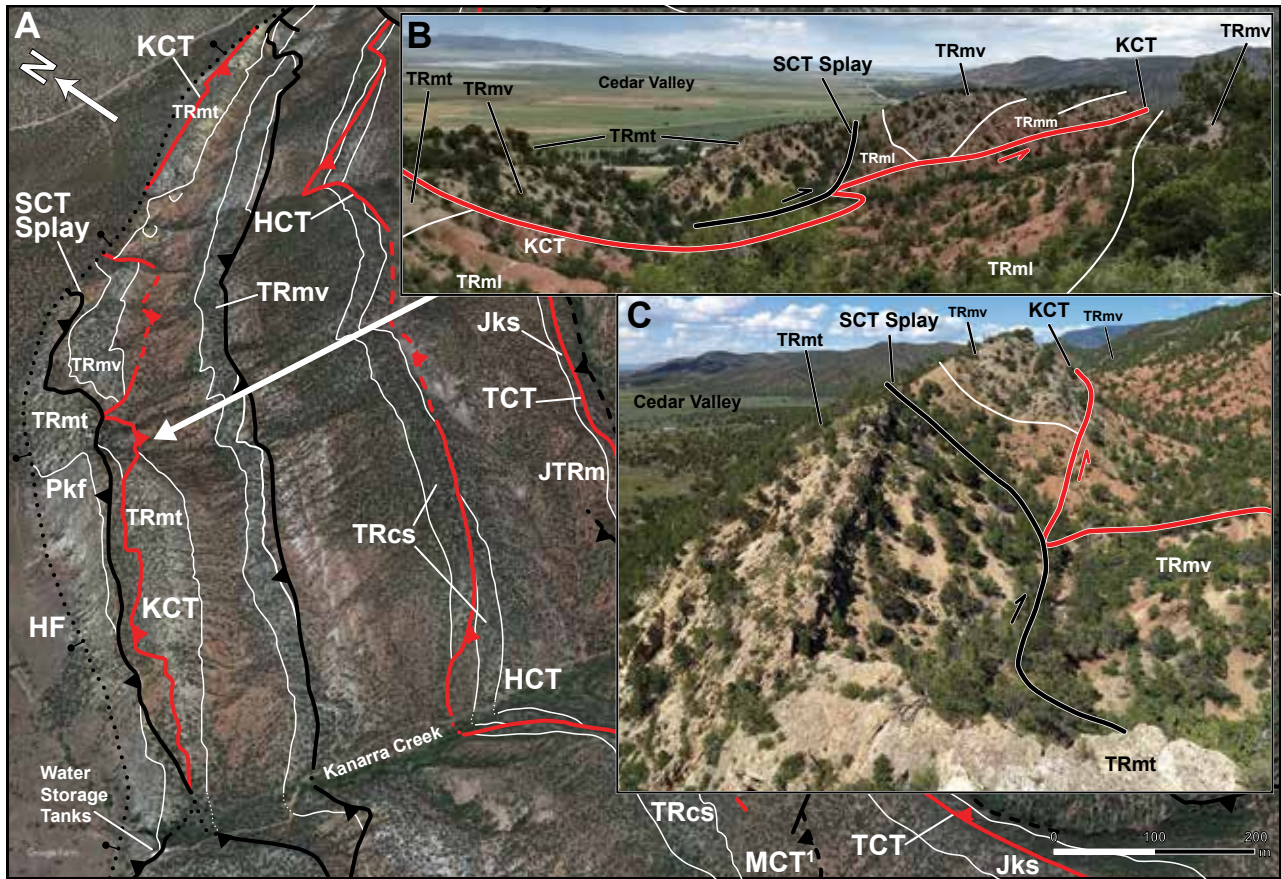


Figure 13. (A) Google Earth 3D terrain view looking northeast into Kanarra Creek. (B) Field photograph of both the Kanarra Creek thrust and the Spring Creek thrust splay, farther to the north along strike. The obliquity of the view distorts the thrust traces to imply gentle apparent dips (see C). Juxtaposition of Virgin Limestone Member against Timpoweap Member of the Moenkopi Formation along the fault here is confirmed by fossils, lithology, and topographic signature. Part of the purple-gray mudstone at the top of the Timpoweap Member can be seen in the left midground, juxtaposed against the Virgin Limestone Member. (C) Along-strike view of the faults in (B), taken standing on the Timpoweap looking north. Structure initializations: HF—Hurricane fault; KCT—Kanarra Creek thrust; SCT—Spring Creek thrust; HCT—Hicks Creek thrust; TCT—Taylor Creek thrust; MCT¹—Murie Creek thrust¹; RRTT—Red Rock Trail thrust. See plate 2B (stratigraphic column) for explanation of map unit symbols.

dipping and duplicates thin, competent ridge formers within the Dinosaur Canyon Member of the Moenave Formation and the Springdale Sandstone Member of the Kayenta Formation, and it soles into detachment layers within the Petrified Forest Member of the Chinle Formation (lower) and the main body of the Kayenta (upper). At Taylor Creek, several splays duplicating these units form a system of thrusts, which likely share the same detachments. Several other west-directed flank thrusts crop out along the leading anticline, (e.g., the Kanarra Creek thrust fault, plates 2A and 3), for clarity we restrict the term Taylor Creek thrust to the west-directed

thrusts duplicating Lower Jurassic units, primarily the Springdale Sandstone Member, as seen in the type area.

The Taylor Creek thrust is well exposed at Camp Creek (figure 15). Here, a single splay of the thrust duplicates nearly the entire Dinosaur Canyon Member and the Springdale Sandstone Member. Erosion through the duplicated section produced a broad hill underlain by two ridge-forming ledges of the Springdale Sandstone. South of this ridge top, shallow, east-dipping ledges of the Springdale Sandstone define a broad, gentle fold nose in the hanging wall of the Taylor Creek thrust, indicating west-directed transport (figure 15B)

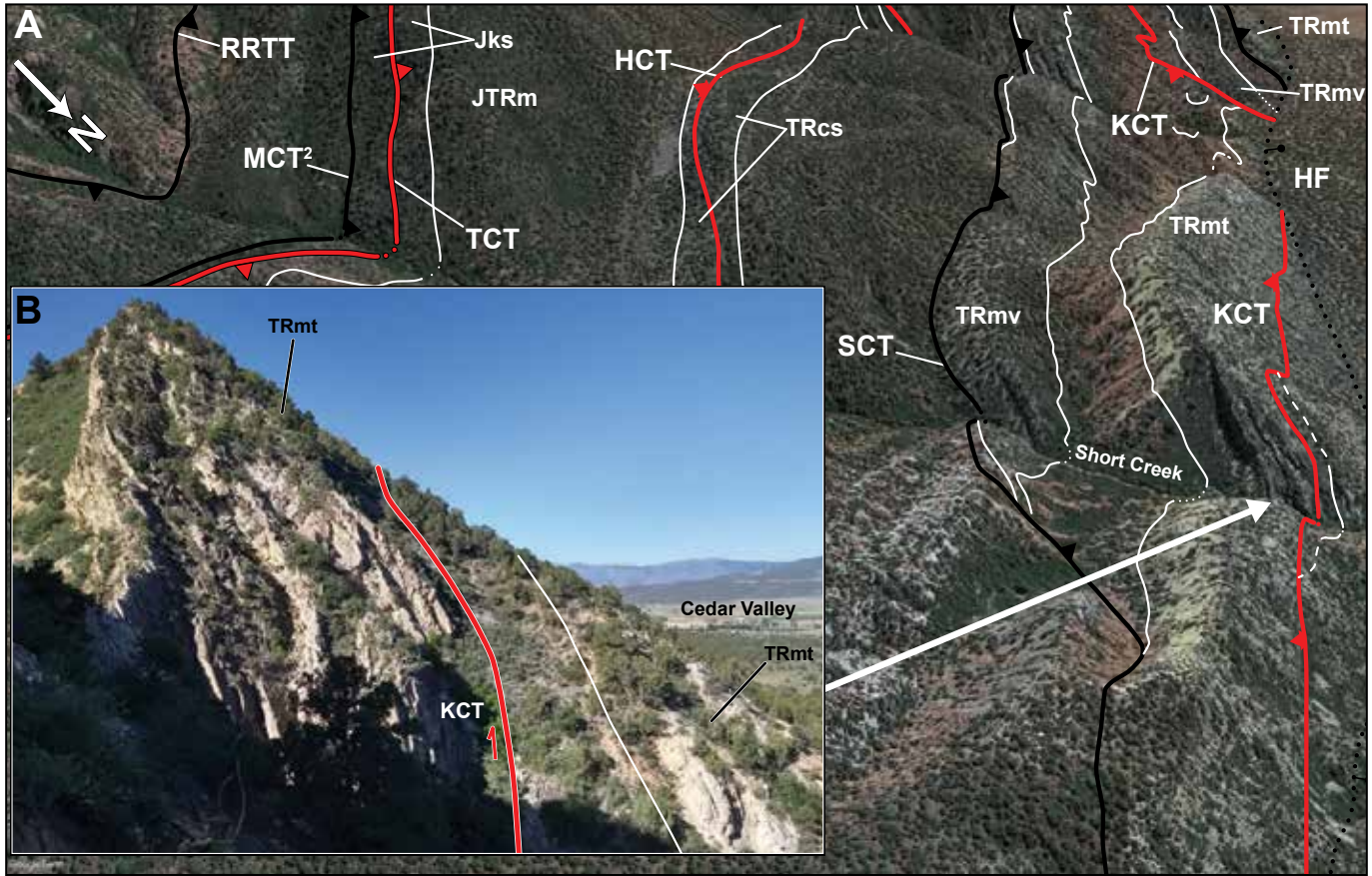


Figure 14. (A) Google Earth 3D terrain view southwest into Short Creek. Selected faults and sedimentary contacts are included for reference to the map. These contacts show the overturned fold limb, overturned thrusts (Taylor Creek, Hicks Creek, and Kanarra Creek thrusts) and the Spring Creek thrust. Here, the Kanarra Creek thrust duplicates the full section of Timpoweap Member. (B) South-facing, along-strike view of duplicated Timpoweap Member along the Kanarra Creek thrust. Structure initializations: HF–Hurricane fault; KCT–Kanarra Creek thrust; SCT–Spring Creek thrust; HCT–Hicks Creek thrust; TCT–Taylor Creek thrust; MCT²–Murie Creek thrust²; RRTT–Red Rock Trail thrust. See plate 2B (stratigraphic column) for explanation of map unit symbols.

(307320 m E.; 4152110 m N.). This fold in the hanging wall mimics the broad fold in the Springdale Sandstone in the hanging wall of the easternmost thrust fault of the Taylor Creek thrust system (plate 2A; cf., figure 4 on plate 3, in Biek, 2007a).

Analysis of shear fracture data in the Camp Creek area yield a fault plane solution of (022, 55) with a rake of 122°, indicating a thrust fault with a minor left-lateral component of displacement. This result is indicated in table 3 by the bolded great circle and slip vector. It is consistent with the attitude of the fault (033, 54), determined from the orientation of its map trace (plates 2A

and 3). Bedding in the footwall near the creek bed dips about 38° (plates 2A and 3). Thus, at Camp Creek the Taylor Creek thrust is best characterized as a shallow thrust ramp, forming an angle about 16° from bedding and thickening the Springdale Sandstone Member.

The Taylor Creek thrust is less well exposed in Spring Creek. Here, the steeply dipping overturned Springdale Sandstone Member is double to nearly triple its stratigraphic thickness because of multiple duplications (plate 2A). The tectonically imbricated and overthickened sandstone ledges form a prominent topographic ridge that has been eroded by the creek



Figure 15. (A) Google Earth 3D terrain view south into Camp Creek showing the Taylor Creek thrust duplicating the Springdale Sandstone Member of the Kayenta Formation and the Dinosaur Canyon Member of the Moenave Formation over the Springdale Sandstone in its footwall. Here, the stratigraphic section and the Taylor Creek thrust are upright, and the fault verges westward. (B) Edge-on field photograph of the Taylor Creek thrust duplication. The apparent fold nose formed by the Springdale is not simply an effect of the view angle; the Springdale at the top of the hill dips about 20° less than the Springdale in the creek, which conforms to the thrust. Structure initializations: HF–Hurricane fault; KCT–Kanarra Creek thrust; TCT–Taylor Creek thrust. See plate 2B (stratigraphic column) for explanation of map unit symbols.

(figure 16). Along the southern ridge isolated, slickensided outcrops of Springdale Sandstone on the hillside mark the presence of the thrust. A minor kink fold defined by shallow-dipping Springdale Sandstone ledges (dashed white line, figure 16B) indicates the thrust splay cropping out along the ridge is a ramp, which folded the overturned strata to very shallow inclinations (30 to 40° W.). This kink fold continues up the ridge. At the top of the ridge (top right), a late thrust exploited the shallow-dipping strata and displaced sandstone of the Dinosaur Canyon Member over itself to form a conspicuous truncation (figure 16; plates 2A and 3; 307900

m E.; 4154060 m N.). Along the topographic ridge on the north side of Spring Creek, the primary indication of the Taylor Creek thrust system is that the Springdale Sandstone is nearly double its normal stratigraphic thickness, suggesting at least one thrust flat is confined within the unit (figure 17; plates 2A and 3).

In Spring Creek, shear fractures are best preserved on the southern ridge of Springdale Sandstone, where the thrust begins to ramp up section (figure 18). The unrotated fault plane solution is presented in plate 3 and table 3. To compare to Camp Creek, the data were rotated 82° clockwise along a bearing of 185° so that the

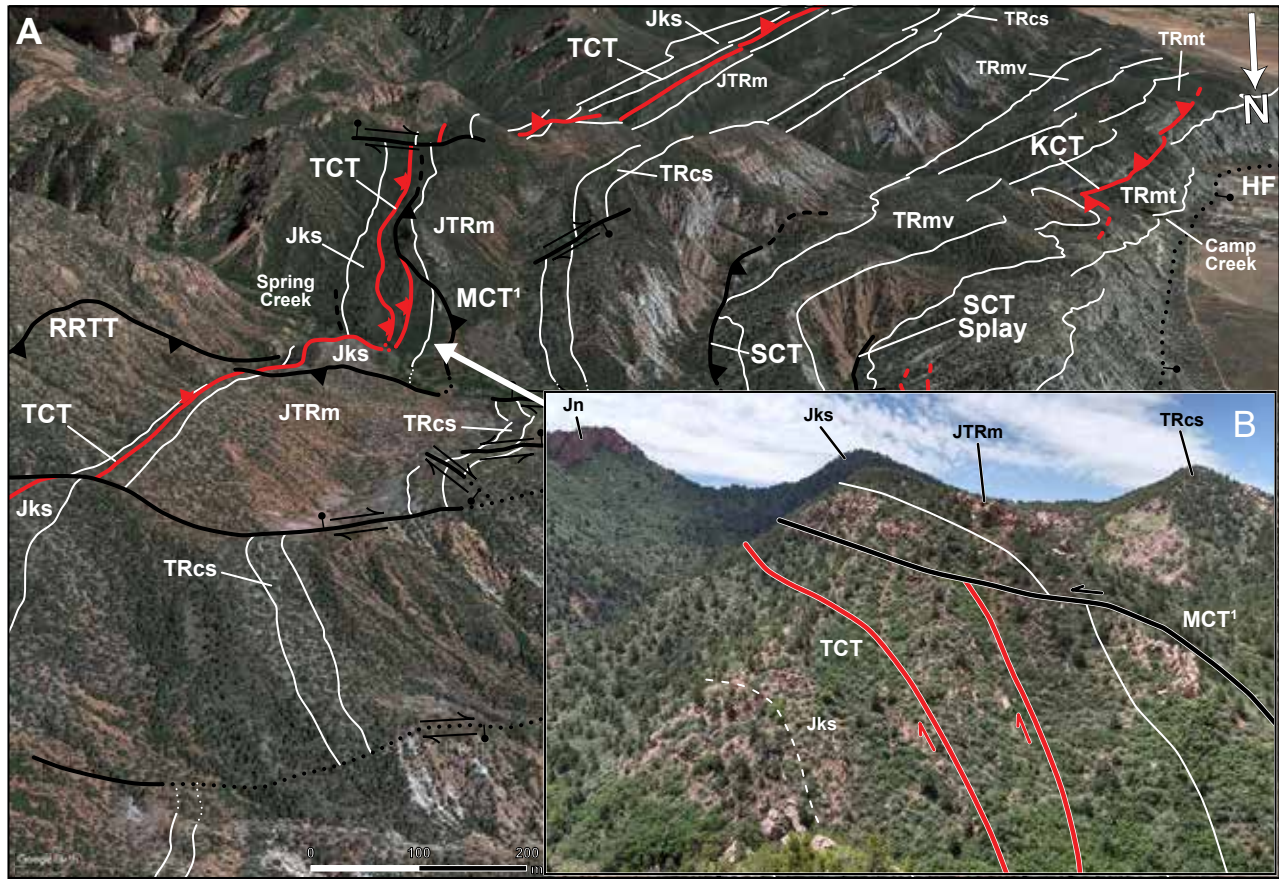


Figure 16. (A) Google Earth 3D terrain view south into Spring Creek. Structures outcropping in Camp Creek are in the background. Here, duplication of the Springdale Sandstone on the Taylor Creek thrust is readily apparent on the southern ridge formed by the Springdale Sandstone of Kayenta Formation in Spring Creek (midground). (B) Close-up of the southern Springdale Sandstone ridge and the Taylor Creek thrust duplications. The Dinosaur Canyon Member-Springdale Sandstone contact is outlined in white. At the bottom of the ridge, above the second duplication, strata are gently overturned, whereas adjacent (footwall) strata are steeply overturned, consistent with an early formed, overturned thrust ramp. The Murie Creek thrust¹ (MCT¹) appears to sole into the shallow, overturned strata in the Taylor Creek thrust hanging wall. Structure initializations: HF—Hurricane fault; KCT—Kanarra Creek thrust; SCT—Spring Creek thrust; TCT—Taylor Creek thrust; MCT¹—Murie Creek thrust¹. See plate 2B (stratigraphic column) for explanation of map unit symbols.

bedding inclination in the footwall (185, 60) coincides with the footwall at Camp Creek (38°). Upon this rotation, the fault plane solution (table 3) yields a pre-overturning fault orientation of (353, 57)—a close match with the fault exposure in Camp Creek both in dip and angle to bedding.

At Kanarra Creek, outcrop patterns and slickensides indicate the Taylor Creek thrust continues within the Springdale Sandstone Member. Slickensided outcrops are exposed along the thrust trace. Creep of the rock may introduce more scatter in measurements along this steep ridge, but data collected along the thrust trace

produce thrust-sense fault plane solutions (plate 3; table 3). When data are rotated so that local bedding matches the Taylor Creek thrust footwall at Camp Creek, the fault plane solution indicates a likely thrust at (003, 39)—i.e., a flat compared to Camp Creek (plate 3; table 3). This solution also matches the present-day map pattern of an overturned thrust flat within the Springdale Sandstone Member.

North of Kanarra Creek, the outcrop pattern of the Springdale Sandstone Member changes. Discordantly dipping sets of sandstone ledges in the Springdale, near the head of the canyon north of Kanarra Creek (310036

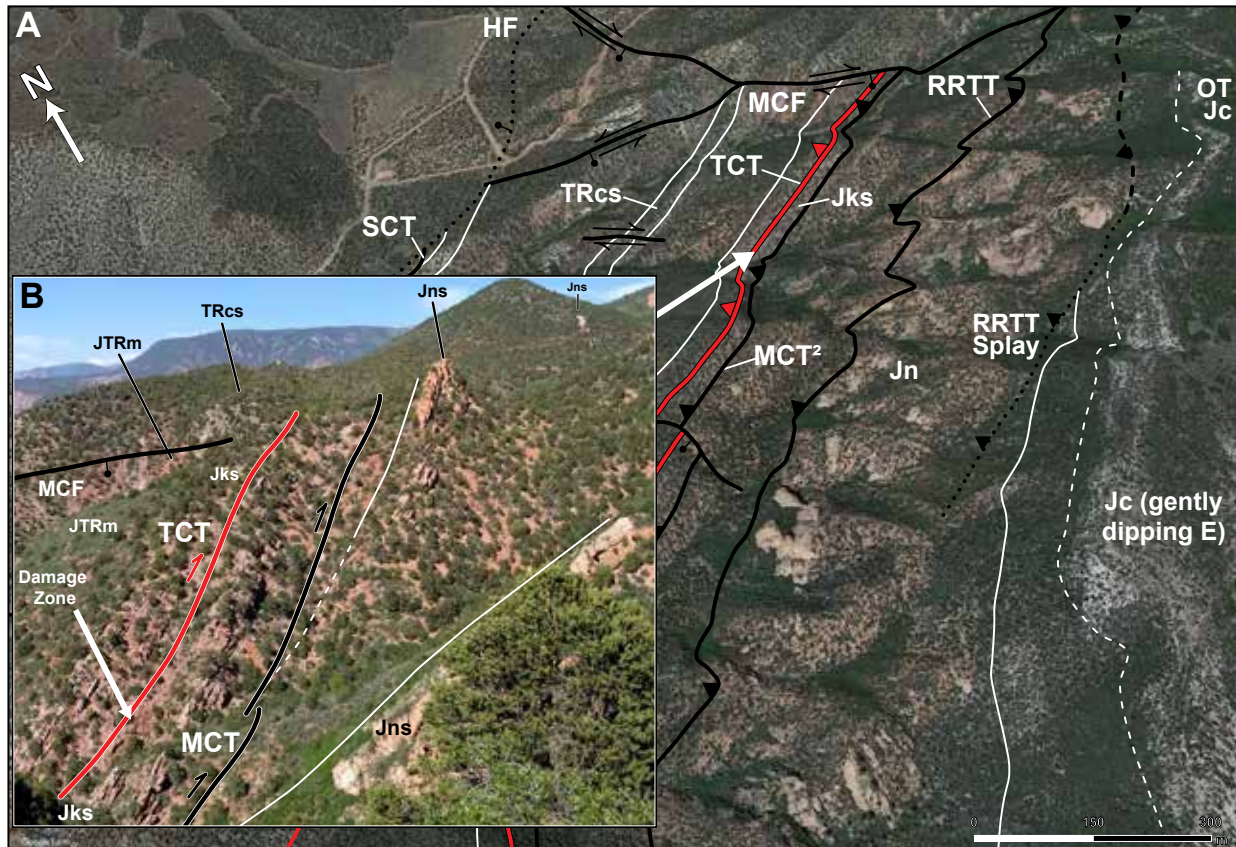


Figure 17. (A) Google Earth 3D terrain view of the overturned Kanarra fold limb, looking northwest into Short and Murie Creeks. Selected faults and sedimentary contacts are shown for reference to the map. Potential reactivation of the Taylor Creek thrust is reflected in the position and style of the thrust barbs. (B) The Taylor Creek thrust as seen looking north along strike from the Short Creek saddle into Murie Creek. A double sandstone ledge with minor siltstone interbeds marks the duplication. Here, a damage zone of altered rock (white arrow) outcrops near the creek bed. Adjacent to the eastern Springdale Sandstone ledge of the Kayenta Formation, the main body of the Kayenta is cut through by the late-formed Murie Creek thrust, nearly displacing the Springdale Sandstone onto the Shurtz Tongue of the Navajo Sandstone. The white arrow points to the location of (B). Structure initializations: SCT—Spring Creek thrust; TCT—Taylor Creek thrust; MCT²—Murie Creek thrust²; MCF—Murie Creek fault; RRTT—Red Rock Trail thrust. See plate 2B (stratigraphic column) for explanation of map unit symbols.

m E.; 415799 m N.), indicate minimal, tops-to-the-east reactivation of the Taylor Creek thrust (plates 2A and 3). Additional evidence for reactivation can be seen in the slickenside data collected near Short Creek (plate 3; table 3). The rotated fault plane solution produces a thrust at (036, 60), and outcropping Riedel shear zones (e.g., figure 18) show shear sense matching an overturned thrust. Yet, the fault plane solution for unrotated (present-day) data includes a potential fault, which closely matches the local orientation of the thrust trace at (225, 56). Based on the outcrop pattern farther south,

this cannot be discounted. We show the potential for reactivation along this part of the thrust trace with a slightly different style of the thrust fault barbs (figure 17). In addition, the barb style and side of the thrust are switched to indicate the location where the thrust appears to have begun limited, east-directed, movement (plates 2A and 3).

At Murie Creek, isolated slickensided outcrops indicate the Taylor Creek thrust trace is exposed near the top of the southern and middle ridges of Springdale Sandstone (311667 m E., 4159286 m N.; plate 3). At-



Figure 18. (A) View to the north looking upon Riedel shears along overturned Springdale Sandstone beds (dipping about 65° W.) defined by deformation bands. Here, shear surfaces that form low angles to bedding intersect R' shear surfaces at high angles to bedding. The sense of motion prior to overturning is tops to the west, synthetic with the Taylor Creek thrust. (B) View to west of shear fracture surface north of (A) within the Taylor Creek thrust damage zone. R shears along the fracture surface indicate the missing block moved upwards (tops-to-the-west). Right hand rule strike, dip, and slip direction rake: 054, 77, and 69. Inset: close-up of R shears on the fracture surface in (B) with arrow pointing in the direction of motion. Lower right: diagram of R shears along a fracture surface, arrow pointing in the direction of motion of the missing block. (C) View to south of Dylan Webb measuring local bedding and shear fractures. Outcrop with the shear fractures in (B) is just beyond Webb along bedding strike. Inset: close-up of P-T type shears with tops-to-the-east motion prior to overturning, antithetic to the main thrust. Right hand rule strike, dip, and slip direction rake: 235, 73, and 87. Lower right: diagram of P-T shears along a fracture surface, arrow pointing in the direction of motion of the missing block. (D) View to west of an outcrop-scale overturned thrust with tops-to-the-east motion prior to overturning. Right hand rule strike, dip, and slip direction rake: 240, 78, and 86. Inset: close-up of R shear steps along thrust surface with black arrow indicating motion of the missing block. All panels from Springdale Sandstone Member of the Kayenta Formation outcrops within the Taylor Creek thrust damage zone (see plate 3 for locations). For all panels, arrow with "TOP" points to stratigraphic top. Diagrams in (B) and (C) panels from Petit (1987) and Allmendinger and others (1989).

tenuation of intervening siltstones between duplicated Springdale Sandstone ledges, and a zone of well-indurated, altered siltstone between the Springdale ledges, mark the trace of the thrust (figure 17B). Rotation of the shear fracture data (for comparison) produces a thrust fault plane solution (062, 39), closely resembling the

result at Kanarra Creek. The unrotated (present-day) data does not produce a viable thrust for either potential fault plane. This result indicates that if the Taylor Creek thrust was reactivated, only an approximately 1.8 km segment between Kanarra and Short Creeks underwent renewed, eastward movement. We trace the Tay-

lor Creek thrust past the northern fork of Murie Creek, where it is truncated by the Murie Creek fault (figure 17).

Hicks Creek thrust: The thin, competent Shinarump Conglomerate Member of the Triassic Chinle Formation locally hosts the Hicks Creek thrust, a flank thrust with the same style and vergence as the two previously described faults (cf., Averitt, 1962, the Hicks Creek fault). Here, in comparison to where it crops out in the Shurtz Creek amphitheater and at The Red Hill, the Hicks Creek thrust is less significant and its trace semi-continuous (plates 2A and 3). Averitt (1962) mapped this thrust as a normal fault at Hicks Creek, but its observed style in adjacent quadrangles to the north and south (Averitt, 1967; Biek, 2007b; Knudsen, 2014a; Biek and Hayden, 2016; this paper) negates this interpretation. Similar, west-directed flank thrusts cut through the upper red member and Chinle Formation at Kolob Canyon (Biek, 2007a) and at The Red Hill (Knudsen, 2014a).

The Hicks Creek thrust is well exposed at Kanarra Creek (figure 19). Here, it forms a conspicuous duplication of the Shinarump Conglomerate Member. The overturned Hicks Creek flank thrust, previously interpreted as an upright, east-directed reverse fault (Averitt, 1967), hosts an about 500-m-long duplication of the Shinarump Conglomerate and crosses the creek near UTM 308496 m E.; 4156677 m N. The lower detachment of the thrust is within the lower unit of the Chinle Formation, and the upper detachment is in the Petrified Forest Member. The trace of the Hicks Creek thrust is shown by Averitt (1962) to die out near the Murie Creek fault. A near-identical duplication is exposed in the canyon north of Kanarra Creek, and we trace the Hicks Creek thrust from here into Short Creek where it truncates against a small cross fault. It is likely that the thrust soles into a higher detachment layer in the Petrified Forest Member; this was not mappable in the field, so we query the trace of the thrust between these two Shinarump Conglomerate duplications. The Hicks Creek thrust becomes a major fault north of Murie Creek and at The Red Hill. Along its northern trace, the thrust cuts deeper down section, soling into a lower detachment in the Shnabkaib Member.

Late Contraction Faults

Late contraction thrust faults (tables 1 and 2) associated with formation of the Kanarra fold-thrust structure are east-verging and cut across bedding. These faults include the Spring Creek thrust, Murie Creek thrust, and Red Rock Trail thrust faults. Many of these faults are kilometer-scale features (plates 2A and 3). A lack of piercing points precludes determining their slip, but minimal displacement can be estimated in cross section by measuring the fault trace orientation and the magnitude of displacement consistent with the map pattern. These displacements can be tens to hundreds of meters; at Kanarra Creek, smaller thrusts displace strata up to 80 m along their length, whereas larger thrusts have minimum displacements of up to 300 m. The late thrusts commonly tectonically thin, fold, and/or truncate less competent stratigraphic units (e.g., red beds of the Moenkopi Formation). Tectonic thinning of stratigraphic layers reflects ductile flow and/or truncation along the hanging wall. The trace of late thrust faults tends to parallel the strike of bedding. Thrust fault inclinations are discordant to bedding and can achieve steep orientations, particularly when cutting through mechanically stiff layers to form ramps (e.g., the Navajo Sandstone). Where these faults are well exposed and cut through competent strata, they are associated with cataclastic breccia zones several meters to tens of meters wide with varying degrees of induration. These late contraction thrusts and their connecting splays are best observed within the creek valleys that erode across the strike of the limb of the leading anticline (plate 3).

Spring Creek thrust: The primary splay of the Spring Creek thrust and the Kanarra Creek thrust are closely associated spatially in the field (plates 2A and 3). However, as previously discussed, the Kanarra Creek thrust is overturned by folding and cross-cut by the upright primary splay of the Spring Creek thrust (figures 7 and 20; plate 3). This demonstrates that the Spring Creek thrust and its splays are younger and distinct from the Kanarra Creek thrust.

The trace of the Spring Creek thrust is well exposed along the northern side of Spring Creek, east of the leading anticline hinge zone, along its overturned

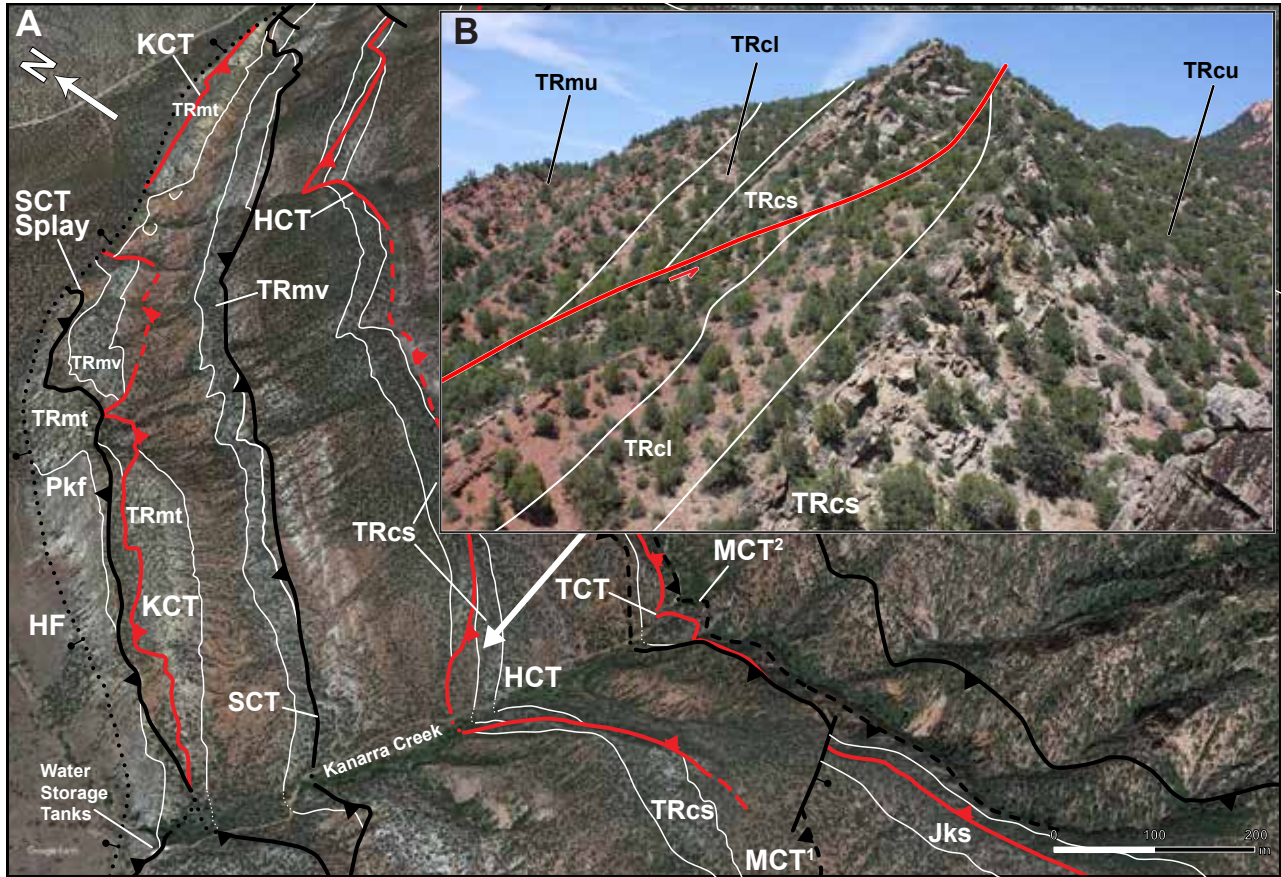


Figure 19. (A) Google Earth 3D terrain view looking northeast into Kanarra Creek. The Hicks Creek thrust Vs gently west into the creek in the foreground and displaces the Shinarump Conglomerate Member and lower members of the Chinle Formation and part of the upper red member of the Moenkopi Formation. Another duplication is visible in the background. Other early and late structures shown for reference to the map. (B) Along-strike view of the Hicks Creek thrust duplication, from the perspective of the hanging wall on the southern side of Kanarra Creek. Gently dipping Shinarump Conglomerate in the hanging wall conforms to the thrust, which truncates Shinarump strata in the background. Structure initializations: HF–Hurricane fault; KCT–Kanarra Creek thrust; SCT–Spring Creek thrust; TCT–Taylor Creek thrust; HCT–Hicks Creek thrust; MCT^{1,2}–Murie Creek thrust^{1,2}. See plate 2B (stratigraphic column) for explanation of map unit symbols.

limb. The fault trace begins just south of Spring Creek and continues northwards for several kilometers (figure 20; plates 2A and 3). Its tortuous map pattern consists of several thrust splays, which branch and curve through Moenkopi strata. Like the Taylor Creek thrust, the Spring Creek thrust is a thrust system, and this adds significant structural complexity to the overturned section along the Kanarra fold (figure 7; plates 2A and 3). We identify the main trace of the Spring Creek thrust system as the easternmost continuous thrust within the system of splays. At the surface, the main trace commonly cuts across the eastern fold limb of the leading

anticline, from the Virgin Limestone Member into the Shnabkaib Member (figure 7; plates 2A and 3).

The primary splay of the Spring Creek thrust system is exposed just east of the mouth of Spring Creek, where the Timpoweap Member and part of the lower red member are thrust eastward (figure 20; plates 2A and 3). To the north, and to the south, the lower red member is truncated by this same thrust (plates 2A and 3). The primary splay continues to the north where the Timpoweap Member is overturned, and here subsidiary splays of the Spring Creek thrust system displace the Virgin Limestone Member. These splays form a

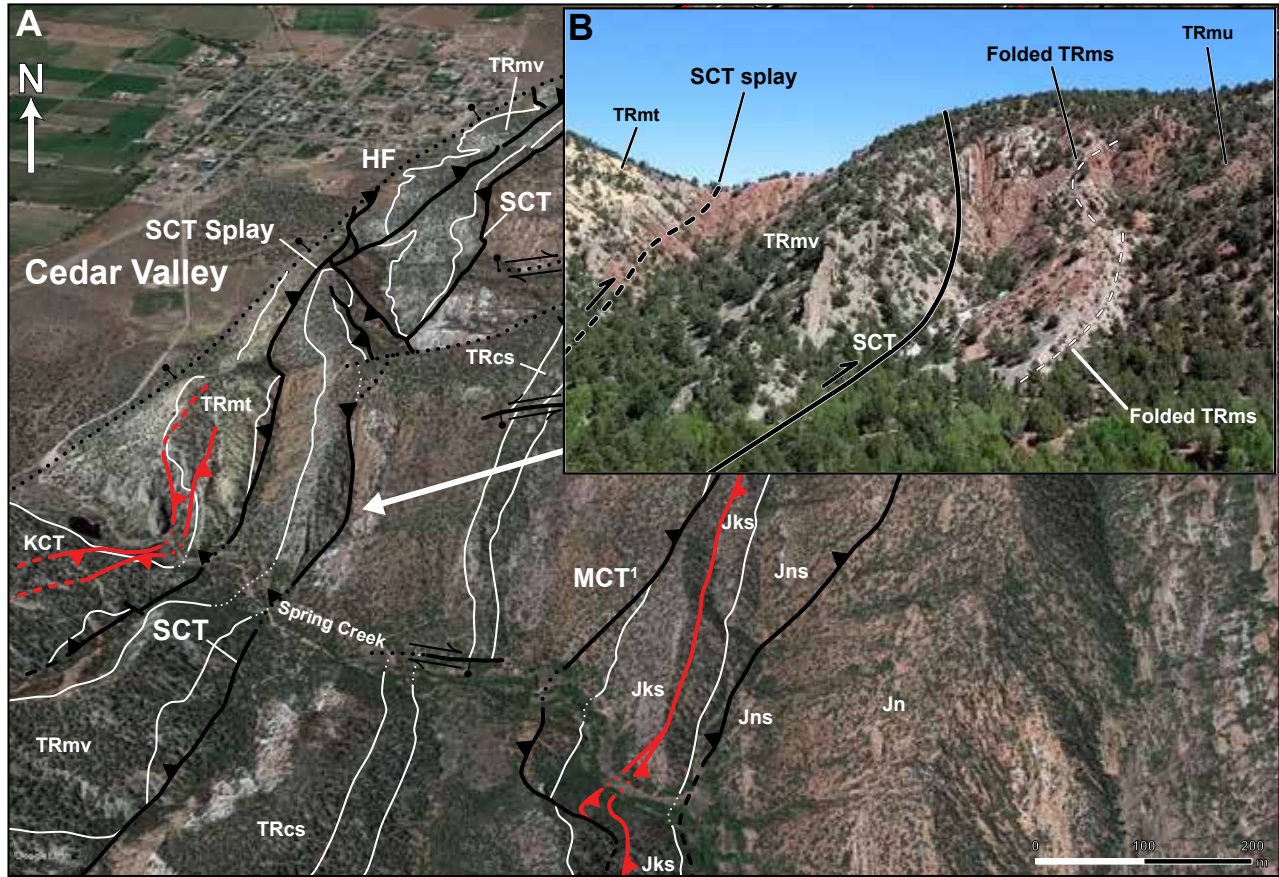


Figure 20. (A) Google Earth 3D terrain view looking northeast into Spring Creek. To the west, the Spring Creek thrust primary splay cuts the Timpoweap Member and displaces it over the lower red member and Virgin Limestone Member of the Moenkopi Formation. To the east, the Spring Creek thrust main trace breaks across the more competent Virgin Limestone and displaces it over the middle red member and part of the Shnabkaib Member of the Moenkopi. Selected fault and sedimentary contacts are included for reference to the map. (B) Close-up of the Spring Creek thrust deformation zone. Here, it is clear the Virgin Limestone is displaced over a large part of the Moenkopi section, cutting out the middle red member and much of the Shnabkaib Member. The displacement is accompanied by folding, as seen in the trace of a folded Shnabkaib gypsum layer (black dashed line). Structure initializations: HF—Hurricane fault; KCT—Kanarra Creek thrust; SCT—Spring Creek thrust; MCT¹—Murie Creek thrust¹. See plate 2B (stratigraphic column) for explanation of map unit symbols.

complex zone of faulting that has been dissected by the Hurricane fault, leaving discontinuous remnants of the Spring Creek thrust system along the hinge of the leading anticline (figure 9; plates 2A and 3).

The primary splay of the Spring Creek thrust system reemerges at Kanarra Creek and displaces the Fossil Mountain Member and part of the Timpoweap Member over a ridge of lower red member and Timpoweap in the hanging wall of the Kanarra Creek thrust (figure 21, also see figures 11A and 11B, lower left). On the south side of Kanarra Creek, a connecting splay branches from the main trace of the Spring Creek thrust sys-

tem (figure 11A, lower left), accommodating displacement of the Virgin Limestone Member over the lower red member that had been previously duplicated by the Kanarra Creek thrust. This connecting splay merges with the primary splay of the Spring Creek thrust on the north side of Kanarra Creek (plates 2A and 3). A smaller thrust splay displaces the Timpoweap Member onto the Virgin Limestone Member ridge on the south side of Kanarra Creek. Here, along the trail from the parking area (307994 m E.; 4156823 m N.) leading to the creek mouth, yellow limestone, shale, and tan, sand-rich limestone crops out discordantly against the Virgin

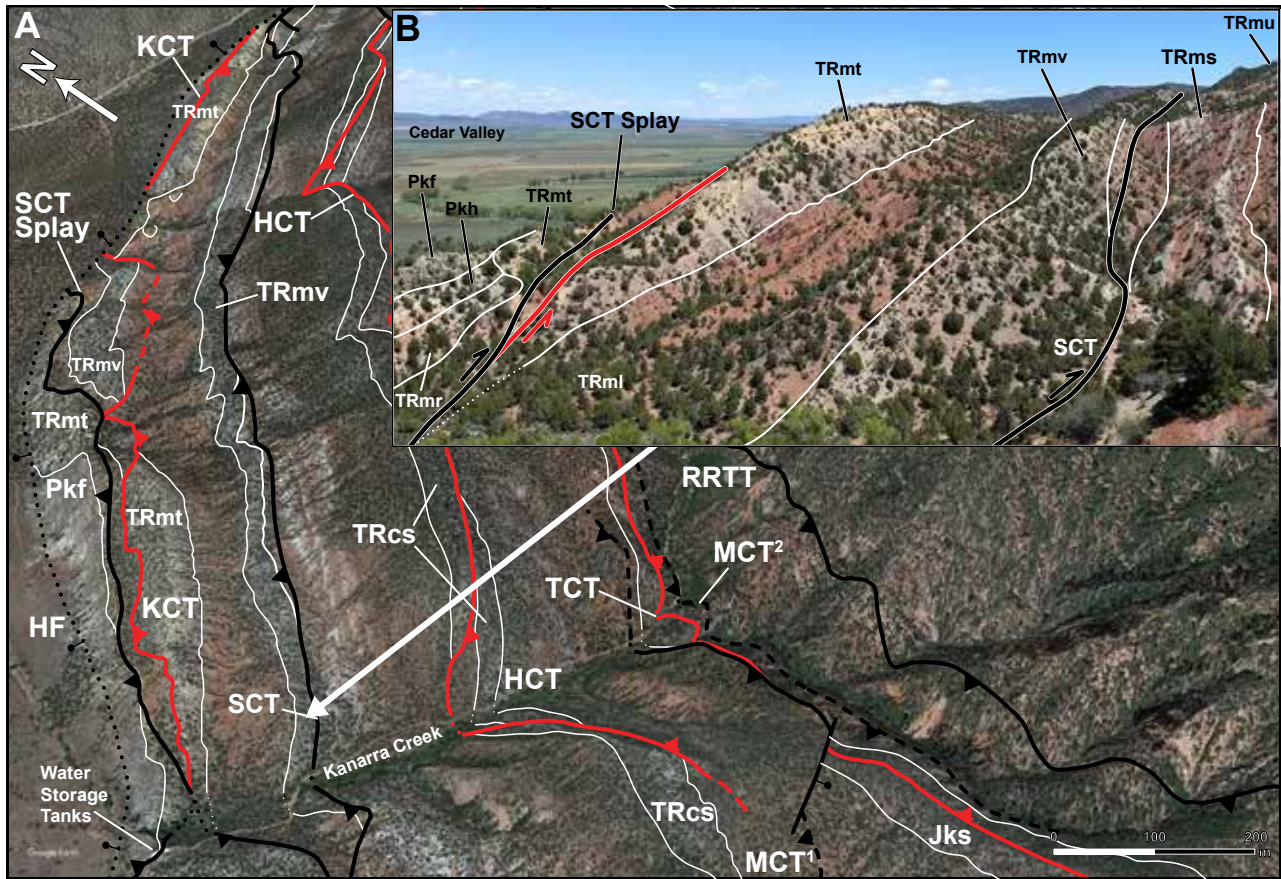


Figure 21. (A) Google Earth 3D terrain view looking northeast into Kanarra Creek. To the west, the Spring Creek thrust primary splay displaces the Fossil Mountain Member of the Kaibab Formation and the Timpoweap Member over the lower red member of the Moenkopi Formation. To the east, the main trace of the Spring Creek thrust continues roughly parallel to the strike of bedding, displacing the Virgin Limestone Member over the Shnabkaib Member of the Moenkopi Formation. (B) Along-strike view to the north of the Spring Creek thrust main trace truncating the middle red member and Spring Creek thrust primary splay. Structure initializations: HF–Hurricane fault; KCT–Kanarra Creek thrust; SCT–Spring Creek thrust; TCT–Taylor Creek thrust; HCT–Hicks Creek thrust; MCT^{1,2}–Murie Creek thrust^{1,2}; RRTT–Red Rock Trail thrust. See plate 2B (stratigraphic column) for explanation of map unit symbols.

Limestone. Yellow Timpoweap shale beds on the side of the path are contorted into meter-scale, complex folds. Steep eastward dips on the Timpoweap Member above the trail indicate folding along an east-directed thrust (plates 2A and 3). Near the Timpoweap-Virgin juxtaposition, mass wasting of the Virgin Limestone Member obscures the exact location of the thrust splay and presumably the lower red member along the western side of the ridge. Along this ridge, a minor normal fault associated with the Hurricane fault zone cuts obliquely across strike and truncates the Spring Creek thrust splays (plates 2A and 3).

The primary splay of the Spring Creek thrust sys-

tem continues northward from Kanarra Creek along the west side of the topographic ridge held up by the duplicated Timpoweap Member (figures 13 and 21; plates 2A and 3). Near the end of the ridge, the primary splay ramps down section, exposing more of the Timpoweap in the hanging wall than seen at Kanarra Creek. The primary splay also truncates part of the overturned Kanarra Creek thrust and cuts out most of the lower red member (figure 13C; plates 2A and 3). From this location, the primary splay continues along strike to the north where it is truncated by the Hurricane fault (309191 m E.; 4158719 m N.).

The main trace of the Spring Creek thrust system

first appears south of Spring Creek to the east of the primary splay (figures 9 and 20; plate 2A). It cuts through the hinge zone of the leading anticline on the eastern side of a gently folded ridge of Virgin Limestone Member, at the upright-to-overtured transition on the eastern limb of the fold (307342 m E.; 4154074 m N.). The thrust thins the middle red member and truncates the lower double-layer of gypsum. A few tens of meters north of the truncation, the fault is marked by a calcite-encrusted, well-indurated fault megabreccia (cataclasite), which hosts cobble- to boulder-sized clasts of slickensided and folded Virgin Limestone Member limestone (figure 22). The trace of the main Spring Creek thrust fault can be followed along strike to the north, where west-dipping, overturned middle red gypsum layers crop out and the trace of the thrust is within the middle red member. On the north side of Spring Creek, a prominent wall of vertical Virgin Limestone Member fins crops out in the hanging wall of this thrust—these fins were transported east and over the middle red member (figure 20; plates 2A and 3).

From Spring Creek, the main trace of the Spring Creek thrust system continues northward towards Kanarra Creek, juxtaposing steep overturned beds of the Virgin Limestone Member onto the Shnabkaib Member. Here, the hanging wall of the main Spring Creek thrust includes a 1-km-long, nearly-recumbent, overturned fold in the Virgin Limestone (figure 9). This fold is part of the hinge zone of the leading anticline that was displaced east on the thrust. The folded Virgin Limestone forms a low ridge, with shallow west-dipping strata (about 10 to 25° W.) on its western side and steeper, overturned (about 45 to 55° W.) strata on its eastern side. On the eastern side of the ridge, the trace of the main Spring Creek thrust system displaces overturned Virgin Limestone beds and the middle red double gypsum layer over the middle red member (307924 m E.; 4156400 m N.).

At Kanarra Creek, the main trace cuts out much of the middle red member in the same structural style seen at Spring Creek. Here, the thrust cuts shallow dipping (about 45 to 50°), duplicated Virgin Limestone Member in the Kanarra Creek thrust hanging wall (figure 21). Near the creek bed, slickenside measurements on the Virgin Limestone indicate two populations of shear

fractures—a set of normal-sense slickensides, which mostly form low angles to bedding, and a set of thrust-sense slickensides, also at low angles to bedding (figures 23B and 23D; plates 2A and 3; table 3). Both populations include strike-slip shear fractures with minor normal-sense and thrust-sense displacement, indicated by their slickenline rakes (figures 23B inset and 23C). Rotation of the normal sense shear fracture data to where bedding dips 38° E. (analogous to an earlier stage of folding at Camp Creek) yields a fault plane solution with a west-directed thrust at 27° to bedding. Once restored, the normal-sense shear fractures are consistent with movement along the early Kanarra Creek thrust, which was later folded and overprinted (table 3). Fault plane solutions from the thrust-sense shear fracture population indicate a steep, east-directed thrust, which matches the local orientation (208, 64) of the main trace of the Spring Creek thrust (plates 2A and 3; table 3). The Spring Creek thrust shallows to the north to (209, 45), where it exploits the shallow bedding on the duplicated Virgin Limestone.

North of Kanarra Creek, the main trace of the Spring Creek thrust ramps up section and places the Virgin Limestone Member over the Shnabkaib Member (figure 24). This juxtaposition of the Virgin Limestone against the Shnabkaib continues another 3.5 km from Kanarra Creek into Short Creek. Only the main thrust trace is present within Short Creek, again placing the Virgin Limestone Member against the Shnabkaib Member (plates 2A and 3). The thrust trace veers westwards as it ramps down section from the Shnabkaib Member to the lower red member. As the thrust truncates the Virgin Limestone, it veers northward into sub-parallelism with the strike of bedding (310690 m E., 4159590 m N.). Within Murie Creek, displacement along the main trace completely cuts out the lower red member, placing the Timpoweap Member against the Virgin Limestone Member. Just to the north of the creek mouth, the thrust is truncated by the Hurricane fault (311370 m E., 4159990 m N.).

Murie Creek thrust: East of Spring Creek, several late, east-directed thrusts are exposed in the Jurassic section near the syncline axis of the Kanarra fold-thrust structure. We group the first two of these thrusts together



Figure 22. (A) Kink fold (layering traced by dashed white lines) on outcrop of brecciated limestone in the Virgin Limestone Member of the Moenkopi Formation along the Spring Creek thrust. View sub-parallel to local strike (about 30°) and kink axial trace. Hammer beneath Dylan Webb is placed parallel to the fold axis. (B) View nearly parallel to strike southeast along same structure as (A). Flaggy breccia clasts (examples outlined in white), variably slickensided and oriented. (C) Cobble-sized, slickensided clasts (white arrow) within a recrystallized calcite matrix. (D) Calcite-encrusted outcrop containing several boulder-sized, angular clasts. Well-developed calcite steps are exposed on the clast marked by the white arrow just above William Chandonia.

as the Murie Creek thrust system. From west to east, the first Murie Creek thrust (MCT¹ in plates 2A and 3; figure 16) is a shorter, discontinuous thrust in the Dinosaur Canyon Member of the Moenave Formation. We show it as an independent thrust rather than a splay of the longer Murie Creek thrust (e.g., MCT² in figure 17; plates 2A and 3). The second Murie Creek thrust is a longer, continuous thrust that crops out near Kanarra Creek (308910 m E.; 4156517 m N.) within the Kayenta Formation and can be traced for 5 km to the north. Displacement along this thrust is revealed by folding and truncation of Kayenta strata at the upper contact of the Springdale Sandstone Member in Kanarra Creek.

The first Murie Creek thrust crops out south of Spring Creek where it displaces the Dinosaur Canyon Member over the Springdale Sandstone (307900 m E., 4154070 m N.). The thrust is well exposed where Spring

Creek erodes through the topographic ridge underlain by sandstones of the Springdale Sandstone Member. Looking south along this ridge, a thick, persistent sandstone ledge in the Dinosaur Canyon Member forms a prominent “T” discordance where it is folded and displaced over itself along the thrust plane (figure 16; plates 2A and 3). Bedding above the thrust is overturned and shallow dipping (about 30°), whereas bedding beneath the thrust is steeply overturned (about 65 to 70°). Looking north of Spring Creek along the continuation of this topographic ridge, the structural pattern is repeated but partially obscured by mass wasting and vegetation (figure 25). High on the topographic ridge, the thrust displaces the lower Springdale Sandstone Member contact before it dies out. Farther north towards Kanarra Creek, the first Murie Creek thrust recurs for a short distance where it again thrusts the Dinosaur Canyon Member



Figure 23. (A) Overturned, slickensided outcrop of the Virgin Limestone Member. Examples of slickensided shear fractures marked by white arrows, slip direction by black arrow. View northeast, Daniel Quick for scale (1.84 m). Lower right: diagram of mineral fiber steps characteristic of fault-related shear fractures in carbonates. Slip direction is down the mineral fiber steps, and arrow points in the direction of motion of the missing block (from Allmendinger and others, 1989). (B) View to northeast of another overturned, slickensided limestone outcrop nearby. White arrow points to a thrust-sense shear fracture (hanging wall moved up and east) exposed near the rock hammer; right hand rule strike, dip, and slip direction rake: 210, 84, and 83. Inset: close-up of the same shear fracture showing the mineral fiber steps, with black arrow showing the slip direction of the missing block. (C) Slickensided outcrop near the Spring Creek thrust contact, north of Kanarra Creek, view to west. White arrows show shear surfaces that are out of the plane of view, whereas black arrows show slip direction on the visible shear surfaces. The shear fracture set contains strike- and thrust-slip conjugate shear surfaces. Closest fracture to viewer (long sub-horizontal slip direction arrow) is dextral strike-slip; right hand rule strike, dip, and slip direction rake: 187, 87, and 5. (D) View west onto a slickensided outcrop northeast of (A). Stereonet shows the spatial relationship here between bedding (black) and the shear fracture (red), produced with the Stereonet 11 software (Allmendinger and others, 2013; Cardozo and Allmendinger, 2013).

over the Springdale Sandstone Member (figure 25; plates 2A and 3). Truncation of the Petrified Forest Member of the Chinle Formation indicates the thrust may initiate farther down section, but the contact is complicated by mass wasting and by a late, across-strike normal fault (308220 m E.; 4155780 m N.). North of Kanarra Creek, fractured Dinosaur Canyon Member and discordance with Springdale Sandstone bedding at the contact indicate the presence of the first Murie Creek thrust, but displacement is visibly diminished, and the thrust dies out (308940 m E., 4156670 m N.).

The trace of the second Murie Creek thrust initiates just south of Kanarra Creek where the main body of the Kayenta Formation is dramatically thinned by the fault (plates 2A and 3; 308730 m E., 4156050 m N.). The thrust crops out along the Kanarra Creek Falls trail, where the creek has eroded through the topographic ridge formed by the Dinosaur Canyon and Spring Creek Sandstone Members. The thrust is marked where overturned sandstones of the Springdale Sandstone define an east-verging fold in the hanging wall of the thrust (figure 26). The fold is a composite fold-thrust struc-

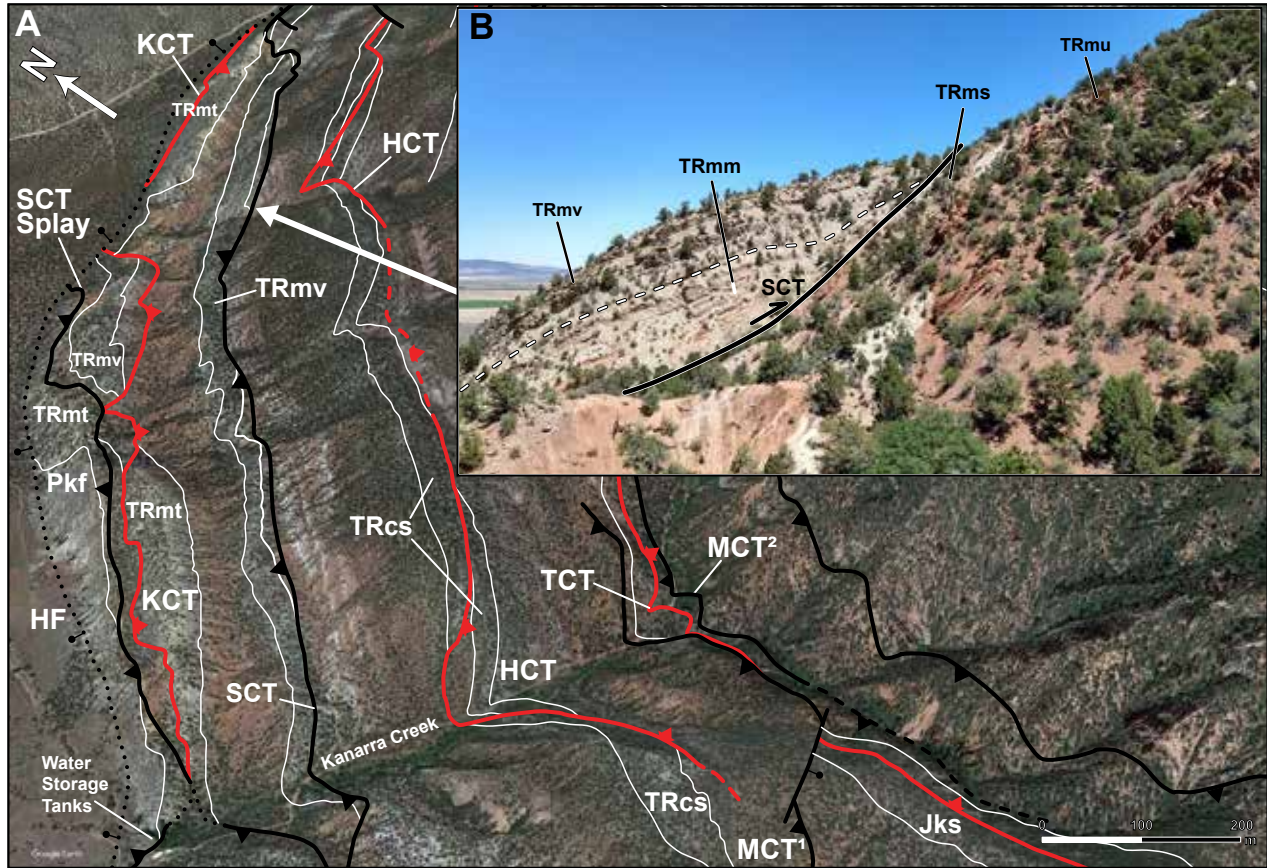


Figure 24. (A) Google Earth 3D terrain view looking northeast into Kanarra Creek. (B) The Spring Creek thrust main trace seen looking north within an unnamed stream cut just north of Kanarra Creek. As in the other two creeks, the structural pattern of the Virgin Limestone Member of the Moenkopi Formation being displaced over and truncating the Shnabkaib Member of the Moenkopi is continued here. A sliver of the middle red member of the Moenkopi containing a thick, double layer of gypsum persists all along the Spring Creek thrust hanging wall. The gypsum layers outcrop below the contact of the Virgin Limestone Member with the middle red member and are indicated here by the dashed white and black line. Structure initializations: HF–Hurricane fault; KCT–Kanarra Creek thrust; SCT–Spring Creek thrust; TCT–Taylor Creek thrust; HCT–Hicks Creek thrust; MCT^{1,2}–Murie Creek thrust^{1,2}. See plate 2B (stratigraphic column) for explanation of map unit symbols.

ture. We interpret faults in the nose and on the front limb of this fold as small, older, east-directed thrusts, which were subsequently folded. These faults are well exposed along the trail on the north side of the creek where slickensides show normal separation, but rotation of the steep west-dipping (about 81° W.) bedding back to the local average orientation along the ridge (about 45° W.) shows a pre-folding thrust sense of motion with an average dip about 10° greater than bedding (see table 3). To the north, the Kayenta Formation thins dramatically as the second Murie Creek contin-

ues along the Springdale Sandstone Member-Kayenta Formation contact north towards Short Creek (plates 2A and 3). Thinning of this unit, based on our measurement using GMDE (Allmendinger, 2020) and published thicknesses for the area (plate 2B), indicate a 63% reduction from 120 to 46 m along the main body of the Kayenta Formation. We interpret the reduced thickness is a result of movement along the second Murie Creek thrust, and east-directed thrusting of the Springdale Sandstone Member over the Kayenta Formation. The trace of the second Murie Creek thrust can be followed

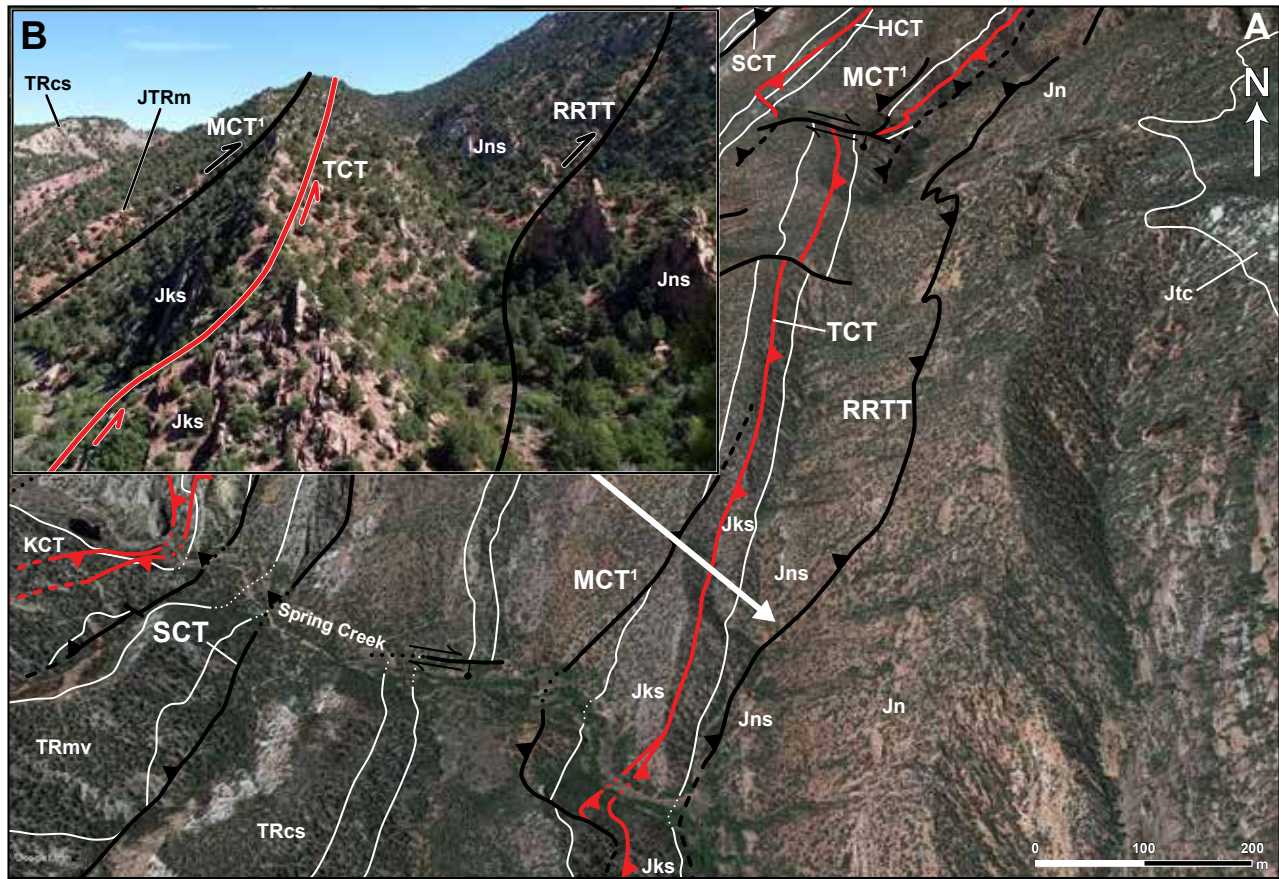


Figure 25. (A) Google Earth 3D terrain view looking north into Spring Creek. The Red Rock Trail thrust cuts the Shurtz Tongue of the Navajo Sandstone as it makes its way up section. The Spring Creek thrust, Taylor Creek thrust, and cross faults shown for reference to the map. (B) Along-strike view northward of the Red Rock Trail thrust cataclasite zone, seen here as thinned Kayenta Formation and offset Shurtz Tongue—through outcrop observations in the field, we connect this displacement to the Red Rock Trail cataclasite along a steep, late-formed, east-verging thrust, the Red Rock Trail thrust. Also shown is the overturned Taylor Creek thrust and the Murie Creek thrust¹. Structure initializations: KCT—Kanarra Creek thrust; SCT—Spring Creek thrust; TCT—Taylor Creek thrust; HCT—Hicks Creek thrust; MCT¹—Murie Creek thrust¹; RRTT—Red Rock Trail thrust. See plate 2B (stratigraphic column) for explanation of map unit symbols.

north to Murie Creek where the thrust is truncated by the Murie Creek fault, along with the rest of the fold limb (plates 2A and 3).

The Red Rock Trail thrust: The Red Rock Trail thrust is the largest and easternmost thrust in the map area (plates 2A and 3). Minor thrusts and buckle folds, which we associate with the Kanarra fold-thrust structure, do crop out farther to the east of the Red Rock Trail thrust (plates 2A and 3). The Red Rock Trail thrust can be traced from Spring Creek to where it abuts the Murie Creek fault. In the Cedar Mountain quadrangle (Averitt, 1962; Doelling, 1972), the trace of the fault

is less obvious but can be inferred by the presence of the cataclasite in the Navajo Sandstone (T.R. Knudsen, Utah Geological Survey, written communication, 2022). The Red Rock Trail thrust outcrops in the Cedar City 7.5-minute quadrangle (plate 2A) and we suggest it crops out in Parowan Gap as well (see discussion below). It begins within the Kayenta Formation near the Springdale Sandstone Member contact in Spring Creek and cuts up section through the Navajo Sandstone, forming a persistent, poorly consolidated cataclasite zone at the Kayenta–Navajo contact (plates 2A and 3; figures 25 and 27). Here, a resistant lens of the Shurtz Tongue of the Navajo crops out from the creek bed,

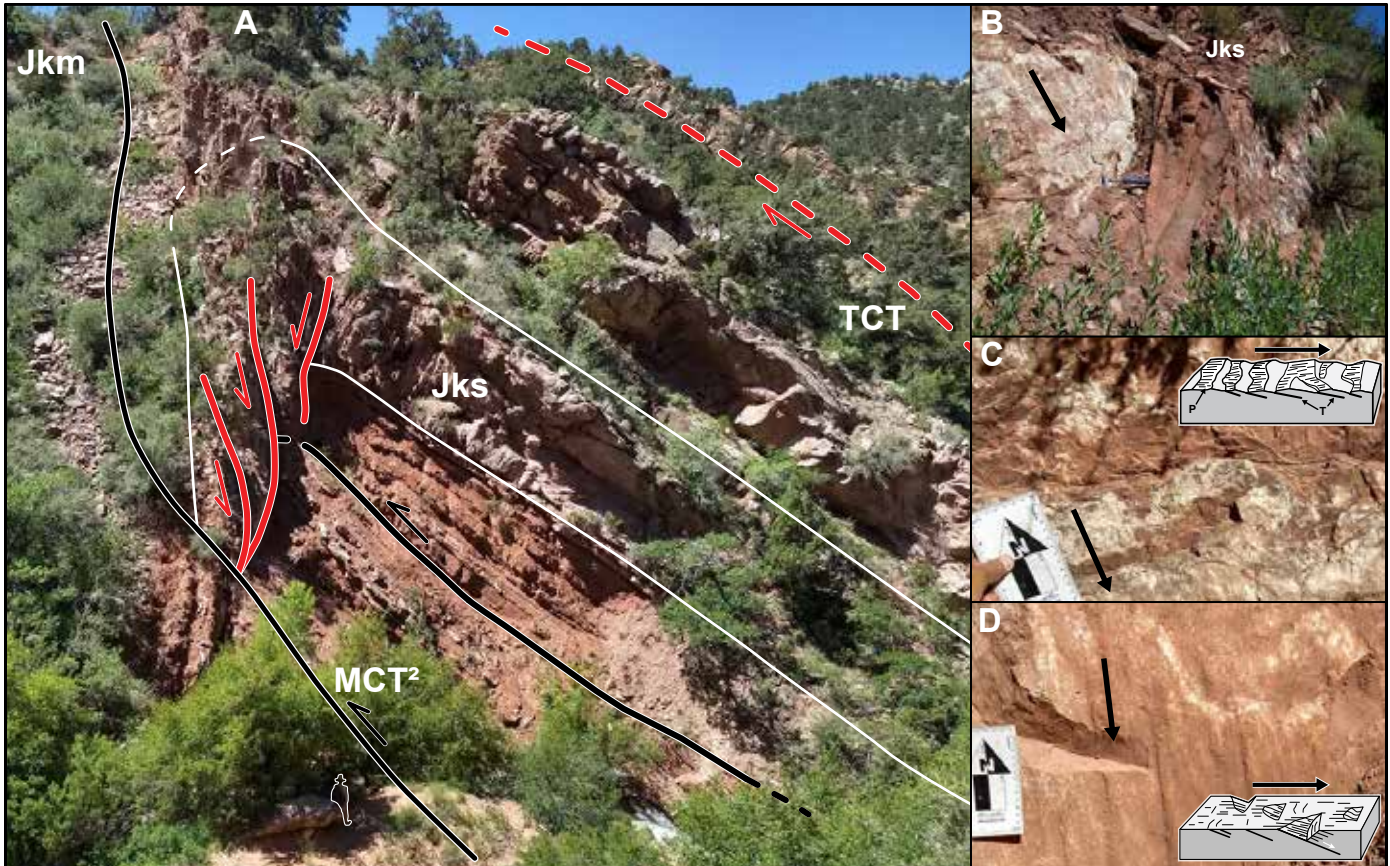


Figure 26. (A) View to south upon a fold-thrust structure in the Springdale Sandstone Member and part of the main body of the Kayenta Formation on the Murie Creek thrust² hanging wall. Vergence demonstrates tops-to-the-east motion. Daniel Quick (outlined in white, bottom foreground) takes in the view to the south closer to the outcrop. Earlier thrusts with tops-to-the-east motion, which are now folded within the hanging wall are in solid red. (B) Outcrop of the fold limb where it is exposed looking northwest on the trail at the north side of Kanarra Creek, containing bedding-discordant, slickensided shear surfaces; right hand rule strike, dip, and slip direction rake of marked white slickenside: 218, 88, and 82. Slip direction of the missing block (black arrow) is consistent with earlier, tops-to-the-east folded thrusts. (C) P-T shear fractures along the fold limb outcrop in (B) with black arrow showing slip direction of the missing block; right hand rule strike, dip, and slip direction rake: 42, 83, and 68. Upper right: diagram of P-T shears along a fracture surface, arrow pointing in the direction of motion of the missing block. (D) Slickensided shear fracture surface with well-developed, lunate R shear, black arrow points to direction of motion of missing block; right hand rule strike, dip, and slip direction rake: 210, 87, and 84. Lower right: diagram of R shears along a fracture surface, arrow pointing in the direction of motion of the missing block. Diagrams in (C) and (D) from Petit (1987) and Allmendinger and others (1989). Structure initializations: TCT–Taylor Creek thrust; MCT²–Murie Creek thrust². See plate 2B (stratigraphic column) for explanation of map unit symbols.

striking obliquely to adjacent strata. This lens is truncated and offset 150 m to the north along the southernmost expression of the Red Rock Trail thrust as it ramps up section. The cliffs near the contact are mantled with talus of pervasively slickensided clasts derived from the fault damage zone. The cataclasite zone is well exposed and readily accessible on the Red Rock Trail (308700 m E.; 4155320 m N.). The fault damage zone associated

with the Red Rock Trail thrust is mapped as a cataclasite derived from the Navajo Sandstone (i.e., Jnc, see plates 2A and 3). As with other thrusts along the Kanarra fold, the Red Rock Trail thrust is more likely a thrust fault system, but individual thrusts within the cataclasite are difficult to trace. Within the central section of the Kanarra fold-thrust structure, the Red Rock Trail thrust forms the contact between the Kayenta Formation and

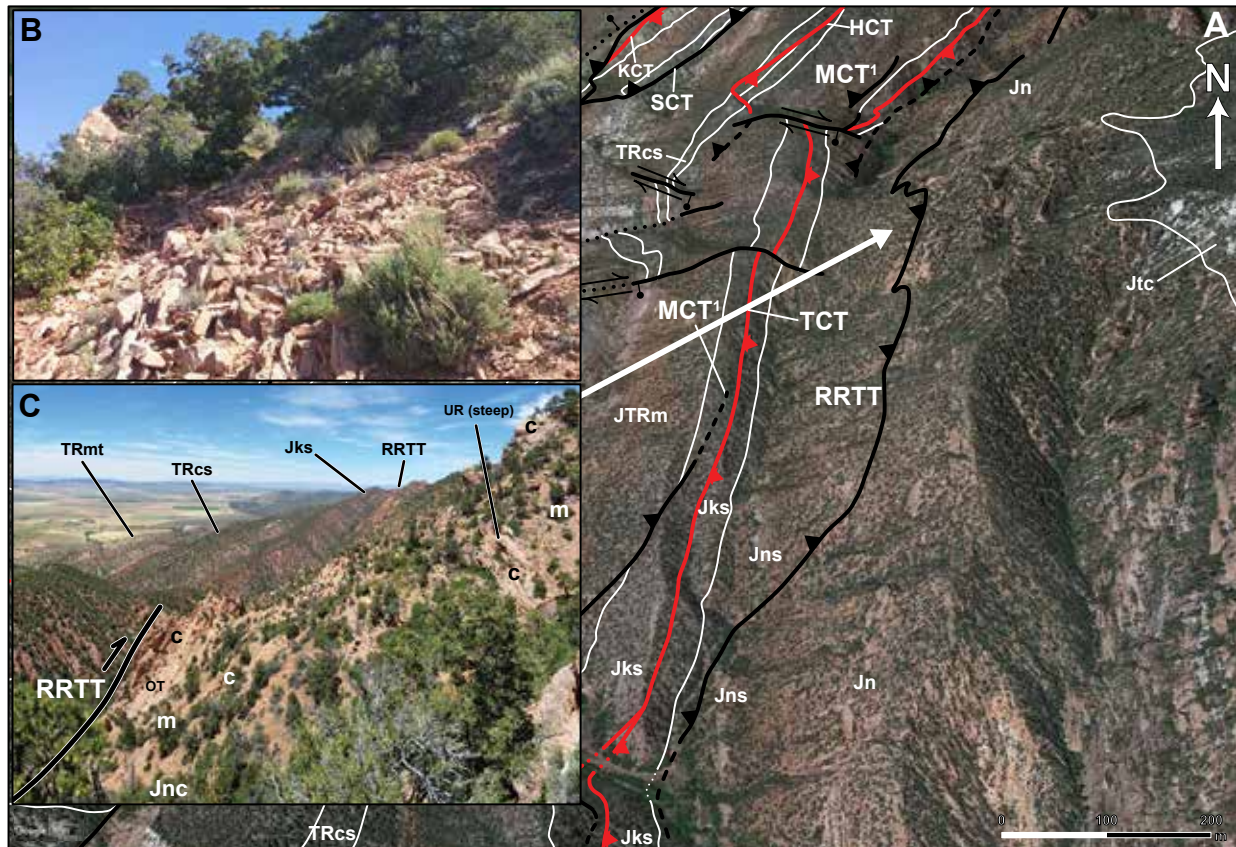


Figure 27. (A) Google Earth 3D terrain view looking north into Spring Creek. Selected faults and sedimentary contacts shown for reference to the map. (B) View looking north on the Red Rock Trail above the Kayenta Formation-Navajo Sandstone contact. Foreground: flaggy, slickensided clasts of Navajo cataclasite eroding off an outcrop above that is out of the view of the photograph. (C) View of the Red Rock Trail thrust, looking northeast while standing on the Red Rock Trail after crossing the thrust contact. Cobble-sized and smaller slickensided clasts (m, matrix) surround larger boulder to outcrop sized clasts (c, clast). Overturned (OT), west-dipping Navajo sandstone beds are thrust over steep, upright (UR), east-dipping beds. Prominent, overturned ridge formers on the exposed front limb of the Kanarra fold-thrust structure are marked for reference. Photograph by John P. Hogan. Structure initializations: KCT–Kanarra Creek thrust; SCT–Spring Creek thrust; TCT–Taylor Creek thrust; HCT–Hicks Creek thrust; MCT'–Murie Creek thrust'; RRTT–Red Rock Trail thrust. See plate 2B (stratigraphic column) for explanation of map unit symbols.

the cataclasite developed in the Navajo Sandstone.

North of Spring Creek, talus aprons of cataclasite appear on the Kayenta-Navajo cliff face, indicating the presence of the Red Rock Trail thrust damage zone. Direct accessibility is poor due to the steepness of the cliff. The Red Rock Trail thrust crops out along the Red Rock Trail, and it is here that a damage zone consisting of a moderately indurated fault megabreccia—outcrop-sized clasts of faulted Navajo surrounded by a matrix of smaller clasts (e.g., see “C” and “M” on figure 27C)—is well exposed at the fault contact with the Kayenta Formation and Navajo Sandstone and the planar-bedded, steeply

overturned Navajo Sandstone is pervasively slickensided and host sets of deformation bands. Farther east into the damage zone, remnant steep, upright bedding indicates fault-related discordance with overturned Navajo in the hanging wall of the thrust. Approximately 100 m east along the Red Rock Trail and farther into the Navajo, the megabreccia gives way to intact rock.

At Kanarra Creek, near the entrance to the Kanarra Falls slot canyon, the trace of the Red Rock Trail thrust is marked by strong discordance in bedding dips between channel sands in the Kayenta Formation and planar-bedded sandstone of the Navajo Sandstone (figure

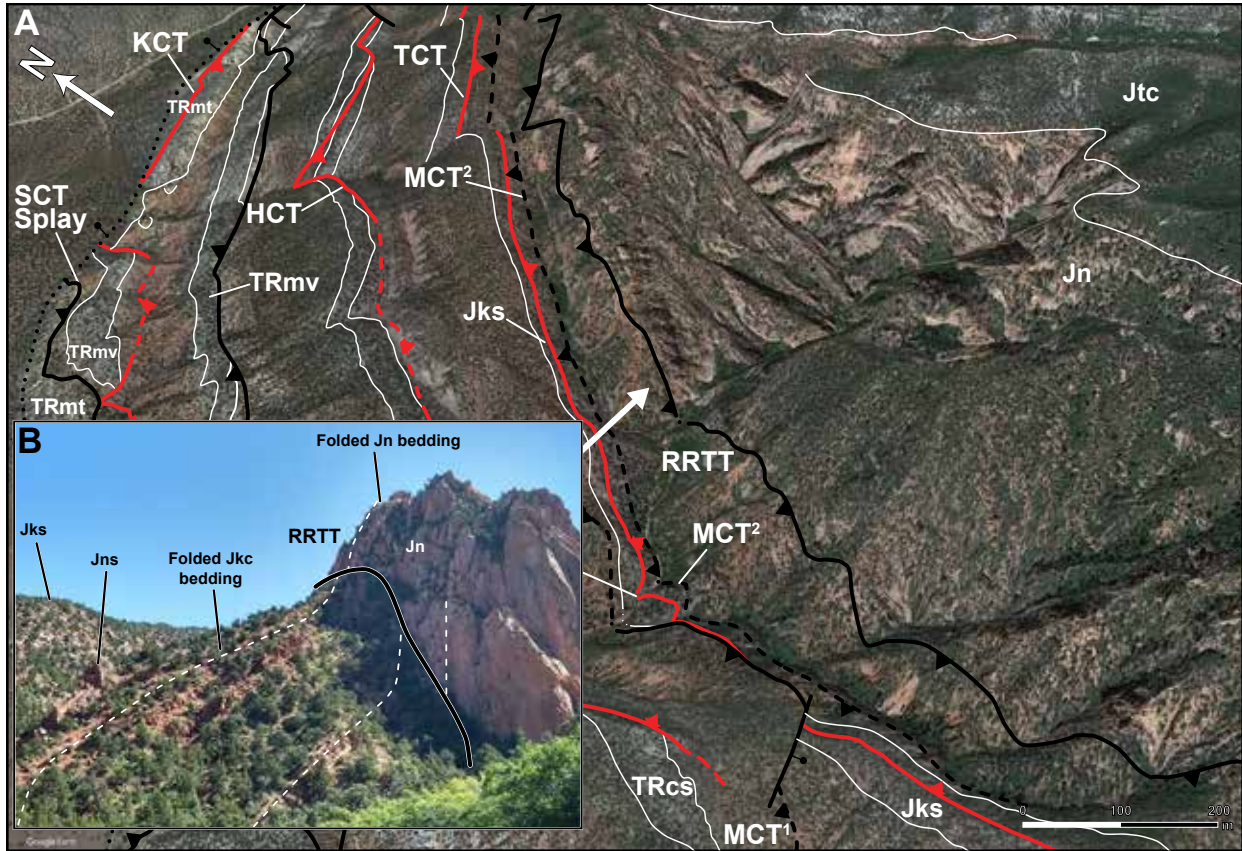


Figure 28. (A) Google Earth 3D Terrain view of the Red Rock Trail thrust, looking northeast into Kanarra Creek. Late-formed thrusts (Spring Creek thrust, Murie Creek thrust) shown for reference to the map. (B) View looking northeast onto Jurassic units exposed near Kanarra Creek. Folded Kayenta Formation (beds outlined in dashed white lines) abuts steep, overturned Navajo Sandstone along the Red Rock Trail thrust. Part of this contact may be complicated by the presence of an older, east-dipping thrust (e.g., Averitt, 1967). Structure initializations: KCT–Kanarra Creek thrust; SCT–Spring Creek thrust; TCT–Taylor Creek thrust; HCT–Hicks Creek thrust; MCT^{1,2}–Murie Creek thrust^{1,2}; RRTT–Red Rock Trail thrust. See plate 2B (stratigraphic column) for explanation of map unit symbols.

28; plates 2A and 3). This discordance reflects folding of the Kayenta Formation along the thrust (figure 28B). In the foreground of figure 28B, beds of Navajo Sandstone have been rotated to vertical and in the canyon to the east they return to upright, gentle eastward dips. To the north of the slot canyon, steeply overturned, folded planar beds of the Navajo Sandstone, seen in the background of figure 28B, are in fault contact with significantly thinned, shallow-dipping, overturned strata of the Kayenta Formation. Though the Red Rock Trail thrust appears to dip steeply to the east (i.e., verge west) at Kanarra Creek, the dominant vergence along

the thrust is to the east. Here the thrust contact may be complicated by the presence of an older, east-dipping thrust (see Averitt, 1967). However, we associate this earlier interpretation with sinistral, out-of-the-syncline flexural slip and disharmonic folding of thin Kayenta sandstone lenses adjacent to a thick, competent control unit, the Navajo Sandstone—see the **Discussion** section for further details.

At the saddle by the next canyon to the north (plate 2A; figure 3; 310000 m E., 4157700 m N.) the Cedar City Tongue of the Kayenta Formation is attenuated with a minimum 62% reduction, measured using GMDE

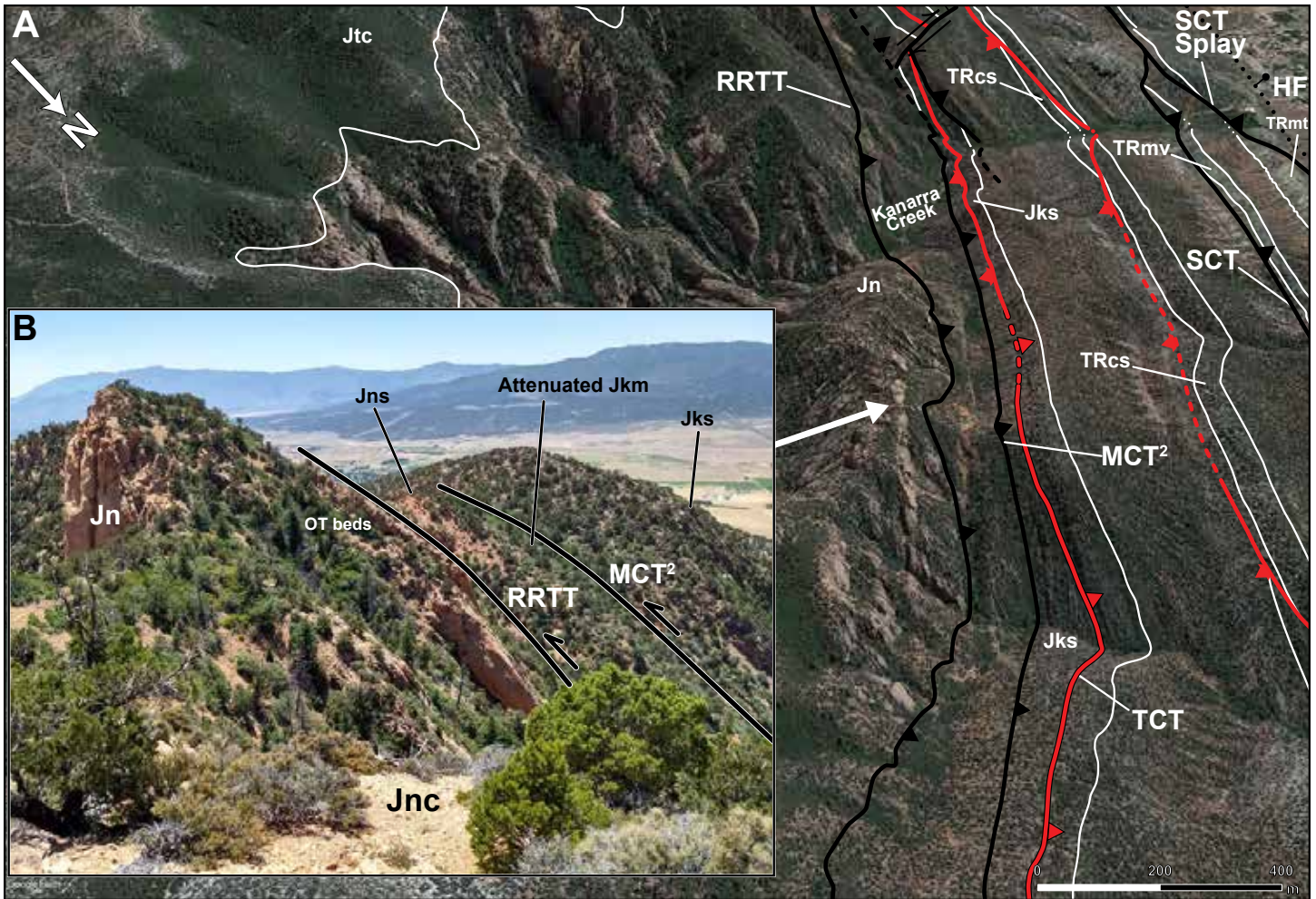


Figure 29. (A) Google Earth 3D terrain view looking south towards Kanarra Creek. Selected faults and sedimentary contacts are shown for reference to the map. (B) View to the southwest of the Red Rock Trail thrust contact at the head of the stream cut north of Kanarra Creek. Here the Navajo Sandstone is overturned (OT). The contact is partially occluded where it Vs westward, down the cliff. Beginning here at the contact, isolated outcrops of pervasively fractured Navajo mantled by slickensided talus define a megabreccia shear zone tens of meters wide. The main body and Cedar City Tongue of the Kayenta Formation are thinned near the contact. Structure initializations: HF–Hurricane fault; SCT–Spring Creek thrust; TCT–Taylor Creek thrust; MCT²–Murie Creek thrust²; RRTT–Red Rock Trail thrust. See plate 2B (stratigraphic column) for explanation of map unit symbols.

(Allmendinger, 2020), in thickness along the Red Rock Trail thrust (figure 29). The thrust contact dips moderately westward (about 50°), and overturned beds of the Kayenta Formation are displaced over steeply dipping, overturned Navajo Sandstone. East of the fault contact, the damage zone persists for 200 to 300 m into the Navajo Sandstone. Talus of slickensided cataclasite mantle the top of the cliff (figure 29B). In this view, the damage zone can be traced from the foreground, through the vegetation, into the background to include steeply dip-

ping, isolated outcrops of Navajo Sandstone.

The Red Rock Trail thrust and damage zone continue northward along the cliffs in the Navajo Sandstone. In the northeast part of the map area between Short and Murie Creeks, dips on the Carmel Formation as high as 39° are observed (plates 2A and 3); the Carmel is steeply overturned (about 85° W.) at Murie Creek. At the flatiron near the head of Murie Creek (311970 m E.; 4159330 m N.) both the Kayenta Formation and the Navajo Sandstone are overturned and dipping about 45 to

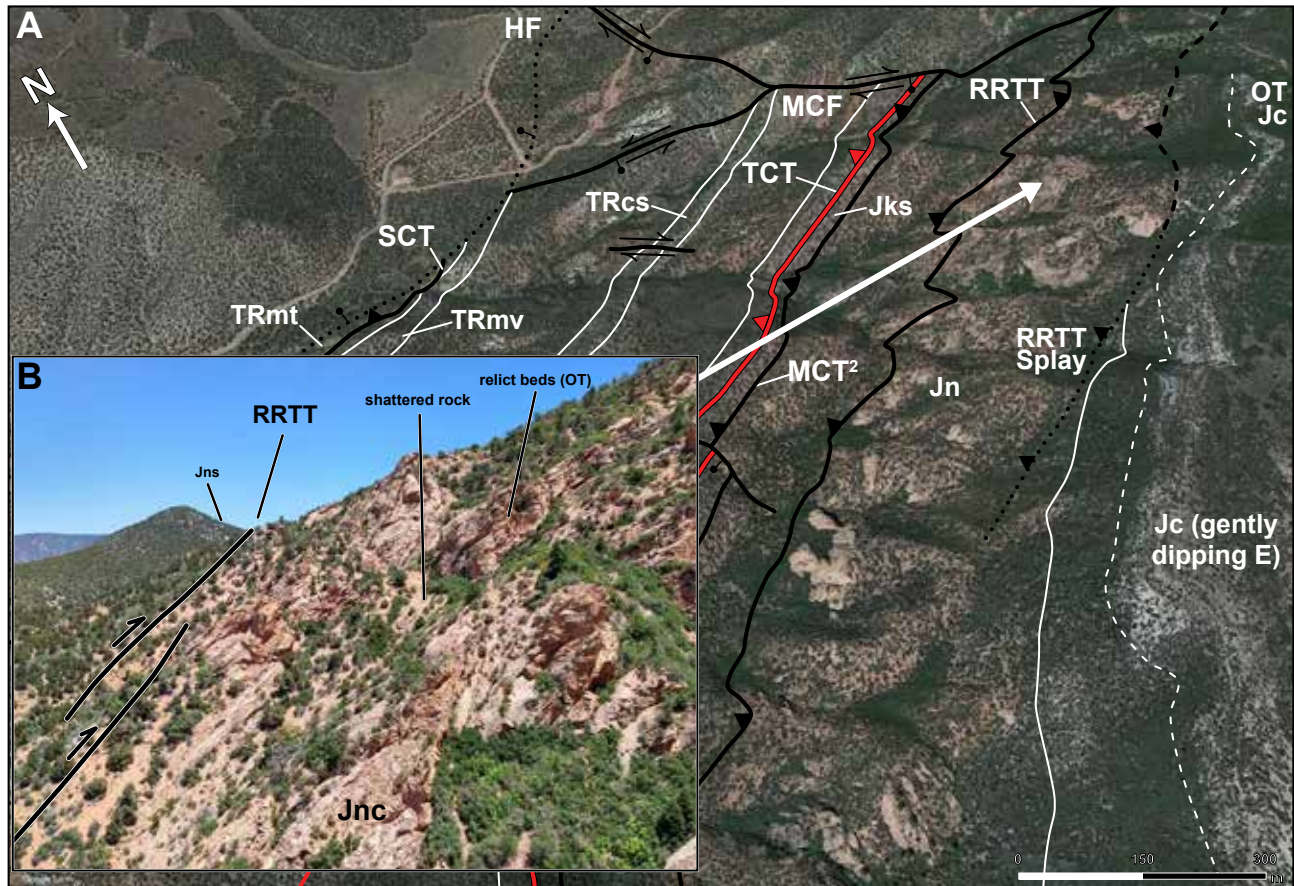


Figure 30. (A) Google Earth 3D terrain view looking north into Short and Murie Creeks. Traces of the Spring Creek, Taylor Creek, and Murie Creek² thrusts are shown for reference. To the east, a splay of the Red Rock Trail thrust truncates the Navajo-Carmel contact, denoted by the solid white line (T.R. Knudsen, Utah Geological Survey, written communication, 2022). Gently east-dipping Carmel steepens and overturns east of the fault zone. The outcrop pattern of a white layer in the upper Co-op Creek Limestone Member of the Carmel Formation (bottom of white layer shown by white dashed line) and associated west-dipping flatiron emphasizes the overturning of the unit (OT) near the thrust. (B) View of the Red Rock Trail thrust contact on the southern fork of Murie Creek. Relict bedding along isolated outcrop-sized clasts within the Navajo Sandstone cataclasite (Jnc) shear zone is overturned beyond 40° in some places, and the thrust appears to exploit the shallow-dipping Navajo bedding planes and weak Kayenta siltstone beds. Structure initializations: HF—Hurricane fault; SCT—Spring Creek thrust; TCT—Taylor Creek thrust; MCF—Murie Creek fault; MCT²—Murie Creek thrust²; RRTT—Red Rock Trail thrust. See plate 2B (stratigraphic column) for explanation of map unit symbols.

55° to the west along the east verging thrust (figure 30). Sharp deflection of Carmel strata into steep, overturned orientations (figure 30A, right, dashed white line in the Carmel) suggests the thrust cuts up section. The high-strain zone is characterized by a great density of fractures, imparting a shattered appearance (i.e., cataclasite) to the Navajo Sandstone within the fault damage zone (figure 30B). Movement within the fault megabreccia cataclasite zone appears to have rotated isolated outcrops of clasts of Navajo Sandstone with relict bedding

to shallow, westward dips (figure 30B, right midground). A splay of the Red Rock Trail thrusts crops out to the east of the main trace and displaces Navajo Sandstone eastward on top of the upper Co-op Creek Limestone Member of the Carmel Formation (T.R. Knudsen, Utah Geological Survey, written communication, 2022). The Red Rock Trail thrust, splay, and damage zone continue northwards and abut against the Murie Creek fault (figure 30; plate 2A; 313000 m E.; 4159750 m N.).

Cross Faults

Other faults with ambiguous temporal relationships between Sevier folding and Basin and Range tectonism are cross faults. Where exposed along the Kanarra fold-thrust structure, cross faults vary in size from tens of meters to kilometers in length (e.g., the Murie Creek fault), tend to cut across bedding, nearly orthogonal to strike, and appear to be exclusive to the overturned limb of the leading anticline (see plates 2A and 3). Estimates of displacement along many of these cross faults indicate a greater horizontal (i.e., strike slip) component than vertical (i.e., dip slip) component (e.g., the Murie Creek fault, also see Averitt, 1962). Cropping out at The Red Hill is a cross fault, similar in size to the Murie Creek fault but with opposite polarity that we refer to as the Thunderbird Gardens Trail fault (plate 1, also see Knudsen, 2014a). These two prominent cross faults displace much of the “salient” northern section of the Kanarra fold-thrust structure upward and to the east (plate 1). The Murie Creek and Thunderbird Gardens Trail faults indicate many of the cross faults associated with the Kanarra fold-thrust structure are likely tear faults or lateral ramps that developed during folding.

Other cross faults include the approximately 800-m-long cross fault along the Spring Creek saddle. This cross fault affected units from the Shnabkaib Member to the Springdale Sandstone Member (figures 16 and 27; plates 2A and 3; also see Biek and Hayden, 2016). Notable cutoffs of the Shinarump crop out north of the saddle (308150 m E.; 4155290 m N.) and along the Springdale Sandstone (308390 m E.; 4155290 m N.). This cross fault exhibits right-lateral separation and limited down-to-the-south vertical displacement. The extent of this fault is unclear, as its western trace is concealed beneath a landslide deposit along part of the Red Rock Trail. Spatial relationships between the Shnabkaib Member north and south of the Spring Creek saddle (plates 2A and 3) indicate the fault may either disturb or truncate against the Spring Creek thrust fault. Another, smaller cross fault, antithetic to the Spring Creek saddle cross fault, is revealed by offset across the Shnabkaib Member (plates 2A and 3) farther to the north (308150 m E.; 4155654 m N.). Along the rest of the fold limb other, smaller cross faults are endemic to competent units in the Jurassic section,

and particularly affect the Dinosaur Canyon Member, Springdale Sandstone, and Shurtz Tongue of the Navajo Sandstone.

Extension Faults—Hurricane Fault Zone

The Kanarra fold-thrust structure is crosscut by later extension faults. These notably include the Hurricane fault, as well as other faults also associated with the Basin and Range transition zone (figure 1; plate 1). Faults of the transition zone are largely restricted to the High Plateaus immediately adjacent the Kanarra fold-thrust structure. Prominent examples of transition zone faults are the Cougar Mountain, Bear Trap Canyon, and Lone Tree Mountain faults (Gregory and Williams, 1947; Averitt, 1962; Biek and others, 2009; Knudsen, 2014a; Biek and Hayden, 2016). Displacement along the transition zone faults rotates the regional dip adjacent to the Kanarra fold-thrust structure syncline axis, which approaches 6° east in the field area and 3 to 5° west near Cedar City.

The Hurricane fault crosscuts the Kanarra fold-thrust structure, displacing the trailing western limb of the anticline in the hanging wall down to the west (plates 2A and 3). The main trace of the Hurricane fault is largely concealed beneath colluvium and alluvial-fan deposits from the Hurricane Cliffs. However, subsidiary normal faults associated with Basin and Range extension can produce complex horse configurations (Biek, 2003b, 2007a; Hurlow and Biek, 2003; Biek and others, 2009). Several large splays of the Hurricane fault, south of the study area, displace Moenkopi strata down onto Permian units or completely cut out the Paleozoic section (plate 1; Biek 2007a; Biek and others, 2009). Within the central part of the Kanarra fold-thrust structure, far fewer splays of the Hurricane fault are present and crop out near (less than 150 m) the main trace of the Hurricane fault. We recognize one notable splay just south of Kanarra Creek along the Kanarra Creek Trail; the other splays are largely restricted to Camp Creek.

The best exposed Hurricane fault splays in the central area of the fold crop out en échelon at the mouth of Camp Creek, where they complicate the leading anticline hinge zone (figure 3; 305800 m E.; 4153000 m N.). Here, short (less than 250 m long), low-displacement

normal faults form gently curved fault traces sub-parallel to the local strike of bedding. In figure 11, two of the three mappable splays can be seen; the largest (westernmost) is a synthetic fault splay, and the eastern, middle splay is antithetic to the Hurricane fault. Slickenside measurements and map patterns indicate down-to-the-west movement on the western and eastern splays, with little lateral motion (most slickenline rakes are between 87 to 93°). The middle, antithetic splay forms a miniature horst of Rock Canyon Conglomerate Member of the Moenkopi Formation (figure 8; plate 3). The largest and westernmost splay at Camp Creek forms a prominent, steeply west-dipping (65 to 70°) fault scarp along the Rock Canyon Conglomerate Member of the Moenkopi Formation. A trail leading into Camp Creek directly follows the scarp strike for about 50 m as it climbs in elevation, allowing good access to slickensides. Near the start of the trail, black banded, chert-rich Fossil Mountain Member is exposed in the footwall of the splay, with Rock Canyon Conglomerate unconformably mantling it (figure 8C, inset). The splay displaces an outcrop of ledge-forming lower Timpoweap Member down to the west, where it rests beside the upper contact of the Fossil Mountain Member. Thus, based on the observed dip slip movement, minimal stratigraphic separation along this splay (i.e., throw) is in the tens of meters. Farther east into Camp Creek, steep, west-dipping fractures with minimal detectable displacement outcrop on the canyon walls (figure 8B). These observations indicate more deformation and may represent a damage zone associated with the fault. This suggests a short zone (tens of meters) of decreasing displacement east from the main Hurricane fault zone.

DISCUSSION

The Kanarra Fold-Thrust Structure

In southwestern Utah, deformation associated with the leading edge of the Sevier fold-thrust belt resulted in formation of multiple thrusts, such as the Square Top Mountain, Iron Springs, and Red Rock Trail thrusts. Deformation was also manifested as prominent folds, such as the Virgin, Pintura, and the Kanarra anticlines (see figure 1; plate 1). These contractional structures are the result of regional layer-parallel compression associ-

ated with plate convergence along the Cordilleran orogen (Yonkee and Weil, 2015). The hanging wall cover rocks were translated along a detachment several hundred meters above the crystalline basement within the Cambrian Bright Angel Shale and, potentially, the lower incompetent layers of the Cambrian Bonanza King Formation (Hintze, 2005; see cross sections A–A' and B–B' in Biek and others, 2009). Folding and thrusting are closely associated, and these fold-thrust structures (e.g., Butler and others, 2020) are thought to have localized blind thrust ramps during folding (e.g., the Virgin Dome; see Biek, 2003a, 2003b).

Early Fold Accommodation Faults

The initial stages of folding likely involved multilayer buckling (break-thrust folds of Willis 1893; Currie and others, 1962; Fischer and others, 1992), followed by thrusting (Eisenstadt and De Paor, 1987; fault propagation folding of Williams and Chapman, 1983; see figure 15, p. 18, in Cawood and Bond, 2020). During buckling, many of these folds developed fold accommodation faults known as limb wedge thrusts or flank thrusts (e.g., Cloos, 1961, 1964; Fail and Wells, 1974, Eisenstadt and De Paor, 1987; Mitra, 2002a). These flank thrusts likely formed due to significant differences in thickness and competence between the currently exposed, relatively thin Paleozoic-Mesozoic ridge formers—namely the Timpoweap and Shinarump Conglomerate Members of the Moenkopi Formation and Springdale Sandstone Member of the Kayenta Formation—and much thicker, incompetent units—the Triassic red beds of the Moenkopi Formation, Petrified Forest Member of the Chinle Formation, and Kayenta Formation. Long-wavelength buckling of thick, competent control units—the Cambrian Bonanza King–Nopah Dolomite, Mississippian Redwall Limestone, Permian Queantoweap Sandstone, and Jurassic Navajo Sandstone—may have determined the development of flank thrusts by inducing more intense buckling of thinner adjacent competent layers (e.g., Currie and others, 1962; Fischer and others, 1992; Davis and others, 2011, p. 384–390). Initial buckling within thin, competent layers transitions to accommodation of folding via thrusting once the layer can no longer fold, as seen on the west flank of the Virgin an-

ticline where an east-directed flank thrust (i.e., a proxy for the Hicks Creek thrust) crops out near Leeds, Utah (see cross section A–A' and B–B' in Biek 2003a, and cross section D–D' in Biek, 2003b).

The Virgin, Pintura, and Kanarra anticlines all exhibit similar structural styles, as they share a stratigraphy with similar mechanical strength properties related to early development of flank thrusts within competent units on the limbs of gentle to open folds (e.g., the thrusts at Leeds, Utah, on the Virgin anticline; see Biek, 2003a; Biek, 2003b). The presence of flank thrusts in the nascent stages of folding greatly affects the structural evolution of the fold as the amount of shortening increases; for example, along the strike of the axis of the leading anticline of the Kanarra fold-thrust structure.

Along most of its length, the Kanarra fold is upright, excepting local displacement by fold accommodation faults, such as that seen in the hanging wall of Hurlow and Biek's (2003) Taylor Creek fault. The deepest structural levels of the fold crop out near its southern terminus between Pintura and Toquerville. At Camp Creek, early formed flank thrusts (e.g., the Kanarra Creek and Taylor Creek thrusts) along the east-dipping, upright limb of the open leading anticline are upright west-verging thrusts (plates 2A and 3). Along strike to the north, the amount of shortening increases and leads to development of a fold style with many attributes of a fault propagation fold, including a gently dipping trailing fold limb and a steeply dipping, overturned leading fold limb (figure 7; cf., Davis and others, 2011, p. 414–428). Early formed flank thrusts along the eastern limb (e.g., Taylor Creek thrusts, plate 3, figures 7 and 15) were rotated, along with the stratigraphy, into steeply dipping to overturned orientations as the fold tightened. The resulting geometry of stratigraphic units juxtaposed along overturned early formed flank thrusts (e.g., Hicks Creek thrust, see figure 19) previously led to a two-dimensional, separation-based interpretation of these faults as normal faults. This is a misrepresentation of these folded thrusts and obscures their true structural significance in the development of the Kanarra fold-thrust structure. Slip will cease along an early formed flank thrust if the fault plane is rotated into an unfavorable orientation for failure with respect to the regional stress field (e.g., Kanarra Creek thrust, figure

11). In contrast, early formed flank thrusts on the trailing limb of the fold, such as the Spring Creek thrust, remain in favorable orientations for slip along the fault plane and continued to do so as the fold tightened. This is demonstrated by displacement of the folded Kanarra Creek thrust by the Spring Creek thrust (figures 7, 11, and 13). Earlier movement along the Spring Creek thrusts at depth resulted in the development of a fault-bend fold in the trailing limb of the anticline, imparting a broad crest profile, similar to a box fold, for the Kanarra anticline (figures 7 and 31).

Late Fold Accommodation Faults

Higher degrees of shortening in the central section of the Kanarra fold-thrust structure resulted in lockup of the leading anticline, syncline, and early formed flank thrusts on the leading overturned limb. In addition to continued slip on faults in a favorable orientation for failure, new, late fold accommodation thrust faults (e.g., Murie Creek and Red Rock Trail thrusts) formed in response to fold lockup within a continued layer-parallel compressive stress field (e.g., see figure 12, p. 122, in Jadamec and Wallace, 2014; see figure 15, p. 686, in Mitra, 2002a; see figure 4, p. 1679, in Mitra, 2002b). These late fold accommodation thrust faults are spatially associated with the locked hinge zones of the leading anticline and syncline, and thus are examples of forelimb shear thrusts (see Mitra, 2002a).

We link the Red Rock Trail thrust with the well-exposed thrust at The Red Hill (plate 1). This inferred linkage is consistent with the position and structural style of the Red Rock Trail thrust and the proposed correlative thrust at The Red Hill as seen in both cross sections (figures 7 and 32). We note that Averitt (1962) does not map the Red Rock Trail thrust in the Cedar Mountain quadrangle. The presence of cataclastic Navajo Sandstone in the Cedar Mountain quadrangle is consistent with such a fault, although a fault contact has yet to be identified (T.R. Knudsen, Utah Geological Survey, written communication, 2022). The possibility exists that the Red Rock Trail thrust is segmented or in a nascent stage of development in the Cedar Mountain quadrangle. Whereas the Murie Creek thrusts are relatively short and of low displacement, the Red Rock

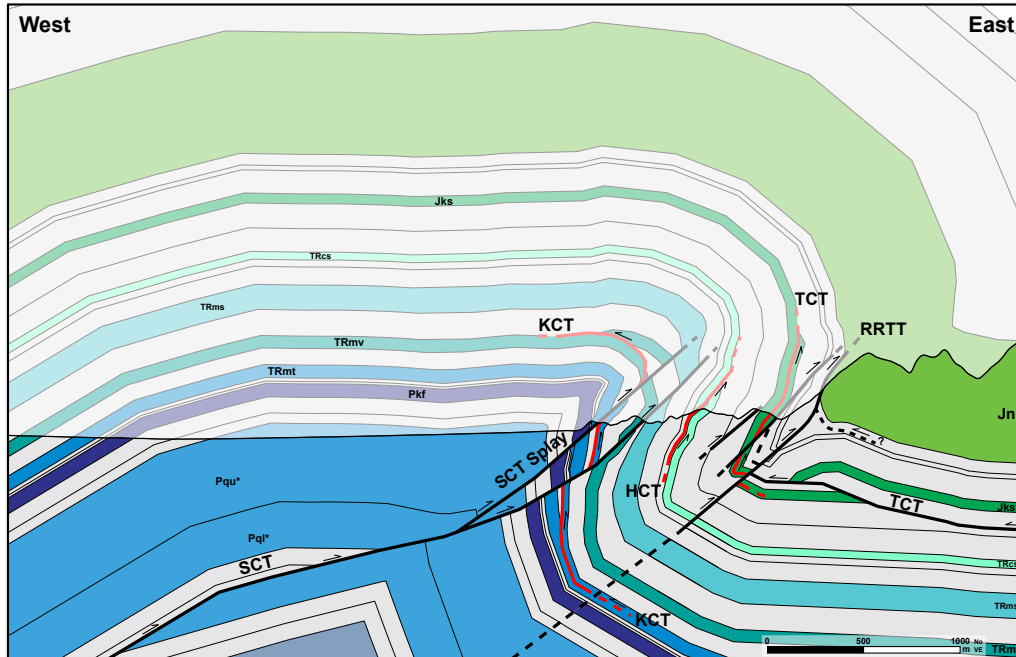


Figure 31. Enlargement of the cross section A–A' of the Kanarra fold-thrust structure at Kanarra Creek. Early formed thrusts (fold accommodation faults), which were overturned at later stages of Kanarra fold development, are colored in red. Here, the late-forming thrusts have formed a dextral shear zone across the fold limb, dissecting earlier flank thrusts. Folding along the Taylor Creek thrust was inferred by extra area in the leading syncline. Displacement along the Red Rock Trail thrust is estimated here to be approximately 250 m. Sinistral flexural slip within the syncline core, which may be responsible for the structural relationships at Kanarra Creek is represented by the dashed, queried detachment beneath the Navajo Sandstone. Structure initializations: SCT–Spring Creek thrust; TCT–Taylor Creek thrust; KCT–Kanarra Creek thrust; RRTT–Red Rock Trail thrust. See plate 2B (stratigraphic column) for explanation of map unit symbols. Line of section shown on plates 1 and 2.

Trail thrust is in a favorable location and orientation to eventually link with the blind thrust deeper in the core of this fold-thrust structure (see dashed fault, figure 7). It is our contention that these two faults are locally hard linked in the subsurface in the vicinity of Short Creek, to form a break thrust (see Eisenstadt and De Paor, 1987; Fischer and others, 1992). Thus, the Red Rock Trail thrust would represent a developing frontal ramp along the leading edge of the Sevier fold-thrust belt in southwestern Utah.

The Pintura Anticline Conundrum

Dissection of the Kanarra fold-thrust structure by the Hurricane fault yielded spectacular exposures of the leading anticline-syncline pair and associated thrust faults of the Kanarra fold-thrust structure in its footwall block, the Hurricane Cliffs. The burial of the hanging wall block of the Hurricane fault, and with it the trail-

ing limb of the Kanarra anticline, beneath Neogene to Quaternary sediments and volcanics of Cedar Valley, obfuscates the full tectonic significance of the Kanarra fold-thrust structure to the Sevier fold-thrust belt. This is borne out in a long-lived debate regarding the relationship between the Virgin, Pintura, and the Kanarra anticlines (see Hurlow and Biek, 2003, for a complete summary) and the timing of Sevier deformation in southwestern Utah (Biek and others, 2009).

The Pintura anticline, from early on, has been depicted as a broad gentle anticline separated from the smaller, tighter Kanarra anticline by an intervening syncline (e.g., figure 2A, p. 249, in Gardner, 1941). The folds were beveled by erosion and the angular unconformity capped by early to late Campanian clastics (Biek and others, 2010). The younger Hurricane fault is pictured cutting the western limb of the Kanarra anticline near the axis of the intervening syncline, isolating the partially eroded Pintura anticline within the rotated hang-

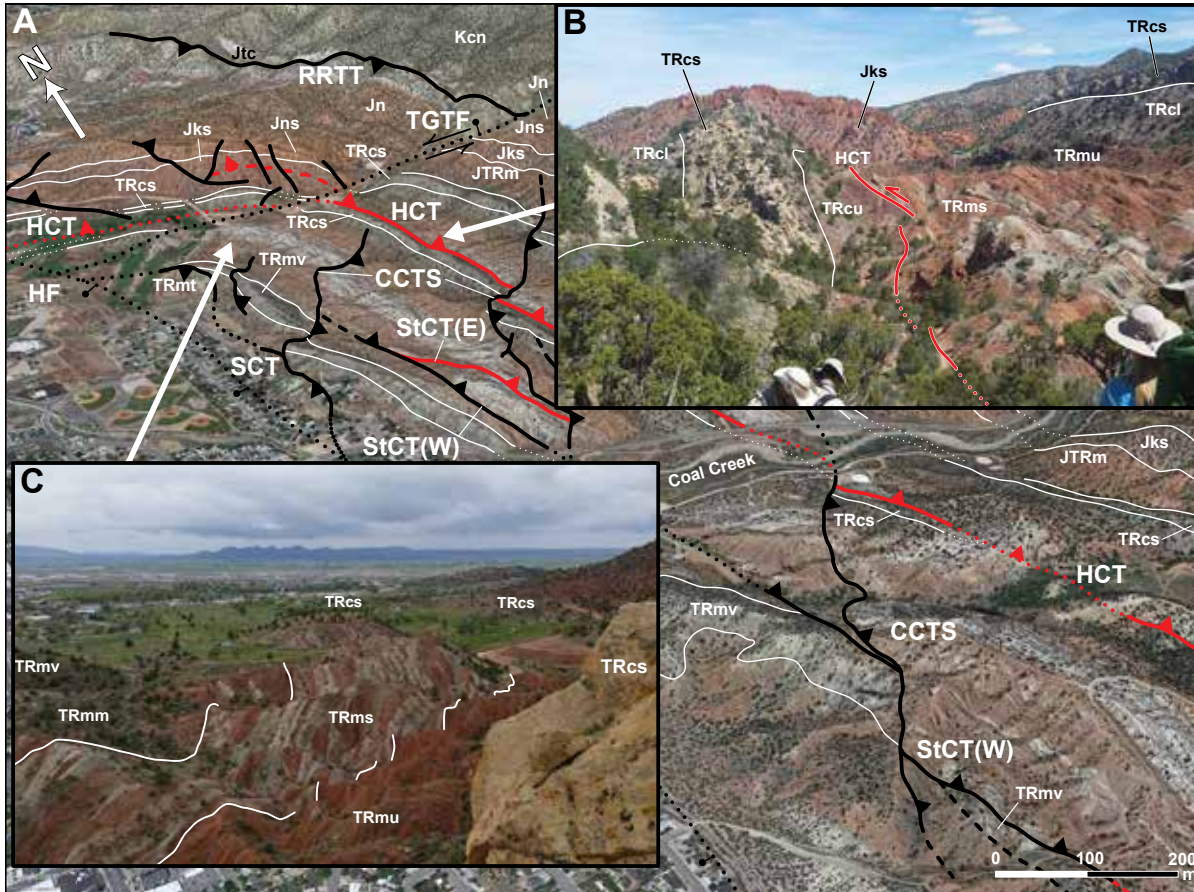


Figure 32. (A) Google Earth 3D terrain view with Landsat/Copernicus imagery looking northeast onto the east limb of the Kanarra fold-thrust structure at The Red Hill adjacent Cedar City. Stephens Canyon forms the low area within the middle red member of the Moenkopi Formation, just east of the Virgin Limestone Member of the Moenkopi (also see plate 1). (B) View looking north upon a ridge of the Shinarump Member of the Chinle Formation, which forms the footwall of the Hicks Creek thrust, east of Stephens Canyon. (C) View northwest showing the curvature of the Shnabkaib Member of Moenkopi as the beds rotate into the fold nose. Structure initializations: CCTS—Coal Creek thrust system; HCT—Hicks Creek thrust; RRTT—Red Rock Trail thrust; StCT(E)—Stephens Canyon thrust (east); SCT—Spring Creek thrust; StCT(W)—Stephens Canyon thrust (west); TGTF—Thunderbird Gardens Trail fault. See plate 2B (stratigraphic column) for explanation of map unit symbols.

ing wall of the Hurricane fault (e.g., see figure 2F, p. 249, in Gardner, 1941). Gardner (1941) notes “down-turning” of the hanging wall strata, as the contact with the Hurricane fault is approached, enhances the intervening syncline, a process Gardner attributes to gravitational “sag.” More recent mapping of the Pintura 7.5-minute quadrangle (Hurlow and Biek, 2003) substantiate these findings and their cross section shows a similar broad Pintura anticline, a faulted intervening syncline, and a tighter faulted Kanarra anticline. We note that in our map area deformation associated with the Hurricane

fault is commonly represented by sparse normal faults that are sub-parallel to the trace of the Hurricane fault (plates 2A and 3). Whereas drag folds may be locally present, we interpret the several locations along the Kanarra fold-thrust structure that preserve westward dips to be associated with the discontinuous remnants of the hinge zone of the leading anticline of the Kanarra fold-thrust structure and these locations record Sevier compression rather than drag along the Hurricane fault (plates 2A and 3).

Cook (1957) called into question the existence of

the Pintura anticline. Cook (1957) noted that when bedding in the Carmel Formation is rotated to horizontal, the contact between the underlying Navajo Sandstone and Carmel Formation everywhere dips more steeply to the northwest; the east-dipping limb of the Pintura anticline is missing or poorly exposed. Hurlow and Biek (2003) confirmed Cook's (1957) result and described two plausible interpretations of the data: (1) the Pintura anticline is a west-dipping homocline (i.e., Cook's model) and (2) the Pintura anticline is a broad anticline that shares an east-dipping limb with the intervening syncline that was modified by reverse drag along the Hurricane fault (i.e., the model preferred by Hurlow and Biek, 2003).

The results of our work have bearing on resolving the Pintura anticline conundrum. The geologic cross section (figure 7) depicts a complete profile through the Kanarra fold-thrust structure restored to the Late Cretaceous (i.e., prior to dissection by the Hurricane fault). In our structural interpretation, the shape of the Kanarra anticline is a compound fold, with a broad, sub-horizontal hinge zone flanked by a leading anticline on the east and by a trailing anticline on the west. The trace of the Hurricane fault closely parallels the trace of the hinge zone of the leading anticline (plates 2A and 3). As previously suggested, during Basin and Range extension, the Hurricane fault exploits the hinge zone of the leading anticline, and likely the underlying thrust as well, of the Kanarra fold-thrust structure (Threet, 1963b; Grant and others, 1994; Biek and others, 2009). Downward displacement of the trailing limb of the composite Kanarra anticline (figure 7) in the hanging wall of the Hurricane fault would result in an apparent west-dipping homocline. The presence of the intervening syncline (i.e., between the Pintura and Kanarra anticlines) can be attributed to the development of a roll-over anticline and antithetic normal faults as the contact with the Hurricane fault is approached (see figure 8.3.1, p. 433, in Davis and others, 2011). However, downward displacement and clockwise rotation of the hanging wall along a listric normal Hurricane fault could create the appearance that the western trailing anticline of the Kanarra fold-thrust structure is a separate anticline—the Pintura anticline. Clockwise rotation of the broad sub-horizontal hinge zone of the Kanarra fold associated with

the Kanarra fold-thrust structure (see figure 7) during normal faulting would then appear to be the east-dipping limb of the Pintura anticline that is shared with the proposed intervening syncline. The dismembered Kanarra anticline of the Kanarra fold-thrust structure would now have the leading anticline (i.e., the Kanarra anticline of Biek and others, 2009) isolated and cropping out in the footwall of the Hurricane fault. Hanging wall strata adjacent to the Hurricane fault would still be subjected to modification by development of a roll-over anticline and antithetic faults. In either scenario, the Pintura anticline is an "accidental anticline" that was cleaved from the compound Kanarra anticline of the Sevier age Kanarra fold-thrust structure during Basin and Range extension rather than a unique fold. The relative stratigraphic ages used previously to constrain the timing of the formation of the Pintura anticline to be between early and late Campanian time (about 84 to 71 Ma; see Biek and others, 2009), and possibly younger, constrain the timing of formation of the Kanarra fold-thrust structure.

The Kanarra Fold-Thrust Structure at The Red Hill

We interpret the Kanarra fold-thrust structure to be well exposed at The Red Hill near Cedar City. The Red Hill is one of Utah's iconic geologic exposures (Hintze, 2005). Again, the fold has been dissected by the Hurricane fault along the axial trace of the leading anticline (plate 1). The western trailing limb of the anticline has been displaced along with the hanging wall beneath the sediment fill in Cedar Valley, with the eastern limb of the anticline and leading syncline well exposed in the footwall. At this structural level, closure of the northerly plunging nose of the fold is well shown by the change in the strike and dip of Upper Triassic and Lower Jurassic strata from northeast to northwest dips (figure 32). The amount of shortening at The Red Hill is greater than along Camp Creek but less than along Kanarra Creek. The lower degree of shortening is reflected in the upright, gentle to steeply dipping stratigraphic section along the leading eastern limb of the anticline with moderate, additional structural complexity from faulting along the limb.

We utilize the structural style of folding and faulting for the Kanarra fold-thrust structure near Kanarraville (this paper) to provide new interpretations for the role of faulting at The Red Hill. For example, some of the faults at The Red Hill (e.g., the Hicks Creek thrust) were also previously classified based upon observed separation as normal faults (e.g., Averitt, 1962; Hintze, 2005), obscuring the true relationship of these faults to folding and to the Sevier fold-thrust belt. Based upon our unpublished in-person and remote geologic mapping as well as published geologic maps (Averitt and Threet, 1973; Knudsen, 2014a; Knudsen, 2014b) and with consideration for the structural style of the Kanarra fold-thrust structure (figure 7), we present a geologic cross section for The Red Hill at Late Cretaceous time and discuss the style of faulting at The Red Hill and why it is part of the Kanarra fold-thrust structure (figures 33, 34B, and 35B).

The profile through the Kanarra fold-thrust structure at The Red Hill shares several features with the central part of the structure at Kanarraville (figure 7). The anticline at The Red Hill is also an asymmetric, composite fold-thrust structure modified by late fold accommodation thrust faults. The structure also likely developed above a basal detachment in the Cambrian Bright Angel Shale and above a blind break-thrust ramp (figure 33). Slip along the early formed Spring Creek flank thrust forms a fault-bend fold within the trailing limb of the anticline to produce a compound fold profile. The influence of kink axes on the fold profile gradually diminishes upwards such that the fold has a rounded profile more typical of buckle folds. The early formed Hicks Creek flank thrust, on the eastern limb of the fold, has been steepened by rotation during folding but remains upright (figures 32 and 33). Duplication of the stratigraphic section along this west-verging flank thrust thickens the east-dipping limb and broadens out the hinge zone of the leading anticline of the fold (figures 33, 34B, and 35B). The Stephens Canyon thrusts are smaller early formed flank thrusts that crop out west of the Hicks Creek thrust (figures 33, 34B, and 35B; table 2). During folding, one of these thrusts duplicates the Shnabkaib Member.

We also interpret several faults, the Coal Creek thrust system, as late fold accommodation faults as sev-

eral of these thrusts truncate the earlier Hicks Creek thrust (figures 33, 34B, and 35B). Displacement of formation contacts by these faults show right-lateral separation on the geologic maps (see figures 33, 34B, and 35B). The two-dimensional separation of formation contacts is compatible with normal-slip, strike-slip, and reverse-slip fault movement and several of these faults have been mapped as normal faults (Averitt and Threet, 1973; Knudsen, 2014a). We use our mapping and GMDE (Allmendinger, 2020) to constrain the dip on these fault contacts to be consistently dipping southeast with dip magnitudes of about 45° and in the range of a low of 36° and a high of 50°. Considering the dip on these faults does not exceed 60°, and that the dips are likely to have been increased as a result of eastward rotation of the fold limb during deformation, the lower dip values for the fault contacts is more typical of thrust faults than normal faults or strike-slip faults (Davis and others, 2011, p. 291). Tops-to-the-northwest movement of the hanging wall on southeast-dipping thrust faults will also produce right-lateral separation of formation contacts on a geologic map of The Red Hill. Thus, we interpret the Coal Creek faults (figures 34 and 35) as a type of late, west-verging, fold accommodation fault known as hinge wedge thrusts (e.g., see figures 12 through 14, p. 113–115, in Cloos, 1961, and figure 8, p. 680, in Mitra, 2002a) and they are represented as such in our cross section through The Red Hill (see figures 33, 34B, and 35B). These thrusts likely formed in response to hinge zone tightening during the development of the Kanarra fold-thrust structure. Accepting that these are thrust faults, in the cross section they duplicate upper Moenkopi and Chinle units in the footwall of the Hicks Creek thrust and displace the Hicks Creek thrust several tens of meters west within the subsurface along the fold limb, though aggregate slip on each splay is higher (hundreds of meters).

At The Red Hill, a late forelimb shear thrust fault is observed (figures 34 and 35). This fault has a highly similar structural style and location within the cross section (figure 33) as the Red Rock Trail thrust at Kanarraville (cf., figure 7). Here, the forelimb shear thrust fault has ramped higher up section compared to Kanarra Creek (figure 35). Like the Red Rock Trail thrust, the forelimb shear thrust fault displaces the Navajo Sandstone over

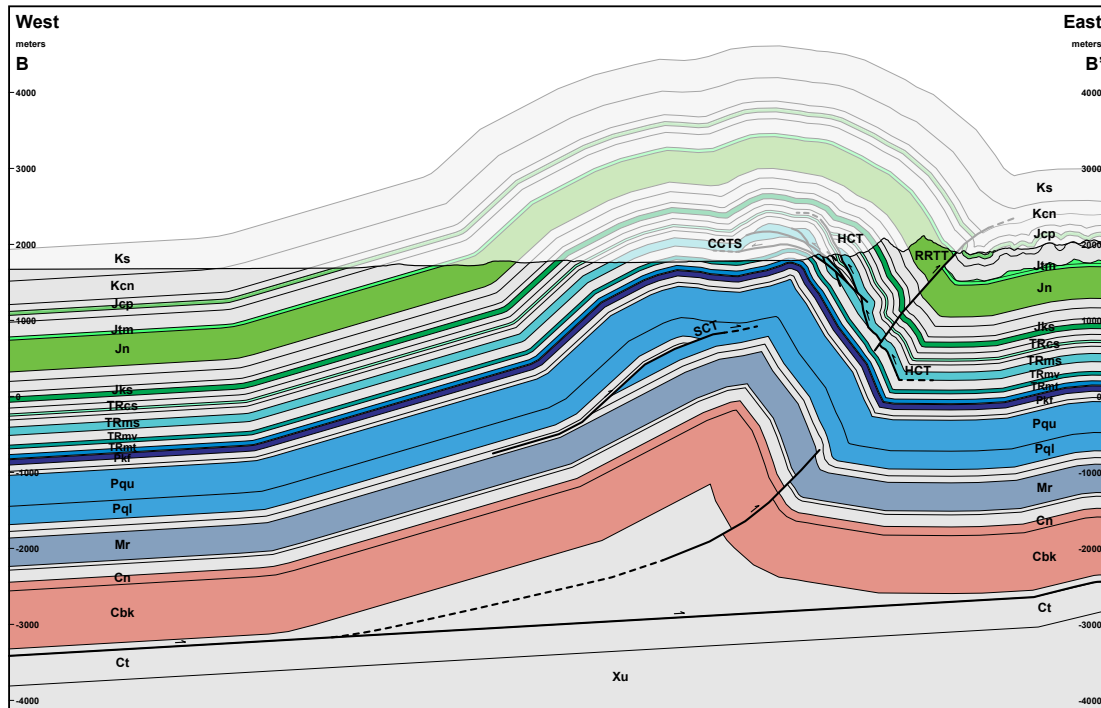


Figure 33. Cross section B–B' of the Kanarra fold-thrust structure showing the restored Sevier structure circa 80 Ma, based on unpublished mapping along Coal Creek and mapping by Knudsen (2014a). Eroded geology is faded out. The pre-extension trailing limb and fold crest are constrained by the tilted, sub-horizontal, west-dipping layering defined by the enveloping surface of the Carmel buckle fold train (the pre-folding Jn–Jtm contact, dotted line) and the shape of the closely related Pintura anticline (Hurlow and Biek, 2003). Unexposed layer thickness and presence are constrained by local data sources (see table 1; Hintze, 1986; Van Kooten, 1988; Hurlow and Biek, 2003; Biek and others, 2009). Unexposed, thick, competent layers (Cbk–Cnd, Mr, Pq) are colored according to age; exposed ridge-former colors correspond to the maps in the study area (figures 3 and 4). Present-day topography is included to emphasize the ridge formers. Structure west of the Hurricane Cliffs, within the present-day Cedar Valley graben, does not represent present-day bedrock geology. Unexposed structure constrained by surface control, fold style, and assumption of buckle folding before break thrust faulting. CCTS—Coal Creek thrust system; HCT—Hicks Creek thrust; RRTT—Red Rock Trail thrust; SCT—Spring Creek thrust. See plate 2B (stratigraphic column) for explanation of map unit symbols. Line of section shown on plate 1.

the Carmel Formation (figure 34). We correlate this fault with the Red Rock Trail thrust. We note that the Carmel Formation in the leading syncline is intensely deformed by a buckle fold train and associated minor thrust faults and duplexes well exposed in road cuts along Cedar Canyon. These buckle folds developed as a result of the Carmel Formation having a shorter dominant wavelength in comparison to the underlying Navajo Sandstone (Fischer and others, 1992). The buckle fold train likely developed above a detachment in the Temple Cap Formation (plate 2, also see Threet, 1963a, p. 113). The proposed detachment along the Temple Cap Formation may also play a role in the development of structures at Parowan Gap (see discussion below).

At The Red Hill, the Red Rock Trail thrust is also in a favorable location and orientation to have had the opportunity to merge with the blind thrust ramp deeper within the fold if horizontal shortening had progressed further. However, construction of the cross section for the amount of shortening required at the Red Hill indicates these two faults are not hard-linked and the frontal ramp was captured in the nascent stages of development (figure 33).

Salient and Recess Development Along the Kanarra Fold-Thrust Structure

The Kanarra fold-thrust structure is defined by

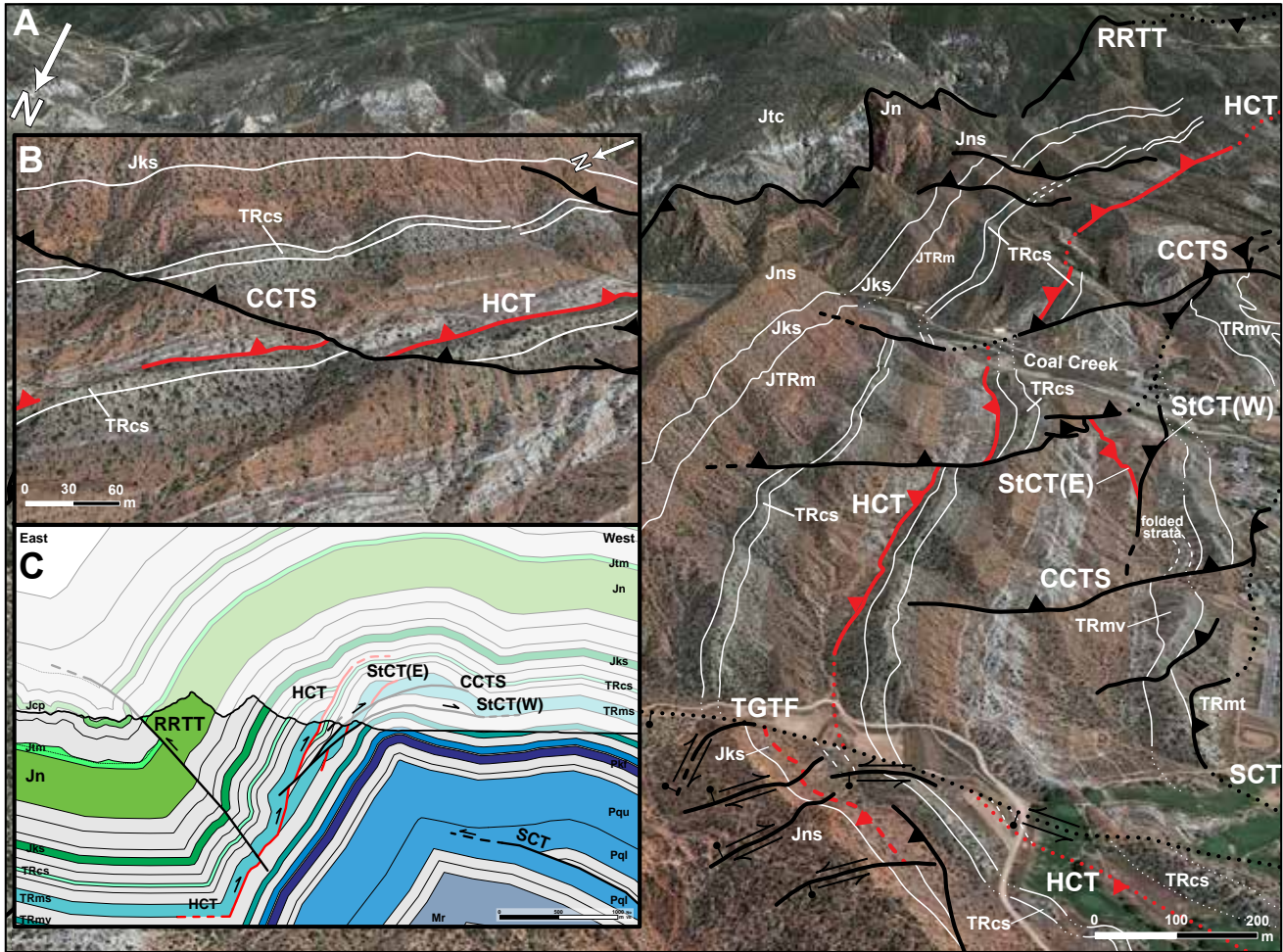


Figure 34. (A) Google Earth 3D terrain view southeast onto the east limb of the Kanarra fold-thrust structure at The Red Hill adjacent Cedar City. Early fold accommodation faults, which were later folded and cut along the CCTS, are colored in red. Nearby, the Spring Creek thrust emerges, bringing up Timpoweap strata. The Thunderbird Gardens Trail cross fault cuts across the fold in the foreground. Contacts from unpublished field and GMDE mapping by the authors, and Knudsen (2014a). (B) The later set of thrusts in the Coal Creek thrust system cuts obliquely across the early set. (C) Partial enlargement of B–B' (see figure 33, section is reversed), reflected vertically to match the southeast view of (A) and with early faults in red. Structure initializations: CCTS–Coal Creek thrust system; HCT–Hicks Creek thrust; RRTT–Red Rock Trail thrust; StCT(E)–Stephens Canyon thrust (east); SCT–Spring Creek thrust; StCT(W)–Stephens Canyon thrust (west); TGTF–Thunderbird Gardens Trail fault. See plate 2B (stratigraphic column) for explanation of map unit symbols.

broad open curves along its strike (plate 1). Near Cedar City the curve is concave towards the hinterland and forms a salient. Just south of Kanarraville, the structure curves to be concave towards the foreland and forms a recess. The presence of salients and recesses is a common feature of many orogens, including the Sevier fold-thrust belt (Quick and others, 2020). The presence of salients and recesses may reflect variation in stratigraphy (e.g., Chapman and DeCelles, 2015), sediment thickness

(Paulsen and Marshak, 1999), and variation in the shape of the rifted continental margin, which is controlled by the embayments and promontories that define the hingeline (Thomas, 2006). The presence of strike-slip transform faults separating different rift basins in the Precambrian basement contributes to development of an irregular hingeline to the extended continental crust. Along strike variation in the temporal and spatial advancement of the leading edge of the Sevier fold-thrust

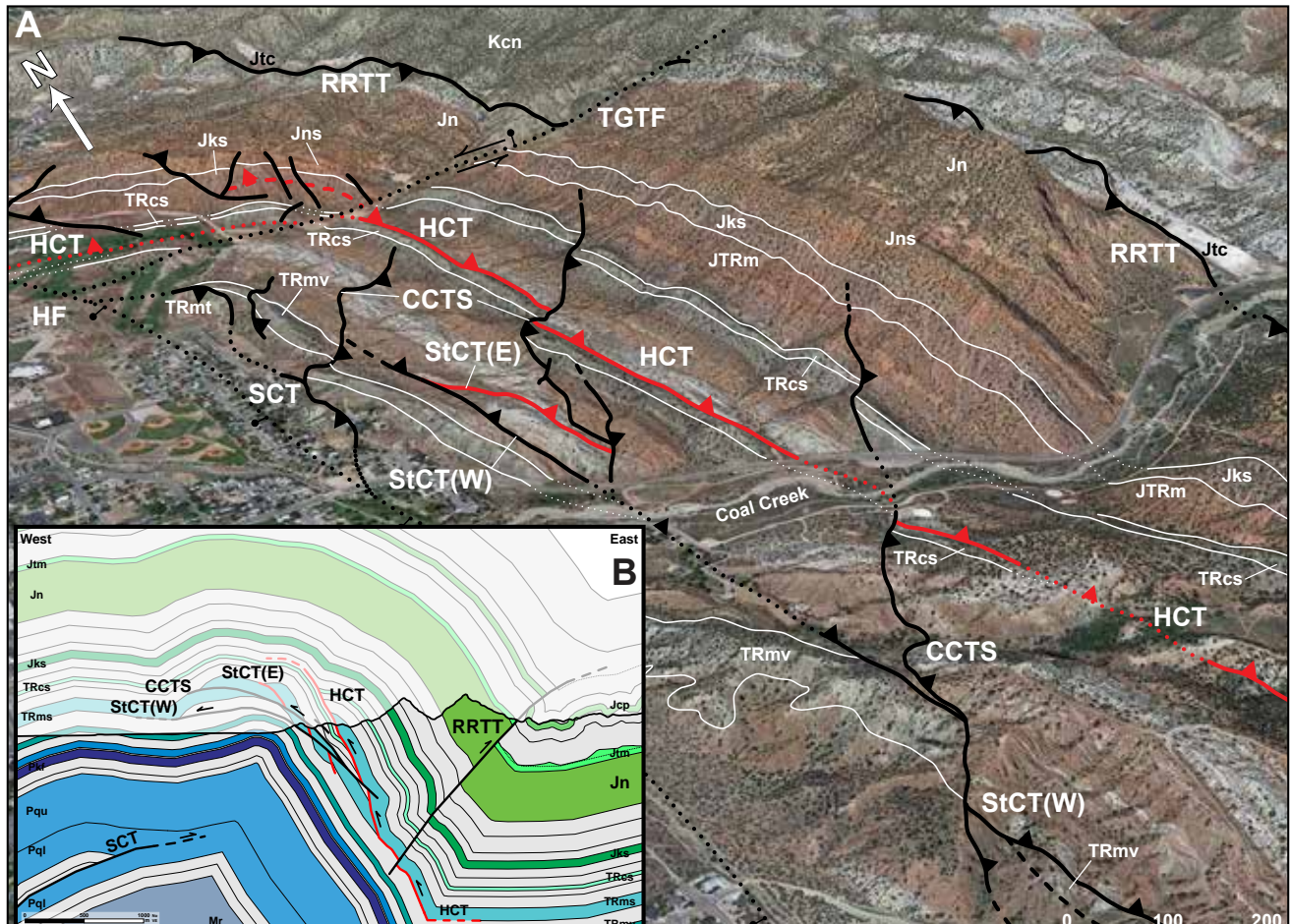


Figure 35. (A) Google Earth 3D terrain view with Landsat/Copernicus imagery looking northeast onto the east limb of the Kanarra fold-thrust structure at The Red Hill adjacent Cedar City. Selected faults and sedimentary contacts are shown for clarity. Early fold accommodation faults, which were later folded and displaced are colored in red. This view is approximately along-strike to the late, northwest-vergent set of Coal Creek thrusts, showing their gentle to moderate dips (e.g., right midground). Contacts from unpublished field and GMDE mapping by the authors and Knudsen (2014a). (B) Partial enlargement of B–B' (see figure 33) with early faults in red. Structure initializations: HF–Hurricane fault; CCTS–Coal Creek thrust system; HCT–Hicks Creek thrust; RRTT–Red Rock Trail thrust; StCT(E)–Stephens Canyon thrust (east); SCT–Spring Creek thrust; StCT(W)–Stephens Canyon thrust (west); TGTF–Thunderbird Gardens Trail fault. See plate 2B (stratigraphic column) for explanation of map unit symbols.

belt front was largely inherited from the structure of the rifted Precambrian crystalline basement of western North America (Picha and Gibson, 1985; Picha, 1986; Quick and others, 2020). We suggest that the close spatial association of the Kanarra fold-thrust structure with the Cordilleran hingeline (figure 1) indicates that structural inheritance is a contributing factor to the formation of salients and recesses that characterize this fold-thrust structure (plate 1).

We interpret the cross faults (e.g., Murie Creek fault)

to reflect reactivation of Proterozoic transfer zone faults (i.e., present-day basement lineaments) along the Cordilleran hingeline in Sevier time (Picha and Gibson, 1985; Paulsen and Marshak, 1999; Thomas, 2006; Quick and others, 2020). For example, the Murie Creek fault just north of Kanarraville and the Thunderbird Gardens Trail fault just north of Cedar City, are both sub-parallel to the Paragonah lineament (figure 1), suggesting they were localized as a result of reactivation of transform faults in the basement and aided along strike displacement of the

fold-thrust structure (plate 1). In addition, early formation of the Murie Creek fault during folding could present a structural discontinuity that hindered the along strike propagation of the Red Rock Trail thrust. The Red Rock Trail thrust abuts the Murie Creek fault (plates 2A and 3) and its trace farther to the north in the Cedar Mountain quadrangle (Averitt, 1962; Doelling, 1972) is inferred from the presence of a cataclastic zone in the Navajo Sandstone, before it is recognized again in the Cedar City quadrangle.

The Leading Edge of the Sevier Fold-Thrust Belt in Southwestern Utah

Several structures have been previously proposed to represent the leading edge of the Sevier fold-thrust belt in southwestern Utah. Biek and others (2015) proposed that the Bryce Canyon anticline in the hanging wall of the Paunsaugunt normal fault initially formed due to thrusting and defines the easternmost extent of Sevier deformation (Biek and others, 2015 p. 91). Their evidence for the presence of an older episode of thrusting along the Paunsaugunt normal fault is based upon the subtle angular discordance between pre-Claron strata and the Paleocene-Eocene Claron Formation on the Paunsaugunt Plateau. We note that the broad Bryce Canyon anticline in the hanging wall of the Paunsaugunt normal fault is similar in style to the folds in the hanging wall of other normal faults on the plateau (e.g., the Sevier fault; see cross section B–B' of Biek and others, 2015) and likely formed as a roll-over anticline (see figure 6.136b, p. 333, in Davis and others, 2011) during younger Basin and Range extension, thus eliminating the need for an earlier episode of cryptic thrusting along the Paunsaugunt normal fault. Alternatively, we suggest that the Kanarra fold-thrust structure, which includes spatially associated minor folds and thrusts in the Late Cretaceous strata, for example at The Red Hill (Knudsen, 2014a) and in Parowan Gap (Threet, 1963a, 1963b) unambiguously defines the leading edge of the Sevier fold-thrust belt in southwestern Utah (figure 1).

The Red Rock Trail thrust is not hard linked along its entire length, for example at Kanarra Creek (figure 7) and The Red Hill (see figure 33). This is consistent with a Sevier deformation front that was in the process of developing a frontal ramp along the Red Rock Trail thrust

before deformation abated. Locally, where a frontal ramp may have developed, the Navajo Sandstone in the hanging wall was transported east and onto the Carmel Formation, for example near the mouth of Short Creek (plates 2A and 3), and we suggest also in Parowan Gap. In the central part of the Kanarra fold-thrust structure, the Red Rock Trail thrust is in a favorable orientation to have formed a hard linkage with the basal decollement in the Bright Angel Shale to create a break thrust (figure 7). The thrust displaces Navajo Sandstone along with its distinctive cataclastic zone over the Carmel Formation.

This same spatial relationship of fault-related units is well exposed along the prominent topographic ridge of Navajo Sandstone at the west entrance to Parowan Gap (Threet, 1963a; Maldonado and Williams 1993; Anderson and Dinter, 2010). The thrust relationships are complicated by Basin and Range deformation. A steep normal fault along the eastern side of the Navajo Sandstone topographic ridge, down-dropped to the east of the Navajo cataclastic zone, the thrust fault, and the Carmel Formation in its hanging wall (figure 36). Cropping out in the low hills in the hanging wall of the normal fault is an east-verging thrust that places cataclastic Navajo Sandstone over folded and fractured, laminated, micritic limestone of the Carmel Formation. We propose the following: (1) this thrust fault contact has a similar structural style and position as the Red Rock Trail thrust and is part of a similar, but unique, fold-thrust structure. This fold-thrust structure at Parowan would be related to the Kanarra fold-thrust structure in a similar fashion that the Virgin anticline is related to the Kanarra fold-thrust structure (see Biek and others, 2015, p. 64) and (2) the westernmost thrust fault in Parowan Gap is correlative with the Red Rock Trail thrust and the fold-thrust structure at Parowan Gap is part of the Kanarra fold-thrust structure as originally proposed by Threet (1963a, 1963b). If the fold-thrust structure at Parowan Gap is related to the Kanarra fold-thrust structure, it is exposed at a higher structural level as it preserves deformation in Upper Cretaceous strata. To the east of the westernmost thrust fault in Parowan Gap (the Red Rock Trail thrust?), two other east-verging thrusts are well exposed in Parowan Gap (Threet, 1963b, Maldonado and Williams, 1993; Anderson and Dinter, 2010; Biek and others, 2015). These thrusts were

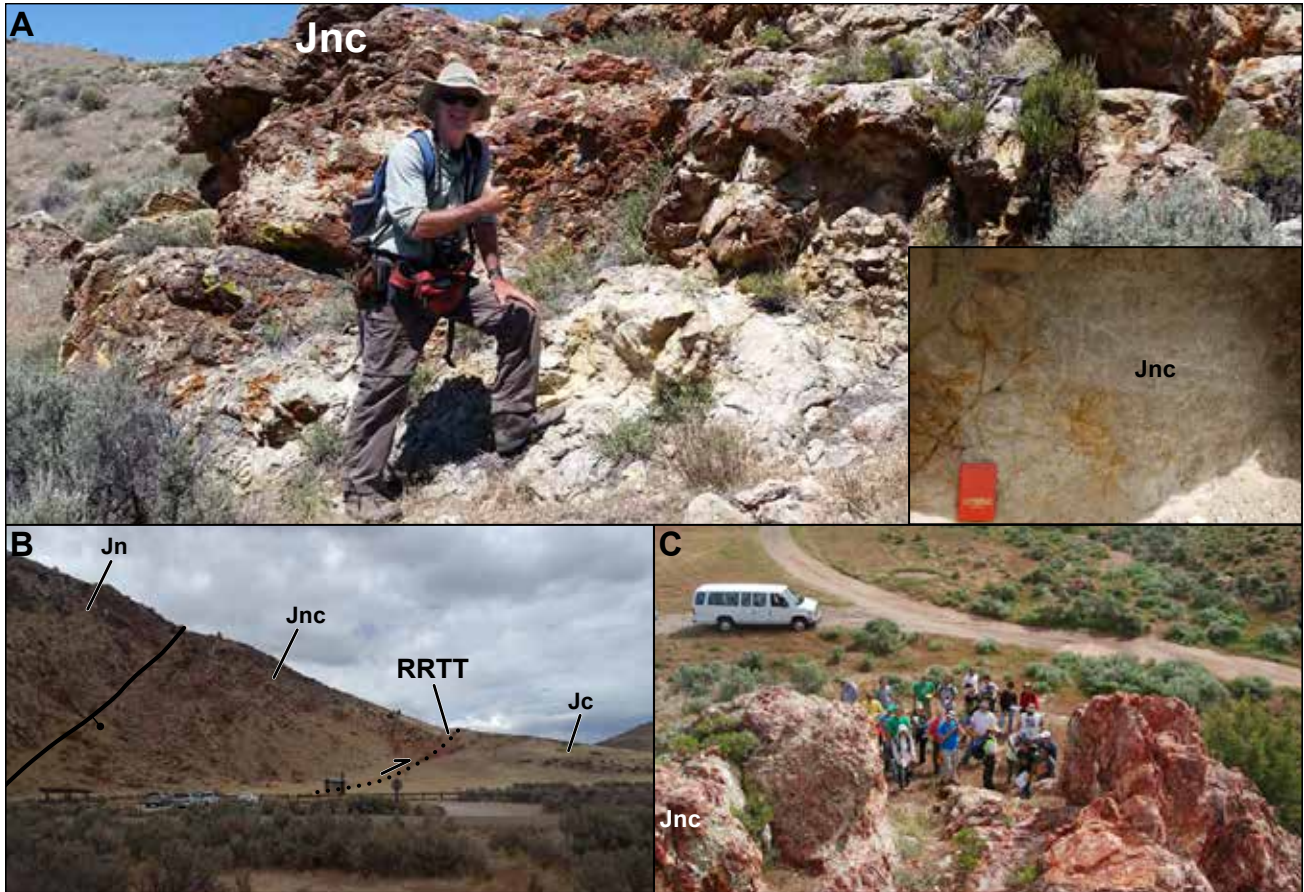


Figure 36. (A) North-facing view of Navajo Sandstone cataclasite (Jnc) at the west entrance to Parowan Gap. John P. Hogan for scale, 1.86 m. Inset: close-up of the Navajo cataclasite a few meters to the east along the same outcrop. Gravel- to cobble-sized sandstone clasts are suspended within a network of fractures and finer cataclastic grains. (B) View to the north of the Red Rock Trail thrust (RRTT) at the west entrance to Parowan Gap tens of meters north of (A). Photograph by John P. Hogan. (C) Cataclastic Navajo near (A), view to the northeast. Photographs in (A) and (C) by Michael Wizevich, Central Connecticut State University.

named “the thrust faults at Parowan Gap” by Maldonado and Williams (1993). They were correlated with the Iron Springs thrust by Goldstrand (1992) and again by Anderson and Dinter (2010) and Biek and others (2015). The original correlation of the thrusts at Parowan Gap to the Iron Springs thrust by Goldstrand (1991, p. 58, and 113) is based upon these thrusts being on trend, exhibiting similar structural style, and stratigraphically correlating Upper Cretaceous rocks at Parowan Gap with the Iron Springs Formation. We note that the along trend correlation of these thrust faults crosses about 30 km of younger sedimentary fill in the Cedar Valley graben and discounts disparate horizontal Basin and Range extension. cursory inspection suggests resto-

ration of the Red Hills horst, and thus Parowan Gap to its pre-Basin and Range extension location, would place it closer to the Markagunt Plateau and on trend with the Kanarra fold-thrust structure. This supports the correlation of Sevier structures in Parowan Gap as part of the Kanarra fold-thrust structure as previously suggested by Threet (1963b). In contrast, restoration of Basin and Range extension would still preserve the Irons Springs thrust in the Three Peaks horst cropping out well west of the Kanarra fold-thrust structure.

The thrusts at Parowan Gap placed Carmel Formation over the lower Iron Springs Formation as well as the lower Iron Springs over upper Iron Springs, suggesting low displacement (Threet, 1963b). The thrusts

are beveled off along an angular unconformity that is capped by the Upper Cretaceous Grand Castle Formation. Slight displacement of the unconformable contact by the thrusting constrains the waning stages of deformation to the early Paleocene (Anderson and Dinter, 2010; Biek and others, 2015). Uncertainty and disagreement in the identification of the Upper Cretaceous units in Parowan Gap, particularly the presence or absence of the Straight Cliffs (e.g., the about 90 to 80 Ma John Henry Member) and Naturita Formations, will affect the interpretation of the displacement and timing of movement on these thrusts (Anderson and Dinter, 2010; Biek and others, 2015; Enriquez St. Pierre and Johnson, 2021). The debate regarding the stratigraphic assignment of Upper Cretaceous units in Parowan Gap with Upper Cretaceous formations that are younger than the Iron Springs Formation at Three Peaks further undermines the validity of correlating the thrusts in Parowan Gap with the Iron Springs thrust at the Three Peaks.

Considering recent findings reported here, and by Quick and others (2020), correlation of the Iron Springs thrust, where it crops out in its type locality in the Three Peaks area, with the thrusts exposed in Parowan Gap is tenuous. The Iron Springs thrust at the Three Peaks crops out to the west of the Kanarra fold-thrust structure and the Red Rock Trail thrust (figure 1). In Parowan Gap, the two eastern thrusts (i.e., those proposed to be the Iron Springs thrust) would reverse this spatial relationship if the westernmost thrust correlates with the Red Rock Trail thrust or a similar style thrust. In contrast, in the context of the structural style of the Kanarra fold-thrust structure, the two eastern thrusts at Parowan Gap would more likely have formed as out of the syncline thrusts east of the overturned limb of the leading anticline (cf., figures 7, 33, 34, and 35). These late fold accommodation faults, which are typically of lower displacement, would then potentially sole into the Middle Jurassic Temple Cap Formation detachment, the same detachment underlying the buckle fold train at The Red Hill (e.g., Averitt and Threet, 1973; Knudsen, 2014a) rather than into the regional basal detachment in southwestern Utah (e.g., Van Kooten, 1988; Biek and others, 2009).

Timing of Sevier Thrusting in Southwestern Utah

Advancement of the Sevier deformation front in southwestern Utah is episodic. Quick and others (2020) connected movement along the Iron Springs thrust at 100 Ma with the late Albian to early Cenomanian magmatic flare up in the Cordilleran arc. They suggested that accelerated subduction, associated with a period of global plate reorganization, contributed to a magmatic flare up in the Cordilleran arc. This event, along with steepening of the orogenic wedge, triggered widespread thrusting across the retroarc Sevier deformation belts. The timing of deformation of the Kanarra fold-thrust structure in southwestern Utah (about 80 to 70 Ma) also corresponds with a period of widespread thrusting in central Utah (e.g., Paxton, Gunnison, and Charleston-Nebo thrusts) and in northern Utah and southwestern Wyoming (e.g., Crawford and Absaroka thrusts) as well as overlapping with major magmatic flare ups in the Cordilleran arc (see figure 9, p. 85, in Quick and others, 2020). This close temporal relationship between magmatic activity in the arc and widespread deformation in the Sevier fold-thrust belt (see Lageson and others, 2001; DeCelles and others, 2009; DeCelles and Graham, 2015; Yankee and others, 2019; Quick and others, 2020) requires further investigation.

Correlation of the Iron Springs thrust at the Three Peaks with the thrusts exposed in Parowan Gap is also unlikely due to disparity in the temporal relationships of these thrusts. Quick and others (2020) constrained initial deposition of the Iron Springs Formation and the initial movement on the Iron Springs thrust in the type location of the Three Peaks to 100 Ma. Stratigraphic relationships at the Three Peaks also constrain the latest movement on the Iron Springs thrust to be as late as early Paleocene (Knudsen and Biek, 2014). This history of movement on the Iron Springs thrust is consistent with episodic pulses of deformation and syntectonic sedimentation during the Sevier orogeny (Quick and others, 2020). The initial movement on the Iron Springs thrust is tens of millions of years earlier than the motion on the easternmost thrusts in Parowan Gap if they cut the John Henry Member of the Straight Cliffs Formation. This episode of deformation may be more in agreement with

the timing constraints on the movement of the Kanarra fold-thrust structure in the south of about 84 to 71 Ma (i.e., the former Pintura anticline of Hurlow and Biek, 2003). The latest motion on the thrust in Parowan Gap is constrained to be Late Cretaceous to Paleocene (Anderson and Dinter, 2010; Biek and others, 2015). If the Iron Springs Formation at Three Peaks is distinct from the Upper Cretaceous strata at Parowan Gap correlation of the Iron Springs thrust with the thrusts at Parowan Gap is considerably weakened considering that initial movement on the Iron Springs thrust is constrained to 100 Ma (Quick and others, 2020), potentially millions to tens of millions of years before the rocks at Parowan Gap were being deposited. We suggest that recognition of the westernmost thrust cropping out in Parowan Gap as the Red Rock Trail thrust and the two easternmost thrust faults as late fold accommodation faults, rather than as the Iron Springs thrust, alleviates the apparent discrepancy in the timing of thrusting in southwestern Utah.

Sediment Dispersal in the Sevier Foreland

The temporal and spatial advancement of topographic highs and lows associated with the progression of the Sevier deformation front across southwestern Utah significantly influences the redistribution of sediment in the Sevier foreland basin. The emergence of the Iron Springs thrust in the late Albanian to earliest Cenomanian correlates with movement on the Keystone-Muddy Mountain thrust, the Pahvant thrust (formerly spelled Pavant), the Charleston Nebo thrust, and the Willard thrust system (see figure 9, p. 85, in Quick and others, 2020). The deformation front advances eastward in southwestern Utah with the development of the Kanarra fold-thrust structure in the Campanian. During this time, the Kanarra fold-thrust structure likely formed a substantial, linear, topographic high with associated strike valleys that extended over a hundred kilometers from Toquerville to north of Parowan Gap along the edge of the Markagunt Plateau (figure 1).

Investigation of Cretaceous stratigraphy in southwestern Utah documented the foredeep of the Sevier orogeny was broken up into several discrete sub-basins presumably due to reactivation of northeast-trending

structures in the basement as normal faults (see figure 10, p. 561, in Enriquez St. Pierre and Johnson, 2021). Creation of northeast-trending topographic highs and lows associated with horsts and grabens is suggested to have controlled the fluvial drainage patterns of the main axial river systems in what is now the plateau province. In this model, the Sevier fold-thrust belt and wedge top was thought to be well west of the edge of what is now the Markagunt Plateau. This interpretation may have merit for the eastern plateaus adjacent to the Cretaceous Western Interior Seaway, however, it mischaracterized the Kanarra fold-thrust structure as a Laramide age monocline rather than the leading edge of the Sevier fold-thrust belt during the Late Cretaceous (see figure 1, p. 548 and figure 2, p. 549, in Enriquez St. Pierre and Johnson, 2021). We agree the distribution of Cretaceous depocenters and fluvial drainage patterns are sub-parallel to the Sevier deformation on the Markagunt Plateau, and to the immediate west, reflect the development of significant topographic features, as well documented by Enriquez St. Pierre and Johnson (2021), but in response to the episodic advancement of the leading edge of the Sevier fold-thrust belt in southwestern Utah rather than due to extensional faulting.

CONCLUSIONS

Detailed geologic mapping and structural analysis of the central part of the Kanarra anticline (Gregory and Williams, 1947; Averitt, 1962; Threet, 1963a, 1963b) demonstrate folding and thrusting are inextricably linked in all stages of deformation such that we identify this structure as the Kanarra fold-thrust structure. The Kanarra anticline of the Kanarra fold-thrust structure has an overall compound form in that its hinge zone includes an open, upright, trailing anticline as well as the leading anticline now exposed at the surface. Secondary structures associated with contractional deformation within the hinge of the leading anticline, as well as a blind thrust beneath the leading anticline, were in a favorable orientation to be reactivated during younger Basin and Range extension resulting in strain localization and formation of the Hurricane fault. The trace of the Hurricane fault variably dissected the hinge zone of the leading anticline such that scattered remnants of

the hinge zone and axial trace crop out discontinuously along the strike of the entire structure. The hinge zone of the composite fold, as well as the trailing anticline, were down dropped in the hanging wall of the Hurricane fault and are obscured by younger Neogene and Quaternary clastics and volcanics in the grabens created along the strike of the fault. The consequences of Basin and Range deformation resulted in recognition of an accidental anticline, the Pintura anticline, and an apparent intervening syncline, separate from the Kanarra anticline. We demonstrate the Pintura anticline is part of the trailing anticline on the broad crest of the composite Kanarra anticline that is part of the Kanarra fold-thrust structure. Stratigraphic relationships associated with the Pintura anticline apply to the Kanarra fold-thrust structure and constrain the timing of deformation to be early to late Campanian but possibly younger (Hurlow and Biek, 2003).

Mapped thrust faults associated with the Kanarra fold-thrust structure can be divided into early (e.g., flank thrusts) and late (out-of-the-syncline) fold accommodation faults. Early formed flank thrusts are common to many folds in this area (e.g., the Virgin anticline). The Taylor Creek thrust system on the eastern limb of the leading anticline of the Kanarra fold-thrust structure is the best-known example of one of these faults (e.g., see Biek, 2007a). Early formed flank thrusts on this eastern limb (e.g., Taylor Creek thrust) were folded and overturned along with the stratigraphic section in the central part of the Kanarra fold-thrust structure. This additional structural complexity resulted in several faults previously being misidentified as normal faults rather than as folded thrusts. Rotation of these thrusts into an unfavorable orientation for continued slip resulted in fault lockup. However, early formed flank thrusts on the trailing western limb remained in a favorable orientation for slip. These thrusts affected both the early development and shape of the Kanarra anticline, as well crosscutting and displacing folded thrusts on the overturned eastern limb (e.g., the Spring Creek thrust). Upon hinge lockup, late-forming forelimb shear thrusts within the overturned eastern limb developed a kilometer-scale, east-directed shear zone (e.g., Mitra 2002a; Jadamec and Wallace, 2014) shared by the leading anticline and syncline. Of these faults, the

Red Rock Trail thrust was in a favorable position and orientation to grow and locally may have merged with the blind thrust beneath the leading anticline to form a break thrust (Eisenstadt and De Paor, 1987; Fischer and others, 1992). The cross section through the Kanarra fold-thrust structure indicates the Red Rock Trail thrust transports the stratigraphic section in the Kanarra anticline to the east and on top of the Jurassic to Upper Cretaceous strata of the now Markagunt Plateau.

The Red Rock Trail thrust and its distinctive Navajo Sandstone cataclasite can be traced from its inception north of Spring Creek along the contact between the Kayenta Formation and Navajo Sandstone well to the north. At The Red Hill, the Red Rock Trail thrust has climbed section and places Navajo Sandstone over folded Carmel Formation. In Parowan Gap, the distinctive pairing of the Navajo Sandstone cataclasite on top of tightly folded and overturned Carmel we interpret as a remnant of the Red Rock Trail thrust at the western end of the gap. The overturned Carmel and Iron Springs Formation(?) in Parowan Gap represent the eastern limb of the leading anticline of the Kanarra fold-thrust structure—a structure, which can be traced for a minimum distance of about 90 km from the southern terminus near Toquerville to north of Parowan Gap (also see Threet, 1963a). We associate the thrusts east of the Red Rock Trail thrust in Parowan Gap as late fold accommodation faults (i.e., out-of-the-syncline thrusts) with the Kanarra fold-thrust structure rather than correlate them with the Iron Springs thrust at the Three Peaks. This reconciles the apparent conflict in the timing of initial movement of the Iron Springs thrust at Three Peaks at about 100 Ma (Quick and others, 2020) with the movement on the Kanarra fold-thrust structure constrained to being between early to late Campanian.

The Kanarra fold-thrust structure represents the leading edge of the Sevier fold-thrust belt in southwestern Utah during the Late Cretaceous. The Sevier fold-thrust deformation front appears to have advanced episodically from the Iron Springs thrust at 100 Ma (Quick and others, 2020) to the Red Rock Trail thrust in the early to late Campanian. This is suggestive that movement on Sevier thrusts may be temporally tied to episodes of magmatic flare ups in the Cordilleran arc (see Lageson and others, 2001; DeCelles and others, 2009; DeCelles and Graham,

2015; Yonkee and others, 2019; Quick and others, 2020). During the Late Cretaceous, and potentially persisting into the Eocene, the Keystone-Muddy Mountain-Tule Spring-Square Top Mountain-Blue Mountain-Iron Springs-Canyon Range thrust system and the Kanarra fold-thrust structure in the Campanian would present substantial north-south, linear topographic highs flanked by linear valleys that stretched over a 100 km in southwestern Utah. These imposing topographic features would have “Sevier” consequences for sediment provenance and dispersal in the associated Cordilleran foreland basin.

ACKNOWLEDGMENTS

John P. Hogan extends his thanks to Robert “Bob” Laudon (Missouri University of Science and Technology) for welcoming him to be a part of the field camp many years ago and sharing his thoughts, as well as his recollections of past conversations with Sheldon “Kerry” Grant (Missouri University of Science and Technology, deceased), on the geology of the area. Additional hearty thanks to Michael Wizevich (Central Connecticut State University), Jonathan Obrist-Farner (Missouri University of Science and Technology), and Jason Kaiser (Southern Utah University), for their insights and discussions regarding the geologic significance of many field exposures to the geology of southwest Utah as well as their friendship and comradery while teaching the Missouri S&T field camp.

William Chandonia would also like to thank Jason Kaiser for his help with logistics in Utah and sharing methods for measuring shear fractures. Tyler R. Knudsen (Utah Geological Survey) gave his time to meet in the field and shared his knowledge of the stratigraphy, which assisted with interpretations in the Chinle Formation. William also acknowledges Brennan Brunsvick (Southern Utah University), Trey Anglim (Missouri University of Science and Technology), Dylan Webb (Missouri University of Science and Technology), and Daniel Quick (Missouri University of Science and Technology) for their valuable assistance helping him in the field. The donation of Petroleum Experts’ Move software was invaluable to the study workflow and creating cross sections. This work was also enhanced by Richard Allmendinger’s (Cornell University) programs GMDE,

FaultKin, and Stereonet. Paul Inkenbrandt’s (Utah Geological Survey) CSL code facilitated the compiling and styling of our references. The study was funded by two grants from the American Association of Petroleum Geologists Foundation Grants-in-Aid program, one grant from the Geological Society of America Graduate Student Research Grant program, and the Chancellor’s Fellowship and Radcliffe Scholarship from Missouri University of Science and Technology.

We acknowledge the substantial effort of Tyler Knudsen and Doug Sprinkel (Azteca GeoSolutions) for their thorough reviews of our manuscript and appreciate their comments as well as the reviews of Grant Shimer (Southern Utah University) and Bob Biek (Utah Geological Survey).

REFERENCES

- Allmendinger, R.W., 2020, GMDE—Extracting quantitative information from geologic maps: *Geosphere*, v. 16, no. 6, p. 1495–1507, doi: <https://doi.org/10.1130/GES02253.1>.
- Allmendinger, R.W., Cardozo, N., and Fisher, D.M., 2013, *Structural geology algorithms—vectors and tensors*: Cambridge, Cambridge University Press, doi: <https://doi.org/10.1017/CBO9780511920202>.
- Allmendinger, R.W., Gephart, J.W., and Marrett, R.A., 1989, Notes on fault slip analysis: Ithaca, New York, Cornell University, notes from Geological Society of America short course “Quantitative interpretation of joints and faults,” 68 p.
- Anderson, L.P., and Dinter, D.A., 2010, Deformation and sedimentation in the southern Sevier foreland, Red Hills, southwestern Utah, *in* Carney, S.M., Tabet, D.E., and Johnson, C.L., editors, *Geology of south-central Utah*: Utah Geological Association Publication 39, p. 338–366.
- Armstrong, R.L., 1968, Sevier orogenic belt in Nevada and Utah: *Geological Society of America Bulletin*, v. 79, no. 4, p. 429–458, doi: [https://doi.org/10.1130/0016-7606\(1968\)79\[429:SOBINA\]2.0.CO;2](https://doi.org/10.1130/0016-7606(1968)79[429:SOBINA]2.0.CO;2).
- Averitt, P., 1962, Geology and coal resources of the Cedar Mountain quadrangle, Iron County, Utah: U.S. Geological Survey Professional Paper 389, 71 p., 3 plates, scale 1:24,000, doi: <https://doi.org/10.3133/pp389>.
- Averitt, P., 1967, Geologic map of the Kanarrville quadrangle, Iron County, Utah: U.S. Geological Survey Geologic Quadrangle Map GQ-694, 1 plate, scale 1:24,000, doi: <https://doi.org/10.3133/gq694>.

- Averitt, P., and Threet, R.L., 1973, Geologic map of the Cedar City quadrangle, Iron County, Utah: U.S. Geological Survey Geologic Quadrangle Map GQ-1120, 1 plate, scale 1:24,000, doi: <https://doi.org/10.3133/gq1120>.
- Biek, R.F., 2003a, Geologic map of the Harrisburg Junction quadrangle, Washington County, Utah: Utah Geological Survey Map 191, 42 p., 2 plates, scale 1:24,000, doi: <https://doi.org/10.34191/M-191>.
- Biek, R.F., 2003b, Geologic map of the Hurricane quadrangle, Washington County, Utah: Utah Geological Survey Map 187, 61 p., 2 plates, scale 1:24,000, doi: <https://doi.org/10.34191/M-187>.
- Biek, R.F., 2007a, Geologic map of the Kolob Arch quadrangle and part of the Kanarraville quadrangle, Washington and Iron Counties, Utah: Utah Geological Survey Map 217, 3 plates, scale 1:24,000, doi: <https://doi.org/10.34191/M-217>.
- Biek, R.F., 2007b, Geologic map of the Kolob Reservoir quadrangle, Washington and Iron Counties, Utah: Utah Geological Survey Map 220, 2 plates, scale 1:24,000, doi: <https://doi.org/10.34191/M-220>.
- Biek, R.F., and Hayden, J.M., 2016, Geologic map of the Kanarraville quadrangle, Iron County, Utah: Utah Geological Survey Map 276DM, 27 p., 2 plates, scale 1:24,000, doi: <https://doi.org/10.34191/M-276dm>.
- Biek, R.F., Rowley, P.D., Anderson, J.J., Maldonado, F., Hacker, D.B., Eaton, J.G., Hereford, R., Sable, E.D., Filkorn, H.F., and Matyjasik, B., 2015, Geologic map of the Panguitch 30' x 60' quadrangle, Garfield, Iron, and Kane Counties, Utah: Utah Geological Survey Map 270DM, 164 p., 3 plates, scale 1:62,500, doi: <https://doi.org/10.34191/M-270dm>.
- Biek, R.F., Rowley, P.D., Hayden, J.M., Hacker, D.B., Willis, G.C., Hintze, L.F., Anderson, R.E., and Brown, K.D., 2009, Geologic map of the St. George and east part of the Clover Mountains 30' x 60' quadrangles, Washington and Iron Counties, Utah: Utah Geological Survey Map 242DM, 101 p., 2 plates, scale 1:100,000, doi: <https://doi.org/10.34191/M-242dm>.
- Burchfiel, B.C., and Davis, G.A., 1972, Structural framework and evolution of the southern part of the Cordilleran orogen, western United States: *American Journal of Science*, v. 272, no. 2, p. 97–118, doi: <https://doi.org/10.2475/ajs.272.2.97>.
- Butler, R.W.H., Bond, C.E., Cooper, M.A., and Watkins, H., 2020, Fold-thrust structures—where have all the buckles gone?, in Bond, C.E., and Lebit, H. D., editors, *Folding and fracturing of rocks—50 years of research since the seminal text book of J.G. Ramsay: Geological Society of London Special Publication 487*, p. 21–44, doi: <https://doi.org/10.1144/SP487.7>.
- Cardozo, N., and Allmendinger, R.W., 2013, Spherical projections with OSXStereonet: *Computers & Geosciences*, v. 51, no. 2, p. 193–205, doi: <https://doi.org/10.1016/j.cageo.2012.07.021>.
- Carpenter, K., 2014, Where the sea meets the land—the unresolved Dakota problem in Utah, in MacLean, J.S., Biek, R.F., and Hunttoon, J.E., editors, *Geology of Utah's far south: Utah Geological Association Publication 43*, p. 357–372.
- Cawood, A.J., and Bond, C.E., 2020, Broadhaven revisited—a new look at models of fault-fold interaction, in Bond, C.E., and Lebit, H.D., editors, *Folding and fracturing of rocks—50 years of research since the seminal text book of J.G. Ramsay: Geological Society of London Special Publication 487*, p. 105–126, doi: <https://doi.org/10.1144/SP487.11>.
- Chapman, J.B., and DeCelles, P.G., 2015, Foreland basin stratigraphic control on thrust belt evolution: *Geology*, v. 43, no. 7, p. 579–582, doi: [10.1130/G36597.1](https://doi.org/10.1130/G36597.1).
- Chidsey, T.C., Jr., DeHamer, J.S., Hartwick, E.E., Johnson, K., Schelling, D.D., Sprinkel, D., Strickland, D.K., Vrona, J., and Wavrek, D., 2007, Petroleum geology of Covenant oil field, central Utah thrust belt, in Willis, G.C., Hylland, M.D., Clark, D.L., and Chidsey, T.C., Jr., editors, *Central Utah—diverse geology of a dynamic landscape: Utah Geological Association Publication 36*, p. 273–296.
- Cloos, E., 1961, Bedding slips, wedges, and folding in layered sequences: *Extrait de Comptes Rendus de la Société Géologique de Finlande*, v. 33, p. 105–122.
- Cloos, E., 1964, Wedging, bedding plane slips, and gravity tectonics in the Appalachians, in *Tectonics of the southern Appalachians: Virginia Polytechnic Institute Geological Sciences Memoir 1*, p. 63–70.
- Constenius, K.N., 1996, Late Paleogene extensional collapse of the Cordilleran foreland fold and thrust belt: *Geological Society of America Bulletin*, v. 108, no. 1, p. 20–39, doi: [https://doi.org/10.1130/0016-7606\(1996\)108<0020:LPECOT>2.3.CO;2](https://doi.org/10.1130/0016-7606(1996)108<0020:LPECOT>2.3.CO;2).
- Constenius, K.N., Esser, R.P., and Layer, P.W., 2003, Extensional collapse of the Charleston-Nebo salient and its relationship to space-time variations in Cordilleran orogenic belt tectonism and continental stratigraphy, in Reynolds, R.G., and Flores, R.M., editors, *Cenozoic systems of the Rocky Mountain region: Denver, Colorado, Society for Sedimentary Geology (SEPM), Rocky Mountain Section*, p. 303–353.
- Cook, E.F., 1957, *Geology of the Pine Valley Mountains, Utah: Utah Geological and Mineralogical Survey Bulletin 58*, 111 p.
- Currie, J.B., Patnode, H.W., and Trump, R.P., 1962, Development of folds in sedimentary strata: *Geological Society of*

- America Bulletin, v. 73, no. 6, p. 655–673, doi: [https://doi.org/10.1130/0016-7606\(1962\)73\[655:DOFISS\]2.0.CO;2](https://doi.org/10.1130/0016-7606(1962)73[655:DOFISS]2.0.CO;2).
- Dahlstrom, C.D.A., 1969, Balanced cross sections: Canadian Journal of Earth Sciences, v. 6, no. 4, p. 743–757, doi: <https://doi.org/10.1139/e69-069>.
- Davis, G.H., Reynolds, S.J., and Kluth, C.F., 2011, Structural geology of rocks and regions (third edition): Hoboken, New Jersey, John Wiley & Sons, 864 p.
- DeCelles, P.G., 2004, Late Jurassic to Eocene evolution of the Cordilleran thrust belt and foreland basin system, western U.S.A.: American Journal of Science, v. 304, no. 2, p. 105–168, doi: <https://doi.org/10.2475/ajs.304.2.105>.
- DeCelles, P.G., and Coogan, J.C., 2006, Regional structure and kinematic history of the Sevier fold-and-thrust belt, central Utah: Geological Society of America Bulletin, v. 118, no. 7–8, p. 841–864, doi: <https://doi.org/10.1130/B25759.1>.
- DeCelles, P.G., Ducea, M.N., Kapp, P., and Zandt, G., 2009, Cyclicity in Cordilleran orogenic systems: Nature Geoscience, v. 2, no. 4, p. 251–257, doi: <https://doi.org/10.1038/ngeo469>.
- DeCelles, P.G., and Graham, S.A., 2015, Cyclical processes in the North American Cordilleran orogenic system: Geology, v. 43, no. 6, p. 499–502, doi: <https://doi.org/10.1130/G36482.1>.
- Di Fiori, R.V., Long, S.P., Fetrow, A.C., Snell, K.E., Bonde, J.W., and Vervoort, J.D., 2021, The role of shortening in the Sevier Hinterland within the U.S. Cordilleran retroarc thrust system—insights from the Cretaceous Newark Canyon Formation in central Nevada: Tectonics, v. 40, no. 5, p. 31, doi: [10.1029/2020TC006331](https://doi.org/10.1029/2020TC006331).
- Doelling, H.H., 1972, Coal and geology map, Cedar Mountain quadrangle: Utah Geological and Mineralogical Survey MO-1-CM, scale 1:42,240.
- Ducea, M.N., Paterson, S.R., and DeCelles, P.G., 2015, High-volume magmatic events in subduction systems: Elements, v. 11, no. 2, p. 99–104, doi: [10.2113/gselements.11.2.99](https://doi.org/10.2113/gselements.11.2.99).
- Dunham, R.J., 1962, Classification of carbonate rocks according to depositional texture, in Classification of carbonate rocks—a symposium: American Association of Petroleum Geologists, p. 108–121, doi: [10.1306/M1357](https://doi.org/10.1306/M1357).
- Dutton, C.E., 1880, Report on the geology of the High Plateaus of Utah, U.S. Geographical and Geological Survey of the Rocky Mountain region: U.S. Government Printing Office Unserialized Monograph, 307 p., 8 plates, doi: <https://doi.org/10.3133/70039920>.
- Eisenstadt, G., and De Paor, D.G., 1987, Alternative model of thrust-fault propagation: Geology, v. 15, no. 7, p. 630–633, doi: [https://doi.org/10.1130/0091-7613\(1987\)15<630:A-MOTP>2.0.CO;2](https://doi.org/10.1130/0091-7613(1987)15<630:A-MOTP>2.0.CO;2).
- Enriquez St. Pierre, G.A., and Johnson, C.L., 2021, Faulty foundations—early breakup of the southern Utah Cordilleran foreland basin: Geological Society of America Bulletin, p. 20, doi: <https://doi.org/10.1130/B35872.1>.
- Fail, R.T., 1973, Kink-band folding, Valley and Ridge Province, Pennsylvania: Geological Society of America Bulletin, v. 84, no. 4, p. 1289–1314, doi: [https://doi.org/10.1130/0016-7606\(1973\)84<1289:KFVARP>2.0.CO;2](https://doi.org/10.1130/0016-7606(1973)84<1289:KFVARP>2.0.CO;2).
- Fail, R.T., and Wells, R.B., 1974, Geology and mineral resources of the Millerstown quadrangle, Perry, Juniata, and Snyder Counties, Atlas 136: Commonwealth of Pennsylvania Department of Environmental Resources, 276 p.
- Fillmore, R.P., 1991, Tectonic influence on sedimentation in the southern Sevier foreland, Iron Springs Formation (Upper Cretaceous), southwestern Utah, in Nations, J.D., and Eaton, J.G., editors., Stratigraphy, depositional environments, and sedimentary tectonics of the western margin, Cretaceous Western Interior Seaway: Geological Society of America Special Paper 260, p. 9–25.
- Fischer, M.P., Woodward, N.B., and Mitchell, M.M., 1992, The kinematics of break-thrust folds: Journal of Structural Geology, v. 14, no. 4, p. 451–460.
- Fleck, R.J., and Carr, M.D., 1990, The age of the Keystone thrust—laser-fusion $^{40}\text{Ar}/^{39}\text{Ar}$ dating of foreland basin deposits, southern Spring Mountains, Nevada: Tectonics, v. 9, no. 3, p. 467–476, doi: <https://doi.org/10.1029/TC009i003p00467>.
- Gardner, L.S., 1941, The Hurricane fault in southwestern Utah and northwestern Arizona: American Journal of Science, v. 239, no. 4, p. 241–260, doi: <https://doi.org/10.2475/ajs.239.4.241>.
- Giallorenzo, M.A., Wells, M.L., Yonkee, W.A., Stockli, D.F., and Wernicke, B.P., 2018, Timing of exhumation, Wheeler Pass thrust sheet, southern Nevada and California—Late Jurassic to middle Cretaceous evolution of the southern Sevier fold-and-thrust belt: Geological Society of America Bulletin, v. 130, no. 3–4, p. 558–579, doi: <https://doi.org/10.1130/B31777.1>.
- Goldstrand, P.M., 1991, Tectonostratigraphy, petrology, and paleogeography of Upper Cretaceous to Eocene rocks of southwest Utah: Reno, University of Nevada, M.S. thesis, 205 p.
- Goldstrand, P.M., 1992, Evolution of Late Cretaceous and early Tertiary basins of southwest Utah based on clastic petro-

- ogy: *Journal of Sedimentary Research*, v. 62, no. 3, p. 495–507, doi: <https://doi.org/10.1306/D4267933-2B26-11D7-8648000102C1865D>.
- Grant, S.K., 1987, Kolob Canyons, Utah—structure and stratigraphy, in Beus, S.S., editor, *Geological Society of America Centennial field guide: Rocky Mountain Section of the Geological Society of America*, p. 139–153, doi: <https://doi.org/10.1130/0-8137-5402-X.287>.
- Grant, S.K., Fielding, L.W., and Noweir, M.A., 1994, Cenozoic fault patterns in southwestern Utah and their relationships to structures of the Sevier orogeny, in Blackett, R.E., and Moore, J.N., editors, *Cenozoic geology and geothermal systems of southwestern Utah: Utah Geological Association Publication 23*, p. 139–153.
- Gregory, H.E., and Williams, N.C., 1947, Zion National Monument, Utah: *Geological Society of America Bulletin*, v. 58, no. 3, p. 211–244, doi: [https://doi.org/10.1130/0016-7606\(1947\)58\[211:ZNMU\]2.0.CO;2](https://doi.org/10.1130/0016-7606(1947)58[211:ZNMU]2.0.CO;2).
- Hautmann, M., Smith, A.B., McGowan, A.J., and Bucher, H., 2013, Bivalves from the Olenekian (Early Triassic) of south-western Utah—systematics and evolutionary significance: *Journal of Systematic Palaeontology*, v. 11, no. 3, p. 263–293, doi: <https://doi.org/10.1080/14772019.2011.637516>.
- Herring, D.M., and Greene, D.C., 2016, The western Utah thrust belt in the larger context of the Sevier orogeny, in Comer, J.B., Inkenbrandt, P.C., Krahulec, K.A., and Pinnell, M.L., editors, *Resources and geology of Utah's West Desert: Utah Geological Association Publication 45*, p. 131–146.
- Hintze, L.F., 1986, Stratigraphy and structure of the Beaver Dam Mountains, southwestern Utah, in Griffin, D.T., and Phillips, W.R., editors, *Thrusting and extensional structures and mineralization in the Beaver Dam Mountains, southwestern Utah: Utah Geological Association Publication 15*, p. 1–36.
- Hintze, L.F., 2005, Utah's spectacular geology—how it came to be: Provo, Utah, Brigham Young University Department of Geology, 203 p.
- Hofmann, R., Hautmann, M., Brayard, A., Nützel, A., Bylund, K.G., Jenks, J.F., Vennin, E., Olivier, N., and Bucher, H., 2014, Recovery of benthic marine communities from the end-Permian mass extinction at the low latitudes of eastern Panthalassa: *Palaeontology*, v. 57, no. 3, p. 547–589, doi: <https://doi.org/10.1111/pala.12076>.
- Hofmann, R., Hautmann, M., Wasmer, M., and Bucher, H., 2013, Palaeoecology of the Spathian Virgin Formation (Utah, USA) and its implications for the Early Triassic recovery: *Acta Palaeontologica Polonica*, v. 58, no. 1, p. 149–173, doi: <https://doi.org/10.4202/app.2011.0060>.
- Hurlow, H.A., and Biek, R.F., 2003, Geologic map of the Pintura quadrangle, Washington County, Utah: Utah Geological Survey Map 196, 20 p., 2 plates, scale 1:24,000, doi: <https://doi.org/10.34191/M-196>.
- Jadamec, M.A., and Wallace, W.K., 2014, Thrust-breakthrough of asymmetric anticlines—observational constraints from surveys in the Brooks Range, Alaska: *Journal of Structural Geology*, v. 62, p. 109–124, doi: <https://doi.org/10.1016/j.jsg.2014.01.012>.
- Kay, M., 1951, North American geosynclines: *Geological Society of America Memoir 48*, 143 p.
- Knudsen, T.R., 2014a, Interim geologic map of the Cedar City 7.5-minute quadrangle, Iron County, Utah: Utah Geological Survey Open-File Report 626, 20 p., 2 plates, scale 1:24,000, doi: <https://doi.org/10.34191/OFR-626>.
- Knudsen, T.R., 2014b, Interim geologic map of the Enoch quadrangle, Iron County, Utah: Utah Geological Survey Open-File Report 628, 12 p., 2 plates, scale 1:24,000, doi: <https://doi.org/10.34191/OFR-628>.
- Knudsen, T.R., and Biek, R.F., 2014, Interim geologic map of the Cedar City NW quadrangle, Iron County, Utah: Utah Geological Survey Open-File Report 627, 18 p., 2 plates, scale 1:24,000.
- Kurie, A.E., 1966, Recurrent structural disturbance of Colorado Plateau margin near Zion National Park, Utah: *Geological Society of America Bulletin*, v. 77, no. 8, p. 867–872, doi: [https://doi.org/10.1130/0016-7606\(1966\)77\[867:RS-DOCP\]2.0.CO;2](https://doi.org/10.1130/0016-7606(1966)77[867:RS-DOCP]2.0.CO;2).
- Lageson, D.R., Schmitt, J.G., Horton, B.K., Kalakay, T.J., and Burton, B.R., 2001, Influence of Late Cretaceous magmatism on the Sevier orogenic wedge, western Montana: *Geology*, v. 29, no. 8, p. 723–726, doi: [https://doi.org/10.1130/0091-7613\(2001\)029<0723:IOLCMO>2.0.CO;2](https://doi.org/10.1130/0091-7613(2001)029<0723:IOLCMO>2.0.CO;2).
- Long, S.P., 2012, Magnitudes and spatial patterns of erosional exhumation in the Sevier hinterland, eastern Nevada and western Utah, USA—insights from a Paleogene paleogeologic map: *Geosphere*, v. 8, no. 4, p. 881–901, doi: <https://doi.org/10.1130/GES00783.1>.
- Long, S.P., 2015, An upper-crustal fold province in the hinterland of the Sevier orogenic belt, eastern Nevada, U.S.A.—a Cordilleran valley and ridge in the Basin and Range: *Geosphere*, v. 11, no. 2, p. 404–424, doi: <https://doi.org/10.1130/GES01102.1>.
- Lovejoy, E.M.P., 1978, Age of structural differentiation between the Colorado Plateaus and Basin and Range provinces in southwestern Utah—comment and reply—comment: *Ge-*

- ology, v. 6, no. 9, p. 572–572, doi: [https://doi.org/10.1130/091-7613\(1978\)6<572a:AOSDBT>2.0.CO;2](https://doi.org/10.1130/091-7613(1978)6<572a:AOSDBT>2.0.CO;2).
- Lucas, S.G., Krainer, K., and Milner, A.R.C., 2007, The type section and age of the Timpoweap Member and stratigraphic nomenclature of the Triassic Moenkopi Group in southwestern Utah, in Lucas, S.G., and Spielmann, J.A., editors, *Triassic of the American West: New Mexico Museum of Natural History and Science Bulletin 40*, p. 109–117.
- Lucas, S.G., and Tanner, L.H., 2006, The Springdale Member of the Kayenta Formation, Lower Jurassic of Utah-Arizona, in Harris, J.D., Lucas, S.G., Spielmann, J.A., Lockley, M.G., Milner, R.C., and Kirkland, J.I., editors, *The Triassic-Jurassic terrestrial transition: New Mexico Museum of Natural History and Science Bulletin 37*, p. 71–76.
- Maldonado, F., and Williams, V.S., 1993, Geologic map of the Parowan Gap quadrangle, Iron County, Utah: U.S. Geological Survey Geologic Quadrangle Map GQ-1712, 1 plate, scale 1:24,000, doi: <https://doi.org/10.3133/gq1712>.
- Marrett, R., and Allmendinger, R.W., 1990, Kinematic analysis of fault-slip data: *Journal of Structural Geology*, v. 12, no. 8, p. 973–986, doi: [https://doi.org/10.1016/0191-8141\(90\)90093-E](https://doi.org/10.1016/0191-8141(90)90093-E).
- Mitra, S., 2002a, Fold-accommodation faults: *American Association of Petroleum Geologists Bulletin*, v. 86, no. 4, p. 671–693, doi: <https://doi.org/10.1306/61EEDB7A-173E-11D7-8645000102C1865D>.
- Mitra, S., 2002b, Structural models of faulted detachment folds: *American Association of Petroleum Geologists Bulletin*, v. 86, no. 9, p. 1673–1694, doi: <https://doi.org/10.1306/61EED-D3C-173E-11D7-8645000102C1865D>.
- Muir, R.J., 2015, Digital field mapping—making the change from paper to touchscreen technology: *Geology Today*, v. 31, no. 6, p. 232–236, doi: <https://doi.org/10.1111/gto.12120>.
- Munsell Color, 2009, Geological rock color chart—with genuine Munsell® color chips: Grand Rapids, Michigan Munsell Color, 8 p.
- Nowir, A.M., and Grant, S.K., 1995, Balanced cross-section across the southern Utah overthrust belt (OTB): *Qatar University Science Journal*, v. 15, no. 1, p. 195–204.
- Page, W.R., Lundstron, S.C., Harris, A.G., Langenheim, V.F., Workman, J.B., Mahan, S., Paces, J.B., Dixon, G.L., Rowley, P.D., Burchfiel, B.C., Bell, J.W., and Smith, E.I., 2005, Geological and geophysical maps of the Las Vegas 30' x 60' quadrangle, Clark and Nye Counties, Nevada, and Inyo County, California: U.S. Geological Survey Scientific Investigations Map 2814, 58 p., 2 plates, scale 1:100,000, doi: <https://doi.org/10.3133/sim2814>.
- Paulsen, T., and Marshak, S., 1999, Origin of the Uinta recess, Sevier fold-thrust belt, Utah—influence of basin architecture on fold-thrust belt geometry: *Tectonophysics*, v. 312, no. 2, p. 203–216, doi: [https://doi.org/10.1016/S0040-1951\(99\)00182-1](https://doi.org/10.1016/S0040-1951(99)00182-1).
- Perry, D.G., and Chatterton, B.D.E., 1979, Late Early Triassic brachiopod and conodont fauna, Thaynes Formation, southeastern Idaho: *Journal of Paleontology*, v. 53, no. 2, p. 307–319.
- Petit, J.P., 1987, Criteria for the sense of movement on fault surfaces in brittle rocks: *Journal of Structural Geology*, v. 9, no. 5, p. 597–608, doi: [https://doi.org/10.1016/0191-8141\(87\)90145-3](https://doi.org/10.1016/0191-8141(87)90145-3).
- Picha, F., 1986, The influence of preexisting tectonic trends on geometries of the Sevier orogenic belt and its foreland in Utah, in Peterson, J.A., editor, *Paleotectonics and sedimentation in the Rocky Mountain region, United States: American Association of Petroleum Geologists Memoir 41*, p. 309–320, doi: <https://doi.org/10.1306/M41456C14>.
- Picha, F., and Gibson, R.I., 1985, Cordilleran hingeline—late Precambrian rifted margin of the North American craton and its impact on the depositional and structural history, Utah and Nevada: *Geology*, v. 13, no. 7, p. 465–468, doi: [https://doi.org/10.1130/0091-7613\(1985\)13<465:CHL-PRM>2.0.CO;2](https://doi.org/10.1130/0091-7613(1985)13<465:CHL-PRM>2.0.CO;2).
- Pipiringos, G.N., and O'Sullivan, R.B., 1978, Principal unconformities in Triassic and Jurassic rocks, Western Interior United States—a preliminary survey: U.S. Geological Survey Professional Paper 1035-A, 29 p, doi: <https://doi.org/10.3133/pp1035A>.
- Pujols, E.J., Stockli, D.F., Constenius, K.N., and Horton, B.K., 2020, Thermochronological and geochronological constraints on Late Cretaceous unroofing and proximal sedimentation in the Sevier orogenic belt, Utah: *Tectonics*, v. 39, no. 7, p. 32, doi: <https://doi.org/10.1029/2019TC005794>.
- Pumpelly, R., Wolff, J.E., and Dale, T.N., 1894, *Geology of the Green Mountains in Massachusetts*: U.S. Government Printing Office, Monographs of the U.S. Geological Survey Monograph 23, 206 p, doi: <https://doi.org/10.3133/m23>.
- Quick, J.D., Hogan, J.P., Wizevich, M., Obrist-Farner, J., and Crowley, J.L., 2020, Timing of deformation along the Iron Springs thrust, southern Sevier fold-and-thrust belt, Utah—evidence for an extensive thrusting event in the mid-Cretaceous: *Rocky Mountain Geology*, v. 55, no. 2, p. 75–89, doi: <https://doi.org/10.24872/rmgjournal.55.2.75>.
- Rowley, P.D., Williams, V.S., Maxwell, D.J., Hacker, D.B., Snee, L.W., and Mackin, J.H., 2006, Interim geologic map of the Cedar City 30' x 60' quadrangle, Iron and Washing-

- ton Counties, Utah: Utah Geological Survey Open-File Report 476DM, 2 plates, scale 1:100,000, doi: <https://doi.org/10.34191/OFR-476dm>.
- Schubert, J.K., Bottjer, D.J., and Simms, M.J., 1992, Paleobiology of the oldest known articulate crinoid: *Lethaia*, v. 25, no. 1, p. 97–110, doi: [10.1111/j.1502-3931.1992.tb01794.x](https://doi.org/10.1111/j.1502-3931.1992.tb01794.x).
- Sprinkel, D.A., Doelling, H.H., Kowallis, B.J., Waanders, G., and Kuehne, P.A., 2011, Early results of a study of the Middle Jurassic strata in the Sevier fold and thrust belt, Utah, *in* Sprinkel, D.A., Yonkee, W.A., and Chidsey, T.C., Jr., editors, Sevier thrust belt—northern and central Utah and adjacent areas: Utah Geological Association Publication 40, p. 151–172.
- Steed, D.A., 1980, Geology of the Virgin River Gorge, northwest Arizona: Brigham Young University Geology Studies, v. 27, pt. 3, p. 96–115.
- Stewart, M.E., and Taylor, W.J., 1996, Structural analysis and fault segment boundary identification along the Hurricane fault in southwestern Utah: *Journal of Structural Geology*, v. 18, no. 8, p. 1017–1029, doi: [https://doi.org/10.1016/0191-8141\(96\)00036-3](https://doi.org/10.1016/0191-8141(96)00036-3).
- Stokes, W.L., 1976, What is the Wasatch line?, *in* Hill, J., editor, Symposium on geology of the Cordilleran hingeline: Denver, Colorado, Rocky Mountain Association of Geologists, p. 11–25.
- Stokes, W.L., Hintze, L.F., and Madsen, J.H., Jr., 1963, Geological map of Utah: Utah State Land Board and University of Utah, scale 1:250,000.
- Thomas, W., 2006, Tectonic inheritance at a continental margin: *Geological Society of America Today*, v. 16, no. 2, p. 4–11, doi: [https://doi.org/10.1130/1052-5173\(2006\)016\[4-TIAACM\]2.0.CO;2](https://doi.org/10.1130/1052-5173(2006)016[4-TIAACM]2.0.CO;2).
- Threet, R.L., 1963a, Geology of the Parowan Gap area, Iron County, Utah, *in* Heylman, E.B., editor, Guidebook to the geology of southwestern Utah—transition between the Basin-Range and Colorado Plateau provinces: Intermountain Association of Petroleum Geologists Twelfth Annual Field Conference, p. 136–145.
- Threet, R.L., 1963b, Structure of the Colorado Plateau margin near Cedar City, Utah, *in* Heylman, E.B., editor, Guidebook to the geology of southwestern Utah—transition between the Basin-Range and Colorado Plateau provinces: Intermountain Association of Petroleum Geologists Twelfth Annual Field Conference, p. 104–117.
- Van Kooten, G.K., 1988, Structure and hydrocarbon potential beneath the Iron Springs laccolith, southwestern Utah: *Geological Society of America Bulletin*, v. 100, no. 10, p. 1533–1540, doi: [https://doi.org/10.1130/0016-7606\(1988\)100<1533-SAHPBT>2.3.CO;2](https://doi.org/10.1130/0016-7606(1988)100<1533-SAHPBT>2.3.CO;2).
- Walker, J.D., Tikoff, B., Newman, J., Clark, R., Ash, J., Good, J., Bunse, E.G., Möller, A., Kahn, M., Williams, R.T., Michels, Z., Andrew, J.E., and Ruffledt, C., 2019, StraboSpot data system for structural geology: *Geosphere*, v. 15, no. 2, p. 533–547, doi: <https://doi.org/10.1130/GES02039.1>.
- Wang, F., Chen, J., Dai, X., and Song, H., 2017, A new Dienerian (Early Triassic) brachiopod fauna from South China and implications for biotic recovery after the Permian–Triassic extinction: *Papers in Palaeontology*, v. 3, no. 3, p. 425–439, doi: <https://doi.org/10.1002/spp2.1083>.
- Wernicke, B., Axen, G.J., and Snow, J.K., 1988, Basin and Range extensional tectonics at the latitude of Las Vegas, Nevada: *Geological Society of America Bulletin*, v. 100, no. 11, p. 1738–1757, doi: [https://doi.org/10.1130/0016-7606\(1988\)100<1738:BARETA>2.3.CO;2](https://doi.org/10.1130/0016-7606(1988)100<1738:BARETA>2.3.CO;2).
- Williams, G., and Chapman, T., 1983, Strains developed in the hanging walls of thrusts due to their slip/propagation rate—a dislocation model: *Journal of Structural Geology*, v. 5, no. 6, p. 563–571, doi: [https://doi.org/10.1016/0191-8141\(83\)90068-8](https://doi.org/10.1016/0191-8141(83)90068-8).
- Willis, B., 1893, The mechanics of Appalachian structure, *in* Powell, J.W., editor, Thirteenth Annual report of the United States Geological Survey to the Secretary of the Interior, 1891–1892—Part 2: Washington, D.C., U.S. Government Printing Office, p. 217–281, doi: <https://doi.org/10.3133/70039920>.
- Willis, G.C., 1999, The Utah thrust system—an overview, *in* Spangler, L.W., and Allen, C.J., editors, Geology of northern Utah and vicinity: Utah Geological Association Publication 27, p. 1–9.
- Yonkee, W.A., Eleogram, B., Wells, M.L., Stockli, D.F., Kelley, S., and Barber, D.E., 2019, Fault slip and exhumation history of the Willard thrust sheet, Sevier fold-thrust belt, Utah—relations to wedge propagation, hinterland uplift, and foreland basin sedimentation: *Tectonics*, v. 38, no. 8, p. 2850–2893, doi: [10.1029/2018TC005444](https://doi.org/10.1029/2018TC005444).
- Yonkee, W.A., and Weil, A.B., 2015, Tectonic evolution of the Sevier and Laramide belts within the North American Cordillera orogenic system: *Earth-Science Reviews*, v. 150, p. 531–593, doi: <https://doi.org/10.1016/j.earsci-rev.2015.08.001>.